



Universidad de Valladolid



**PROGRAMA DE DOCTORADO EN
INGENIERÍA INDUSTRIAL**

TESIS DOCTORAL:

**Desarrollo de Estrategias de
Control Biocoperativo para
Plataformas Robotizadas de
Rehabilitación Neuromotora**

Presentada por Ana Ciscal de la
Rica para optar al grado de
Doctora por la Universidad de
Valladolid

Dirigida por:
Javier Pérez Turiel
Juan Carlos Fraile Marinero



Universidad de Valladolid



**DOCTORAL PROGRAM OF
INDUSTRIAL ENGINEERING**

DOCTORAL THESIS:

**Development of Biocooperative
Control Strategies for
Neuromotor Rehabilitation
Robotic Platforms**

Thesis presented by Ana Ciscal
de la Rica to apply for the Ph.D.
degree
from the University of Valladolid

Directed by:
Javier Pérez Turiel
Juan Carlos Fraile Marinero

A mis padres,



Universidad de Valladolid



PROGRAMA DE DOCTORADO EN INGENIERÍA INDUSTRIAL

Research Stay for the International Mention:

Country	Switzerland
Faculty	Swiss Federal Institute of Technology Zurich (Zurich)
Institute	Institute of Robotics and Intelligent Systems (IRIS)
Department	Department of Health Sciences and Technology
Research Group	Sensory-Motor Systems Lab Spinal Cord Injury Artificial Intelligence (SCAI) Lab
Center	Swiss Paraplegic Center (Nottwill)
Dates	05/09/2022 – 30/12/2022
Duration	3 months and 25 days (116 days)
Supervisor	Prof. Dr. Dr. h.c. Robert Riener



Eidgenössische Technische Hochschule Zürich
Swiss Federal Institute of Technology Zurich



Swiss
Paraplegic
Centre



Agradecimientos

En primer lugar, deseo expresar mis más sinceros agradecimientos a los directores de esta tesis doctoral, Dr. Javier Pérez Turiel y Dr. Juan Carlos Fraile Marinero, por su confianza y apoyo durante todos estos años. Todavía recuerdo allá en 2016, cuando Juan Carlos planteó la posibilidad de hacer una estancia de investigación en el extranjero a sus alumnos de cuarto. Creo que, en ese momento, empezó a definirse mi perfil investigador. Gracias Juan Carlos por brindarme la oportunidad de ir al IBMT, de hacer prácticas en CARTIF y por ofrecerme la posibilidad de empezar a trabajar en ITAP Robótica Médica. Gracias Javier, por todo el rigor que siempre intentas brindar a mi trabajo de investigación, tus valiosas sugerencias y las cuidadosas revisiones que has realizado a los artículos que conforman esta tesis. Gracias a los dos por el respaldo y apoyo incondicional que siempre me habéis brindado desde que comencé a trabajar con vosotros.

Asimismo, agradezco a todos los compañeros que forman o formaron parte del grupo ITAP Robótica Médica. Con especial cariño agradeceré aquellos que estuvieron en sus inicios: a Víctor y David que sin ellos esta investigación no hubiera sido posible. Pero también a los que se incorporaron más tarde: Guillermo, Gonzalo, Alberto, Wiki, Diego, Daniel, Carlos... Gracias por todo el apoyo tanto personal como profesional, y por todos los buenos ratos que hemos pasado.

I would also like to express my sincere gratitude to Dr. Robert Riner and Dr. Diego Páez-Granados for embracing me in their research group. Gracias a Diego por su supervisión, sugerencias y dedicación. Furthermore, I would like to acknowledge and thank all the members of the SCAI Lab, with special attention thanks to Mehdi, Sabrina, Yankee, Siri, and Bertram. They did not only contribute professionally to my research work, but also personally,

providing me with many memorable moments. Please know that you are always welcome to visit your second home in Valladolid.

Pero un trabajo de investigación es también fruto del reconocimiento y del apoyo incondicional que nos ofrecen las personas que nos quieren, sin el cual no tendríamos esa energía que nos anima a mejorar como personas y como profesionales. Gracias a mis padres y amigos, que siempre me han prestado un gran apoyo moral y humano. Pero, sobre todo, gracias a ti Rafael que siempre estás ahí, por tu paciencia y comprensión.

A todos ellos, agradeceremos vuestra amistad, apoyo y aportaciones durante todos estos años. Sin vosotros este trabajo nunca se habría escrito y, por eso, este trabajo es también vuestro. A todos, muchas gracias.

Abstract

Rehabilitation robotics has emerged as a promising solution for promoting motor recovery and functional independence in patients with neurological disorders. Utilizing robotic devices for neurorehabilitation has demonstrated great potential in delivering intensive and repetitive training to promote motor recovery. In contrast to traditional rehabilitation robotics, which primarily considers biomechanical information, biocooperative controls in rehabilitation robotics go further by incorporating psychological and/or physiological measurements, effectively integrating the patient into the feedback loop. These robotic devices offer various types of assistance and can be controlled using diverse input modalities, such as electromyography (EMG), electroencephalography (EEG), and kinematic signals. Among these input modalities, EMG has gained widespread adoption due to its capacity to provide real-time information on muscle activation patterns. It enables a biocooperative control approach, establish a feedback loop between the user and the robot.

The current state of biocooperative systems renders them impractical for clinical settings primarily due to their inherent challenges related to reliability and accessibility. The reliability issues primarily stem from the high cost associated with the necessary physiological acquisition systems, thereby posing a significant constraint on further essential research in this field. Moreover, the lack of processing capabilities of these systems hinders the development of real-time biocooperative control strategies and consequently, efficient human-robot interaction. Additionally, the bulky nature of the physiological acquisition systems adversely affects user acceptance.

In this context, this Doctoral Thesis is focused on the design of affordable, real-time, embedded solutions for physiological data acquisition, coupled with the development of biocooperative control strategies that contribute to providing practical applications for individuals suffering from neuromotor

impairments. The studies included in this compendium of publications primarily address motor rehabilitation of the upper-limb. This is an area of significant importance, considering that upper-limb paresis is among the most frequently observed outcome of stroke and profoundly impacts the quality of life and independence of stroke survivors.

The contributions of this study are based on the design of affordable solutions for the acquisition of physiological signals and the implementation of biocooperative controls in these real-time embedded systems. An EMG recording system and a wearable multimodal physiological acquisition system have been designed to enhance accessibility and facilitate the use of upper-limb biocooperative control in the clinical settings.

First, a non-pattern recognition-based EMG-driven control has been developed for a hand rehabilitation robot. The system operates on a real-time embedded platform and has demonstrated favorable performance, achieving an overall accuracy of 97% for hand gesture detection and exhibiting adequate time responsiveness (motion-selection time of 0.48s, motion-onset time of 0.55s, motion-completion time of 1.9 s, and 100% motion-completion rate). Moreover, EMG-based visual feedback was introduced into the system. Significant statistical differences in subject performance were observed based on the type of provided feedback (p -value = 0.0124). Specifically, the performance was significantly better when only EMG-based visual feedback was present compared to kinesthetic feedback alone (p = 0.0412) or the combination of both (p -value = 0.0497). These findings indicate that the feedback enables subjects to enhance their control over the movement of the robotic platform by monitoring their muscle activation in real-time.

Secondly, the performance of the embedded multimodal acquisition platform has been validated through the implementation of two biocooperative control strategies: an EMG&IMU-based control using virtual reality-based therapy, and an adaptive assistive control (AAN) using a wrist rehabilitation robot. The wearable system, integrating multiple sensors, wireless communication, and a high-efficiency real-time microcontroller, is characterized by its high versatility and configurability. It has been verified that its low cost does not compromise the signal quality and has the potential to facilitate and promote the development of real-time biocooperative controls for a wide range of neuromotor rehabilitation applications.

Overall, the findings of this Doctoral Thesis could pave the way for the development of more affordable and effective robotic devices for upper-limb neurorehabilitation and provide insights into the design and implementation of biocooperative controls for neurorehabilitation platforms.

Acronyms

AAN	Assist-as-needed
ADC	Analog-to-Digital Converter
ADL	Activities of Daily Living
AFE	Analog Front End
AGD	Accurately Gesture Detection
ANN	Artificial Neural Networks
ANOVA	Analysis of Variance
ANS	Autonomic Nervous System
APB	Abductor Pollicis Brevis
ARV	Average Rectified Value
ASIC	Application Specific Integrated Circuit
BCI	Brain-Computer Interface
BLE	Bluetooth Low Energy
BP	Blood Pressure
BVP	Blood Volume Pressure
CART	Classification and Regression Trees
CDTI	Center of Development of Industrial Technology
CLA	Control Law Accelerator
CNN	Convolutional Neural Network

CVA	Cerebrovascular Accident
CVVC	Constant Voltage/Constant Current
DES	Dielectric Elastomer Sensor
DMP	Digital Motion Processor
DoF	Degrees of Freedom
DTW	Dynamic Time Warping
ECG	Electrocardiogram
ED	Extensor Digitorum
EDA	Electrodermal Activity
EE	End-Effector
EEG	Electroencephalogram
EMG	Electromyographic
EOG	Electrooculogram
(e)PWM	(enhance) Pulse Width Modulation
ERDF	European Regional Development Funds
FDS	Flexor Digitorum Superficialis
FE	Flexion/Extension
FIR	Finite Impulse Response
FN	False Negative
FP	False Positive
GBM	Gradient Boosting Machine
GSR	Galvanic Skin Response
HR	Heart Rate
HRV	Heart Rate Variability
IMU	Inertial Measurement Unit
IR	Infrared thermometer
ITAP	Institute of Advanced Production Technology

HRI	Human-Robot Interaction
JCR	Journal Citation Reports
KNN	K-Nearest Neighbors
LCSS	Longest Common Subsequence
LDA	Linear Discriminant Analysis
MCP	Metacarpophalangeal
MCT	Motion Completion Time
MCU	Microcontroller
ME	Motion End
MEMS	MicroElectroMechanical System
ML	Machine Learning
MO	Motion Onset
MOT	Motion Onset Time
MSPS	Mega Samples Per Second
MST	Motion Selection Time
MUAP	Motor Unit Action Potentials
MVC	Maximal Voluntary Contraction
M3Rob	Mind-Hand-Wrist Robot
OTP	One-Time Programmable
PCB	Printed Circuit Board
PIP	Proximal Interphalangeal
PPG	Photoplethysmogram
PPV	Positive Predictive Value
PRISMA	Reporting Items for Systematic Reviews and Meta-Analyses
PS	Pronation/Supination
QOL	Quality of Life
RESP	Respiration

RMS	Root Mean Square
RobHand	Robot for Hand Rehabilitation
ROM	Range of Motion
RR	Respiration Rate
RT	Robot-assisted Therapy
RTP	Repetitive Task Practice
RU	Radial/Ulnar
RVC	Reference Voluntary Contractions
SC	Skin Conductance
SCL	Skin Conductance Level
SCR	Skin Conductance Response
sEMG	surface Electromyography
SKT	Skin Temperature
SMD	Surface Mounted Device
SNR	Signal-to-Noise Ratio
SOC	System-On-Chip
SVM	Support Vector Machine
TN	True Negative
TP	True Positive
TPR	True Positive Rate
VR	Virtual Reality
VRBR	Virtual Reality-Based Rehabilitation
WHO	World Health Organization
WOS	Web of Science

List of Figures

Figure 1.1. Types of strokes: ischemic and hemorrhagic (CNS Traumatic Brain Injury Rehab, 2023).	7
Figure 1.2. Rate of disability in stroke survivals, broken down by degree of disability.	8
Figure 1.3. Commercially available robots for hand rehabilitation (a) Saeboflex (Saebo, Inc., NC, USA), (b) Motus Hand (Motus Nova, GA, USA), (c) Hand of Hope (Rehab-Robotics, China), (d) Amadeo (TyroMotion, Austria) (e) Gloreha (Idrogenet, Italy), (f) HandyRehab (Fourier Intelligence, Singapore).....	10
Figure 1.4. Generic diagram of biocooperative robotic systems, specifying integration of the human into the loop in a biomechanical, physiological, and psychological sense (Riener and Munich, 2010).....	14
Figure 1.5. EMG signal recording using a surface electrode, including a motor unit and muscle fibers (McManus et al., 2020).	18
Figure 1.6. Conceptual block diagram for myoelectric control system.	19
Figure 1.7. Schematic diagram of the 3-element Hill model of the human skeletal muscle: a contractile element, series element, and parallel element modelling acting and myosin cross-bridges, tendons, and connective tissues, respectively (Battista et al., 2017).....	20
Figure 2.1. The RobHand robotic platform and forearm support for hand rehabilitation (Cisnal et al., 2021).....	27
Figure 2.2. The M3Rob robotic platform for wrist rehabilitation, which provides assistance of the pronation/supination, flexion/extension, and radial/ulnar deviation motions.	28

Figure 2.3. EMG differences and thresholds used in the triggered ON-OFF EMG-driven control (Serpelloni et al., 2016). 31

Figure 2.4. EMG signal processing for the FDS muscle in the time-over-threshold EMG-driven control (Polygerinos et al., 2015a). 32

Figure 2.5. Raw EMG signals from the APB and ED muscles and the EMG-triggered status (Ho et al., 2011). 32

Figure 2.6. Simplified diagram of the two-stage fuzzy logic model for generating action primitives in an upper extremity rehabilitation robot (Mihelj et al., 2009). 33

Figure 2.7. Determination of arousal and valence from GSR, EMG and HR information (Mandryk and Atkins, 2007). 34

Figure 2.8. The left-handed subject wearing the 5DT Data Glove on the dominant hand and the exoskeleton on the non-dominant hand. The sEMG electrodes are attached to the target muscles of the forearm of the dominant hand (Cisnal et al., 2021). 35

Figure 2.9. The right-handed subject wearing the hand exoskeleton on the non-dominant hand while the sEMG electrodes are attached to the target muscles of the forearm of the dominant hand (Cisnal et al., 2023). 36

Figure 2.10. Experimental setup diagram, showing the data flow between subsystems: visual information from the computer (yellow lines), EMG and control signals (red lines), data transmission (blue lines), and exoskeleton movement (green lines). The presence of the source of feedback (dotted lines) varies depending on the specific test (Cisnal et al., 2023b). 37

Figure 2.11. Confusion matrix for a binary classification problem. There are two true classes: positive (P) and negative (N). The output of the predicted class is either true (T) or false (F). 39

Figure 2.12. Timing diagram showing the time-related metrics: MST, MOT, MCT (Cisnal et al., 2021). 41

Figure 3.1. EMG acquisition system layout (a) PCB layout (b) final solution (c) board plugged-in the MCU. 47

Figure 3.2. High level block diagram of the proposed multimodal embedded system (Cisnal et al., 2023a). 48

Figure 3.3. Multimodal acquisition system (a) PCB layout (b) Final solution (Cisnal et al., 2023a)..... 50

Figure 3.4. User performing EMG-driven bilateral therapy using the RobHand rehabilitation platform. The exoskeleton is worn on the impaired hand, while disposable electrodes are attached to the forearm muscles of the healthy hand to capture EMG signals (Cisnal et al., 2023b). 51

Figure 3.5. Simplified block diagram of the implementation of the EMG-driven control on the RobHand platform for assisted bilateral therapy (Cisnal et al., 2021)..... 51

Figure 3.6. sEMG signal recording and processing, including filtering, rectification, and normalization (Cisnal et al., 2021). 52

Figure 3.7. Control loop implemented for the calibration process and threshold-based EMG-driven control (Cisnal et al., 2021). 53

Figure 3.8. Threshold EMG-driven control: raw EMG signals of ED and FDS muscles, normalized signals, EMG-based threshold, and recognized gestures (Cisnal et al., 2023b). 54

Figure 3.9. EMG-based visual feedback consisting of two variable length bars (Cisnal et al., 2023b). 54

Figure 3.10. Upper-limb rehabilitation using a VR-based exergame. The embedded platform is place on the arm user and two pairs of surface electrodes are attached to the ED and FDS muscles and the reference electrode is attached to the olecranon (Cisnal et al., 2023a). 55

Figure 3.11. Schematic diagram of the VR-based exergame for upper-limb rehabilitation (Cisnal et al., 2023a). 56

Figure 3.12. Recorded linear acceleration (top plot), recorded angular velocity (middle plot) and estimated orientation (bottom plot). Solid lines indicate raw data and dashed lines indicate filtered data (Cisnal et al., 2023a). 56

Figure 3.13. User undergoing rehabilitation using the wrist robotic platform based on an AAN control strategy, while wearing the embedded platform on the arm to register SKT. To record ECG signals, disposable electrodes are attached to the user’s torso, and electrodes are placed on the fingertips of the hand to capture GSR (Cisnal et al., 2023a). 57

Figure 3.14. AAN control strategy based on a two-stage fuzzy logic model which consider the motor performance and emotional state of the user (Cisnal et al., 2023a). 58

Figure 3.15. R events of an ECG signal from a person at rest (Cisnal et al., 2023a). 59

Figure 3.16. Raw and filtered skin conductance and its tonic (SCL) and phasic (SCR) components (Cisnal et al., 2023a). 59

Figure 3.17. Schematic diagram of the AAN control strategy for wrist rehabilitation..... 60

Figure 3.18. Time delay analysis of the EMG-driven bilateral control with the hand exoskeleton (Cisnal et al., 2021)..... 61

Figure 3.19. Confusion matrix of the EMG-based gesture recognition (Cisnal et al., 2021). 61

Figure 3.20. Target and recognized sequence of gestures of one subject (a) Raw data; (b) Time-synchronized data (Cisnal et al., 2023b). 62

Figure 3.21. L2 distances for the four performed tests (Cisnal et al., 2023b). 63

Figure 3.22. Breakdown of the power consumption for the two scenarios: (a) EMG&IMU-based control and (b) AAN control (Cisnal et al., 2023a). 64

Figure 4.1. The control loop used for the threshold EMG-driven control of the RobHand specifying the origin of each feedback (Cisnal et al., 2023b). 68

List of Tables

Table 1.1: Training modalities for rehabilitation robotics, categorized based on the interaction between the rehabilitation robot and the patient.	11
Table 1.2: Literature review on biocooperative systems, indicating the control type and the employed physiological signals.....	16
Table 2.1: Test configuration for evaluating user performance based on the presence of feedback sources, including kinesthetic and EMG-based visual feedback.....	37
Table 3.1: Technical specifications of the EMG acquisition system, encompassing general characteristics and configuration parameters of the Delta-Sigma ADCs.	48
Table 3.2: Color of the bars of the EMG-based visual feedback depending on the recognized gesture.	54
Table 3.3: Results of the Multifactorial additive ANOVA assessing the impact of the three independent variables (type of test, test order and individual) on the L2 distances.	62
Table 3.4: Results of the Duncan's Multiple Range Test showing pairwise comparisons and significant differences among the variables.....	63
Table 4.1: Published data regarding the accuracy and temporal information of EMG-driven robots for hand rehabilitation.	66

Contents

Abstract.....	I
Acronyms	III
List of Figures	VII
List of Tables.....	XI
1. Introduction.....	1
1.1. Compendium of publications: thematic consistency.....	2
1.2. Context: biocooperative rehabilitation robotics.....	7
1.2.1. Neuromotor rehabilitation robotics.....	7
1.2.2. Biocooperative control in rehabilitation robotics.....	13
1.2.3. Myoelectric EMG-Driven control	17
1.2.4. Current limitations	21
1.3. Hypothesis and objectives.....	22
1.3.1. Hypothesis.....	22
1.3.2. Objectives.....	24
2. Materials and methods	25
2.1. Robotic rehabilitation platforms	25
2.1.1. RobHand, a Robot for Hand Rehabilitation.....	26
2.1.2. M3Rob, a robot for wrist rehabilitation.....	27

2.2.	Biocooperative controls	28
2.2.1.	Physiological signals	28
2.2.2.	Non-pattern EMG-based controls	29
2.2.3.	Multimodal controls	33
2.3.	Experimental design	34
2.3.1.	Accuracy and responsiveness of the EMG-driven control ..	35
2.3.2.	Influence of the feedback on the user’s performance	36
2.4.	Performance assessment	38
2.4.1.	Classification accuracy	38
2.4.2.	Time delay analysis	40
2.4.3.	Time series similarity measurement	41
2.4.4.	Statistical analysis	42
3.	Results	45
3.1.	Embedded systems for physiological signal acquisition	45
3.1.1.	EMG acquisition system	46
3.1.2.	Multimodal acquisition system	47
3.2.	Biocooperative rehabilitation systems	50
3.2.1.	EMG-driven control for hand robotic rehabilitation	50
3.2.2.	EMG&IMU-based control for upper-limb rehabilitation	55
3.2.3.	Assist-as-needed control for wrist robotic rehabilitation ...	57
3.3.	Performance assessment	60
4.	Discussion	65
4.1.	EMG-driven hand rehabilitation robot	66
4.2.	Influence of visual biofeedback on the users’ performance	67
4.3.	Wearable embedded multimodal acquisition system	69
5.	Conclusions	71
5.1.	Contributions	72
5.2.	Main conclusions	73
5.3.	Future research lines	74

A. Articles included in this Doctoral Thesis	77
A.1. (Cisnal et al., 2021).....	78
A.2. (Cisnal et al., 2023b)	78
A.3. (Cisnal et al., 2023a).....	78
B. About the author	79
B.1. Biography	79
B.2. Publications.....	80
B.2.1. Papers indexed in the JCR.....	80
B.2.2. International conferences.....	82
B.2.2. National conferences	82
B.3. International internship	83
B.4. Participation in Research Projects	84
B.5. Other activities.....	86
C. Resumen en castellano.....	89
C.1. Introducción	89
C.2. Objetivos	91
C.3. Materiales y métodos	92
C.4. Resultados y discusión	94
C.5. Conclusiones	98
Bibliography	101

Chapter 1

1. Introduction

The present Doctoral Thesis is focused on the design and development of biocooperative control strategies for neuromotor rehabilitation robotic platforms. In contrast to traditional rehabilitation robots that only employ biomechanical data, the biocooperative approach has been defined as human-centered scenarios where physiological measurements are also extracted to develop control strategies and enhance the human-robot interaction (HRI). However, the cost of the necessary physiological signal acquisition systems has limited the use of biocooperative systems as real-world solutions. Hence, this research does not only focus on designing and developing biocooperative control algorithms, but also providing affordable technology for physiological data recording. This study has led to the publication of a total of three articles in journals indexed in the Journal Citation Reports (JCR) from Clarivate's Web of Science™ (WOS). These articles were published from October 2021 to April 2023. As a result of the scientific productivity, this thesis takes the form of a compendium of publications.

In the present Doctoral Thesis, the development of biocooperative control strategies in the context of upper-limb rehabilitation therapies for patients with neurological impairments is investigated. More precisely, Chapter 1 presents a comprehensive literature review of all scientific and technical fundamentals embraced in this the Doctoral Thesis. The thematic consistency of the publications is provided in section 1.1. The general context is described in section 1.2, which introduces neuromotor rehabilitation robotics and its clinical importance. Section 1.2.2 is focused on providing the basis of biocooperative controls in the context of neuromotor rehabilitation. Section

1.2.3 is devoted to myoelectric EMG-driven control, including different approaches for its implementation and other clinical applications based on EMG signals. Section 1.3.2 defines the general objectives pursued in this study and enumerates the specific objectives.

Chapter 2 describes the materials and methodology used for performing this study. Main results are shown in chapter 3, which are further discussed in the following chapter. Finally, the contributions of this Doctoral Thesis, as well as the final conclusions and future research are presented in the chapter 5. The last sections are intended to complement this document by including: the papers of the compendium of publications (appendix A), information about the author such the scientific achievements achieved during the Ph.D. (appendix B), and a brief summary in Spanish (appendix C).

1.1. Compendium of publications: thematic consistency

The incidence of cerebrovascular accidents (CVA) has been growing in the past decades as life expectancy is increasing in developed countries. Although stroke mortality has been reduced, the increase of survivors results in a rising number of adults with neurological disabilities. Restoring or improving motor skills is essential so that patients can regain independence and improve their quality of life (QOL) (Tran et al., 2021). Although effective, traditional rehabilitation requires considerable time commitment by the rehabilitation specialist (Frick and Alberts, 2007). Robotic devices that allow patients to undergo rehabilitation without continuous medical assistance would make physical therapy more affordable, increasing the potential for better clinical outcomes (Polygerinos et al., 2015b).

Given the prevalence of cerebrovascular accidents, motor recovery using rehabilitation robotic systems has elicited considerable scientific interest. The active participation of the patient in the rehabilitation enhances neural plasticity and motor learning (Blank et al., 2014). In this way, biocooperative rehabilitation robotic systems, based on multimodal information, promote patients' participation by considering their performance, motion intention and even, emotional state (Riener and Munih, 2010). Despite their potential for neurorehabilitation, the first challenge to rehabilitation robotic platforms is accessibility. The presence of robotic devices in clinics and hospitals is greatly restricted since only large medical centers have the financial resources to invest in this technology (Almekkawy et al., 2020).

In the context of neuromotor rehabilitation using biocooperative robots, a part of the budget is allocated to physiological signal acquisition systems. This

research has tackled this obstacle directly by creating a cost-optimized version of biosignal recording systems, hoping to access clinical settings with more modest budgets. Its design was based on a trade-off between complexity, cost, and performance. It is necessary to provide high resolution and reliable measurements for implementing biocooperative controls in an affordable way without compromising their greatest strengths.

Biocooperative systems use biomechanical and/or physiological information to monitor the patient actions, intention of movement and/or cognitive load. The emotional state of the user is not often integrated in the control loop due to the challenges associated with determining it through indirect measurement of their physiological changes (Katsigiannis and Ramzan, 2018). Motion intention can be detected by analyzing EMG signals, which is the most popular signal for implementing biocooperative controls because of its unique nature: a physiological signal that provides reliable and robust biomechanical information.

Due to the nature of EMG signals, myoelectric EMG-driven assistive robots are widely used in neuromotor rehabilitation (Li et al., 2020; Meattini et al., 2018). In addition, this control strategy considers the user's intention of movement, which encourages the patient to actively participate in the rehabilitation. The active participation has been proven to enhance neural plasticity and motor learning (Blank et al., 2014).

On the other hand, in the first stage of rehabilitation, it is common for the muscular electrical activity of the patient to be too weak to effectively detect their motion intention. The EMG signals can be recorded from the unimpaired limb to assist the motion of the impaired limb using the rehabilitation robot. This approach is known as bilateral myoelectric control and can replace or complement the passive therapies, which are typically performed during the first stage of rehabilitation due to the patient's inability to move the paretic limb.

Clinical studies found that passive training only reduces spasticity, while unilateral EMG-driven therapies also improved muscle coordination (Hu, Tong, Song, Zheng, & Leung, 2009). Furthermore, bilateral therapies have been found to be beneficial in motor recovery since the hemispheric interaction enhances the rebalancing of the abnormal brain activity caused by the stroke (Wu et al., 2021). Even though sEMG biofeedback has been found to be beneficial in neuromotor rehabilitation (Giggins et al., 2013; Tate and Milner, 2010), this technique has not been used in combination with robot-assisted rehabilitation.

This thesis focuses on the development of biocooperative control strategies considering the principles of neurorehabilitation after stroke based on motor

learning and brain plasticity mechanisms. Controls are developed for upper-limb neuromotor rehabilitation due to the high prevalence of stroke in upper-limb paresis, especially affecting the hand (Fischer et al., 2007). Additionally, the limited access of rehabilitation robotic technology due to their high cost is also addressed by developing low-cost systems for physiological signal recording.

The first and second papers were focused on EMG-driven assisted neuromotor rehabilitation using a hand robotic exoskeleton and a custom-made low-cost EMG real-time embedded system, while the last one presented a highly versatile, low-cost, and wearable real-time embedded system for the implementation of multimodal biocooperative controls for upper-limb neuromotor rehabilitation. The first article (Cisnal et al., 2021) focused on the design of a low-cost 2-channel EMG real-time embedded solution and its integration in a hand rehabilitation exoskeleton. A bilateral training paradigm based on a threshold non-pattern recognition EMG-driven control was developed. The bilateral assisted therapy detected hand gestures of the healthy hand and replicated the gesture on the exoskeleton placed on the paretic hand. The evaluation of the performance of the rehabilitation system in terms of accuracy and response times yielded satisfactory results.

After this study, we took a step further by including EMG-based visual feedback on the rehabilitation platform. In the second article (Cisnal et al., 2023b), we assessed the influence of visual biofeedback on user performance. The findings of the study indicated that incorporating EMG-based visual feedback enhanced performance by facilitating users to gain control over the motion of the EMG-driven exoskeleton by visually monitoring their muscles activations. This enabled them to adjust the exerted force and acquire proficiency in self-regulating their EMG responses.

After evaluating the performance and reliability of the embedded EMG acquisition system by integrating it into the hand robotic rehabilitation platform, our aim was to design an affordable solution that could not only record EMG signals but also other physiological signals of interest in the field of biocooperative upper-limb neuromotor rehabilitation. Therefore, a multimodal, low-cost and wearable embedded system was presented in the third paper (Cisnal et al., 2023a). It integrated inertial measurement unit (IMU), electrocardiogram (ECG), electromyographic (EMG), galvanic skin response (GSR) and skin thermometer (SKT). Two neuromotor rehabilitation scenarios were implemented to assess the system performance: (1) an upper-limb rehabilitation VR-based exergame that used motion tracking through EMG and IMU information, and (2) an assist-as-needed (AAN) control for a wrist rehabilitation robot, which considered the user's emotional state based on GSR, ECG and SKT data. The quality of the signals, processing capabilities

and battery life of the system met the requirements of the two rehabilitation scenarios.

The present Doctoral Thesis is organized as a compendium of publications. Hence, it is essential to consult each paper for a comprehensive understanding of this manuscript. The three published articles can be found in Appendix A. Furthermore, the citation of each article along with its abstract are shown below:

RobHand: A Hand Exoskeleton with Real-Time EMG-Driven Embedded Control. Quantifying Hand Gesture Recognition Delays for Bilateral Rehabilitation

A. Císnal, J. Pérez-Turiel, J.C. Fraile, D. Sierra and E. de la Fuente, "RobHand: A Hand Exoskeleton With Real-Time EMG-Driven Embedded Control. Quantifying Hand Gesture Recognition Delays for Bilateral Rehabilitation," in IEEE Access, vol. 9, pp. 137809-137823, 2021, doi: 10.1109/ACCESS.2021.3118281.

Assisted bilateral rehabilitation has been proven to help patients improve their paretic limb ability and promote motor recovery, especially in upper-limbs, after suffering a CVA. Robotic-assisted bilateral rehabilitation based on sEMG-driven control has been previously addressed in other studies to improve hand mobility; however, low-cost embedded solutions for the real-time bio-cooperative control of robotic rehabilitation platforms are lacking. This paper presents the RobHand (Robot for Hand Rehabilitation) system, which is an exoskeleton that supports EMG-driven assisted bilateral by using a custom-made low-cost EMG real-time embedded solution. A threshold non-pattern recognition EMG-driven control for RobHand has been developed, and it detects hand gestures of the healthy hand and replicates the gesture on the exoskeleton placed on the paretic hand. A preliminary study with ten healthy subjects is conducted to evaluate the performance in reliability, tracking accuracy and response time of the proposed EMG-driven control strategy using the EMG real-time embedded solution, and the findings could be extrapolated to stroke patients. A systematic review has been carried out to compare the results of the study, which present a 97% of overall accuracy for the detection of hand gestures and indicate the adequate time responsiveness of the system.

Interaction with a Hand Rehabilitation Exoskeleton in EMG-Driven Bilateral Therapy. Influence of Visual Biofeedback on the Users' Performance

A. Císnal, P. Gordaliza, J. Pérez-Turiel and J.C. Fraile, "Interaction with a Hand Rehabilitation Exoskeleton in EMG-Driven Bilateral Therapy: Influence of

Visual Biofeedback on the Users' Performance," in Sensors, vol. 23, 2048, 2023, doi: 10.3390/s23042048.

The effectiveness of EMG biofeedback with neurorehabilitation robotic platforms has not been previously addressed. The present work evaluates the influence of an EMG-based visual biofeedback on the user performance when performing EMG-driven bilateral exercises with a robotic hand exoskeleton. Eighteen healthy subjects were asked to perform 1-min randomly generated sequences of hand gestures (rest, open and close) in four different conditions resulting from the combination of using or not (1) EMG-based visual biofeedback and (2) kinesthetic feedback from the exoskeleton movement. The user performance in each test was measured by computing similarity between the target gestures and the recognized user gestures using the L2 distance. Statistically significant differences in the subject performance were found in the type of provided feedback (p-value 0.0124). Pairwise comparisons showed that the L2 distance was statistically significantly lower when only EMG-based visual feedback was present (2.89 ± 0.71) than with the presence of the kinesthetic feedback alone (3.43 ± 0.75 , p-value = 0.0412) or the combination of both (3.39 ± 0.70 , p-value = 0.0497). Hence, EMG-based visual feedback enables subjects to increase their control over the movement of the robotic platform by assessing their muscle activation in real time. This type of feedback could benefit patients in learning more quickly how to activate robot functions, increasing their motivation towards rehabilitation.

A Versatile Embedded Platform for the Implementation of Biocooperative Controls in Upper-limb Neuromotor Rehabilitation Scenarios

A. Cisnal, D. Antolínez, J. P. Turiel, J. C. Fraile and E. De La Fuente, "A Versatile Embedded Platform for Implementation of Biocooperative Control in Upper-Limb Neuromotor Rehabilitation Scenarios," in IEEE Access, vol. 11, pp. 35726-35736, 2023, doi: 10.1109/ACCESS.2023.3265898.

Biocooperative control uses both biomechanical and physiological information of the user to achieve a reliable human-robot interaction. In the context of neuromotor rehabilitation, such control can enhance rehabilitation experience and outcomes. However, the high cost and large volume of the commercial systems for physiological signal acquisition are major limitations for the development of such control. We present a highly versatile, low-cost and wearable embedded system that integrates the most commonly used sensors in this field: inertial measurement unit (IMU), electrocardiography (ECG), electromyography (EMG), galvanic skin response (GSR) and skin temperature (SKT) sensors. Additionally, the compact system combines wireless communication for data transmission and a high-efficiency

microcontroller for real-time signal processing and control. We tested the system in two common neuromotor rehabilitation scenarios. The first is an upper-limb rehabilitation VR-based exergame, in which the patient must collect as many coins as possible. Movement recognition of the hand and arm is performed based on EMG and IMU information, respectively. The second is adaptive assistive control that adjusts the level of assistance of a wrist rehabilitation robot according to the physiological state and motor performance of the patient using GSR, ECG and SKT data. The quality of the recorded signals and the processing capacity of the system meet the needs of the two upper-limb rehabilitation applications. The wearable system is highly versatile, open, configurable and low cost, and it could promote the development of real-time biocooperative control for a wide range of neuromotor rehabilitation applications.

1.2. Context: biocooperative rehabilitation robotics

1.2.1. Neuromotor rehabilitation robotics

The World Health Organization (WHO) defined stroke as “*the neurological deficit of cerebrovascular cause that persists beyond 24 hours or is interrupted by death within 24 hours*” (World Health Organization, 1978). A stroke is caused by the death of brain cells due to a restricted blood flow, either by a blockage of the blood supply to a part of the brain by a clot (ischemic stroke) or by the rupture of a cerebral blood vessel (hemorrhagic stroke) (Figure 1.1).

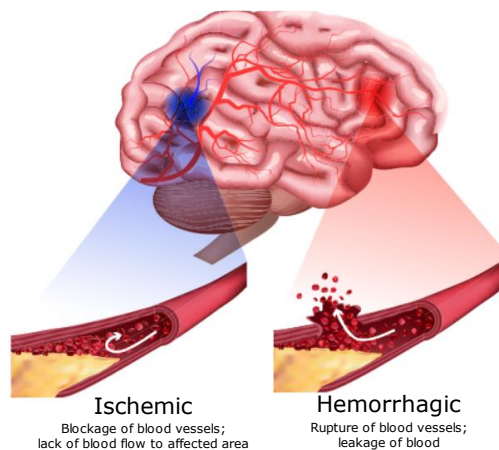


Figure 1.1. Types of strokes: ischemic and hemorrhagic (CNS Traumatic Brain Injury Rehab, 2023).

The brain is an extremely complex organ that controls many vital body functions and different abilities, such as motor and cognitive functions. Therefore, the consequences of a stroke episode depend on the type of stroke and the affected brain area, but can cause lasting brain damage, long-term neuromotor disability, or even death.

In fact, stroke is the second leading cause of death, responsible for approximately 11% of the 55.4 million worldwide deaths recorded in 2019 (World Health Organization, 2020). Additionally, it is one of the leading causes of neurological disabilities, and mainly affects individuals at the peak of their productive life (GBD 2016 Stroke Collaborators, 2019). The rate of disability in stroke survivors is around 64%, with 30% being mildly, 18% moderately, 11% severely and 5% totally disabled (Figure 1.2) (Lv et al., 2021). About 70% of stroke survivors with motor disabilities require long term medical care and live with a poor quality of life (QOL) (Parker and Snyder-Shall, 2013).

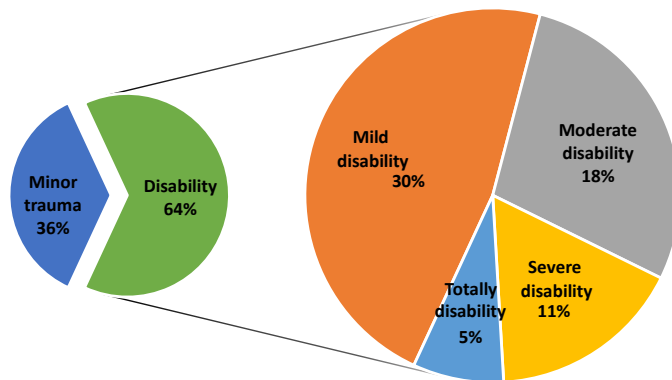


Figure 1.2. Rate of disability in stroke survivors, broken down by degree of disability.

The most common and stable symptom experienced by individuals who have suffered a stroke episode is some degree of their paresis on upper extremities. Around 60% experience upper-limb dysfunction, which are especially prevalent in the hand (Fischer et al., 2007). In fact, motor function of finger extension is usually impaired, and spasticity is often present, leading to reduced range of motion (ROM) of the hand (Kamper et al., 2003). Muscle weakness is also exhibited to varying degrees in most of stroke survivors (Ada et al., 2003; Colebatch and Gandevia, 1989).

Loss of hand function is a major source of impairment in neuromotor disorders, as it is essential for manipulating the environment and thus worsens the abilities of stroke survivors in performing activities of daily living (ADL). Rehabilitation based on physical therapy is the primary mechanism for improving motor function and achievement of independent participation in daily life (Winstein et al., 2016). Early and intensive physical rehabilitation is

of great importance to maximize functional motor recovery (Herpich and Rincon, 2020).

Repetitive task practice (RTP) rehabilitation consists of breaking a ADLs down into individual movements and continuously and intensively practicing them. It has been proved that it promotes hand functional motor recovery, especially leading to improved range of motion and strength (Sterr and Freivogel, 2003). However, RTP rehabilitation costs are very high due to the heavy workload of the rehabilitation specialist (Frick and Alberts, 2007).

Additionally, the aging population is linked to an increase in stroke survivors with neuromotor disabilities and a considerable reduction in the patient-physician ratio. Interest in robotic rehabilitation systems has experienced considerable growth in the last decade not only because of their high costs, but also to increase rehabilitation capacity worldwide and offer adequate rehabilitation to all stroke patients. A system that allows patients to intensively rehabilitate without the continuous assistance of the therapist, would make physical therapy more affordable and accessible.

Clinical studies have shown improvement in hand motor function when performing robot-assisted therapy (RT) (Carmeli et al., 2011; Kutner et al., 2010; Ueki et al., 2008; Wolf et al., 2006). Although the rehabilitation benefits of RT in upper-limb motor recovery of people after stroke is not significantly better than those obtained with conventional rehabilitation, RT offers major advantages in terms of lower manpower cost (Chien et al., 2020; Wu et al., 2021). Furthermore, it improves rehabilitation convenience facilitating independent therapy with the potential outcome of increasing intensity and patient motivation (Kwakkel et al., 2008; Rietman et al., 2014).

Rehabilitation robotic devices can be mainly divided into two categories based on their structural design: exoskeletons and end-effectors (EE). Although clinical results are limited, it has been found that exoskeleton robotic devices provide better rehabilitation outcomes than EE systems in improving hand motor impairments (Moggio et al., 2022).

Upper-limb rehabilitation exoskeletons are more technologically mature when compared to hand exoskeletons due to the anatomical complexity of the hand. The hand has 21 DOFs, while the arm (from wrist to shoulder) has only 7 DoFs. Furthermore, when designing a hand exoskeleton many considerations must be made such as size, weight, dexterous manipulation capabilities, degrees of freedom, joints to directly actuated or which grasp patterns to renounce (Lum et al., 2012).

Some commercially available robotic systems for hand rehabilitation are shown in Figure 1.3, including Saeboflex (Saebob, Inc., NC, USA), the Motus hand (Motus Nova, GA, USA), Hand of Hope (Rehab-Robotics, China), Amadeo

(TyroMotion, Austria), GLOREHA (Idrogenet, Italy) and Waveflex CMP (Remington Medical, Canada) or HandyRehab (Fourier Intelligence, Singapore).

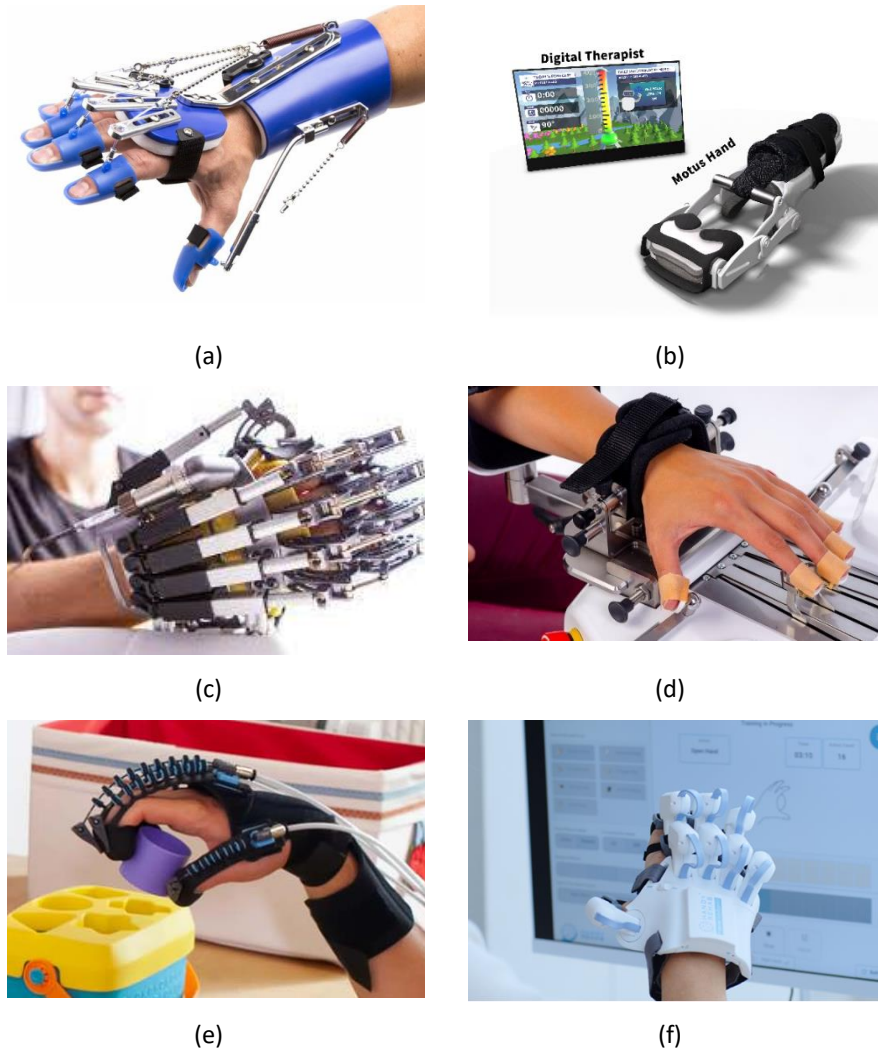


Figure 1.3. Commercially available robots for hand rehabilitation (a) Saeboflex (Saebo, Inc., NC, USA), (b) Motus Hand (Motus Nova, GA, USA), (c) Hand of Hope (Rehab-Robotics, China), (d) Amadeo (TyroMotion, Austria) (e) Gloreha (Idrogenet, Italy), (f) HandyRehab (Fourier Intelligence, Singapore).

In addition to the convenience of RT in terms of cost and intensive rehabilitation, it offers different training paradigms which are used depending on the stroke stage and patient motor function (Kahn et al., 2006). A training paradigm defines the interaction of the rehabilitation robot with the patient, considering their movement intention and applied forces (Yue et al., 2017).

These training paradigms are known as passive, assistive, active-assistive, active, and resistive (Table 1.1).

Table 1.1: Training modalities for rehabilitation robotics, categorized based on the interaction between the rehabilitation robot and the patient.

Training modalities	Patient		Robot
	Intention	Force	Force
Passive	0	0	+++
Assistive	+	+	+
Active-assistive	++	+/0	0/+
Active	++	+	0
Resistive	++	++	-

After suffering a stroke, the person may completely lose mobility of the paretic limb due to muscle spasticity. In the first stage of rehabilitation, passive and active-assistive exercises are optimal since the robot assists the movement of the paretic limb without requiring any motion ability of the patient. Passive therapies have been found to be temporarily effective for reducing hypertonia (Schmit et al., 2000) and for maintaining the ROM of the hand in the early stage of the treatment, but they do not significantly improve motor function (Volpe et al., 2000). Active-assistive exercise were found to be more effective on motor recovery than the passive control since an active engagement of the patient is required (Blank et al., 2014).

In the second stage of the stroke, active and assistive exercises are normally used when the patient has motion capabilities. The robot provides assisting forces to support the patient in completing the desired movement. In the later period of stroke, resistive exercises are used to increase muscle force because the user must complete the motion against a resistive force exerted by the robot (Fasoli et al., 2003).

Evidence has shown that the active participation of the patient induces neural plasticity in motor learning. Hence, robotic systems should monitor the patient's intention and promote patient participation to optimize the therapy outcomes. This can be achieved by providing adaptive exercises or assistance based on the patient motion intent. Assist-as-needed algorithms are based on providing the minimum necessary motion assistance, so the patient can complete a movement, thus requiring significant motion from the patient. In the case of severely impaired patients who are unable to move the limb, active-assistive exercises based on intention detection recognition encourages them to make an effort to move their paretic limb (Blank et al., 2014).

User motion and motor intention are normally detected by measuring position or contact forces. Additionally, motor intention can also be detected

from brain cortical activity by analyzing EEG signals and from the muscles by measuring their electrical activity or EMG signals. The electrical activity can be detected from the paretic hand or the contralateral healthy hand (Yue et al., 2017). In fact, using the electrical activity from the unimpaired side to identify user intention is recommended in the case of patients with severe hand paresis or insufficient muscle tone (Tran et al., 2021). This approach is known as bilateral-assisted therapy.

The robotic device provides motion assistance by referring to detected or intended movement of an unimpaired counterpart. Some studies suggest that bilateral therapies are potentially more effective than unilateral exercise in upper-limb rehabilitation. Motor recovery of bilateral therapies is based on the hemispheric interaction. It increases the excitability of the motor complex and supplementary motor area, resulting in rebalancing the abnormal interhemispheric activities caused by stroke. Additionally, bilateral exercises improve inter-limb coordination (Wu et al., 2021).

One of the primary challenges of neuromotor rehabilitation is maintaining motivation over long periods of time required for significant and lasting functional improvement. RT allows for the integration of virtual reality (VR) environments into the rehabilitation process. Within virtual reality-based rehabilitation (VRBR), three key concepts play a vital role in motor learning: repetition, feedback, and motivation. By offering repetitive practice, augmented feedback, and motivation to endure practice, VR serves as a powerful tool to enhance motor learning and induce cortical and subcortical changes associated with skilled tasks (Holden, 2005).

VRBR offers patients the opportunity to benefit from the robotic rehabilitation experience via serious games. Stroke patients have been shown improved emotional responses to VRBR (Cisnal et al., 2022b). It provides motivation for post-stroke patients (Reinkensmeyer and Housman, 2007), potentially increasing rehabilitation intensity and consequently, promoting motor recovery (Corbetta et al., 2015). Ideally, stroke rehabilitation games should be based on ADLs, while ensuring active patient participation (Sveistrup, 2004). Additionally, incorporating multisensory feedback enhances connectivity between sensory and motor cortices, further promoting motor learning (Maier et al., 2019).

The feedback of serious games such as the score, provides understandable indicators of the patient's performance and stimulates the learning process. Reinforcement learning is one of the most powerful ways of learning new skills. This stimulation of the learning process is based on the release of dopamine in the key areas of the brain. It leads to an improved consolidation of the long-term motor memory and in strengthening the motivation (Bo Nielsen et al., 2015). Hence, providing a rate of recovery feedback encourage

the patient to perform better next session. In general, the use of VRBR has been found beneficial for stroke patients (Subramanian et al., 2013)

1.2.2. Biocooperative control in rehabilitation robotics

The concept of biocooperative control emerged in the field of medical robotics, specifically in rehabilitation robotics during the early years of the 21st century. One of the first formal appearances of the term "biocooperative control" was in a special section of the IEEE Transaction on Neural Systems and Rehabilitation Engineering in 2010, where the basis of biocooperative systems was outlined and formally defined as those that introduced physiological or psychological information into the control loop (Riener and Muih, 2010).

The first rehabilitation robots were based on an open-loop control with fixed position and/or velocity references to execute a predefined trajectory to assist in the patient movement. This technique did not involve either biomechanical or phyco-physiological information. Consequently, these systems were unable to respond to a patient's voluntary effort or spontaneous intentions and an efficient human-machine interaction was practically impossible. In the first decade of this century, rehabilitation robots appeared that employed biomechanical data, such as position, velocity, acceleration, and force to establish robust and adaptive controls. The main goal was to achieve safe, ergonomically acceptable, and user-cooperative systems by controlling the biomechanical interaction between the robot and the patient. This new approach no longer considers the patient as a disturbance applied directly to the robotic system and provides a bidirectional interaction between the robot and the patient enhancing the rehabilitation experience (Koenig et al., 2011).

The biocooperative approach in rehabilitation robotics goes one step further and integrates the patient into the feedback loop by not only considering biomechanical information, but also including psychological and/or physiological measurements. Hence, the appearance of biocooperative controls has led to the emergence of a new generation of rehabilitation robotic platforms, which records and control the patient's physiological signals. They are usually based on multimodal interfaces; information coming from different sources allows for continuously monitoring the patient global status including their actions, intention of movement, emotional state, and even environmental factors. Figure 1.4 shows a generic diagram of biocooperative robotic systems, specifying the integration of the human into the loop in a biomechanical, physiological, and psychological sense.

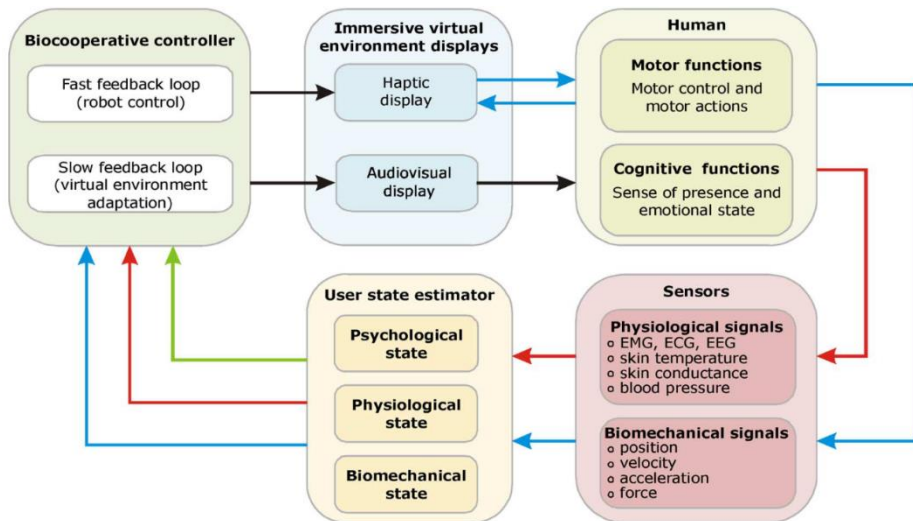


Figure 1.4. Generic diagram of biocooperative robotic systems, specifying integration of the human into the loop in a biomechanical, physiological, and psychological sense (Riener and Muni, 2010).

Emotions are associated with physiological changes produced in response to the autonomic nervous system (ANS). Facial expressions, breathing pattern, heart rate or muscle tension changes are influenced by emotions. Physiological measurements such as cardiovascular parameters, temperature, electrodermal activity, blood oxygenation, photoplethysmography and electromyography have been used to indirectly measure ANS-related responses to external stimuli and hence, determine the emotional state of the person. Although other biomarkers such as cortisol levels or neural changes revealed by neuroimaging can also reveal useful information regarding the emotional state (Jerath and Beveridge, 2020), they are potentially invasive and inconvenient for rehabilitation robotics.

In this field, a diverse number of non-invasive biological signals such as EMG, EEG, EOG, RESP, GSR, SKT and BP are commonly employed to extract valuable physiological information from the user. Signal processing techniques are applied to extract specific features from these signals that are known to exhibit correlations with the user's physiological state. For instance, parameters such as heart rate (HR) and heart rate variability (HRV) derived from ECG signals, and the skin conductance level (SCL) and the frequency of the skin conductance response (SCR) derived from GSR signals, serve as indicators of arousal, physical effort, and mental workload. Consequently, these biosignals allow to determine the cognitive load and physiological response of the user to the rehabilitation session. Additionally, physiological signals can also be used to detect the user intention through non-invasive brain-computers interfaces (BCIs) based on EEG and non-cortical interfaces

based on EOG or EMG, specifically in the case of patients with severe impairments who are able to generate muscle activation or brain activity instead of force for movement (Simonetti et al., 2016).

Table 1.2 shows a summary of biocooperative controls in the context of neurorehabilitation proposed in the literature. In healthy individuals, motor intention is conducted from the brain to the muscle to directly move the limb. However, this natural pathway is damaged in stroke patients and motion intention is detected based on brain or muscle activity or even, eye movement in order for the robot to actuate the motion of the impaired limb. Hence, motion intention recognition (MR in Table 1.2) based on EEG, EMG or EOG is a common approach in biocooperative robots.

Assist-as-needed (AAN) control is widely used in rehabilitation robotics since personalized difficulty has been proved to lead to superior learning outcomes when compared to a fixed difficulty. The difficulty should be adapted to the patient's capabilities without surpassing them as this could have detrimental effects on performance. The adaptive nature of tasks' complexity increases activity in premotor and sensorimotor areas and has beneficial effects on motor recovery (Maier et al., 2019). In this context, an AAN control architecture based solely on myoelectric information from the muscles (EMG-ANN in Table 1.2) has been proposed. Biomechanical information of the user typically extracted from position or force sensors is replaced by information based on EMG signals, such as the user's applied torque, to adapt the assistance level of the rehabilitation robot.

More complex AAN architectures in terms of the number of physiological signal modalities have also been proposed in the literature (BIO-AAN in Table 1.2). The level of assistance or task difficulty is adapted according to the user performance, muscle fatigue or emotional state. While user performance is normally determined by biomechanical variables, muscle fatigue is determined by analyzing EMG signals. The emotional response of the user, including the level of arousal, valence, or stress, is also included in the control loop.

Other works have mainly focused on the emotional estimation (ES in Table 1.2) using multimodal information. The development of emotion recognition algorithms, also known as affective computing, is still a major challenge. Efficient and robust affective computing would significantly increase the quality of human-machine interaction, not only in the context of neuromotor rehabilitation, but also in other fields ranging from preventive medicine to the multimedia industry (Katsigiannis and Ramzan, 2018). Physiological parameters such as HR, SKT, electrodermal activity (EDA), and respiration rate (RR) are known to be associated with autonomic responses related to emotions and are therefore often employed as inputs for emotion classifiers.

Table 1.2: Literature review on biocooperative systems, indicating the control type and the employed physiological signals.

Ref	Type	E O G	E E G	E C G	E M G	IMU/ ACC	G S R	S K T	RESP	B V P	Other
(Zhang et al., 2019)	MR	X	X		X						
(Krasoulis et al., 2019)	MR				X	X					
(Landgraf et al., 2018)	MR				X						x ¹
(Fougner et al., 2011)	MR				X	X					
(Teramae et al., 2018)	EMG-AAN				X						
(Gui et al., 2020)	EMG-AAN				X						
(Cisnal et al., 2019)	EMG-AAN				X						
(Scotto Di Luzio et al., 2018)	BIO-AAN				X	X					
(Novak et al., 2011)	BIO-AAN			X			X	X	X		
(Mihelj et al., 2009)	BIO-AAN						X	X	X		
(Guerrero et al., 2013)	BIO-AAN										
(Badesa et al., 2014)	AAN						X	X	X		
(Gümüslü et al., 2020)	ES		X				X	X			X
(Khezri et al., 2015)	ES	X		X	X		X				X
(Hariharan and Adam, 2015)	ES		X				X				
(Koelstra et al., 2012)	ES	X	X		X		X	X	X		
(Kim and André, 2008)	ES			X	X		X		X		
(Mandryk and Atkins, 2007)	ES			X	X		X				
(Liu et al., 2008)	ES			X	X		X	X			X ²
(Picard et al., 2001)	ES				X		X		X		X
(Zhai et al., 2005)	ES	X					X				X

¹DES (Dielectric Elastomer Sensor) ²Bioimpedance, heart sound and PPG (photoplethysmogram).

Biocooperative controls allow the implementation of more advanced and personalized AAN control paradigms than the traditional ones that only rely on user performance based on biomechanical information. These controls also employ other physiological signals to consider other variables, such as cognitive load, physiological state or even muscle fatigue. This is of great importance since negative emotions such as anxiety, frustration or stress can have a large impact on motor learning. Despite the proven benefits of personalized adaptive controls in facilitating motor recovery, the advancement of biocooperative controls has been hindered by a sluggish pace of progress. This may be due to the complexity of developing robust and efficient algorithms that analyze the physiological response of the human body to a stimulus triggered by the ANS and determine emotions, combined with the high cost and bulky physiological signal recording systems.

Most of the reviewed studies relied on expensive, bulky and lacking computational capabilities commercial products such as the MP150 system (BIOPAC, CA, USA), the Neuroscan NuAmps Express system (Compumedics Ltd., Australia), the ActiveTwo system (Biosemi, Netherlands), and the ProComp/FlexComp Infiniti system (Thought Technology Ltd., Canada). Only a few studies utilized specific wearable technology from Biometrics Ltd (UK), g.tec medical engineering GmbH (Austria), or Delsys Incorporated (MA, USA).

1.2.3. Myoelectric EMG-Driven control

Electromyography (EMG), sometimes referred to as myoelectric activity, is a technique that focused on the development, recording and analysis of the information present in the electric potential generated by the motor units. Motor units are the smallest functional units that describe the neural control of the muscular contraction process when the muscle is activated (Konrad, 2005).

EMG is classified into intramuscular and surface EMG (sEMG). While intramuscular EMG uses tiny needles or fine-wires that are inserted into the muscle through the skin, sEMG uses surface electrodes. sEMG signals represent the electrically superimposed motor unit action potentials (MUAP) of all active motor units detectable under the electrode site (Figure 1.5). The main advantages of sEMG are that it is non-invasive, easy to record, and allows for estimation of the overall muscle activity. The disadvantage of sEMG compared to intramuscular EMG is that it is only suitable for recording superficial muscles and may experience possible contamination with nearby muscles, especially when recording small muscles. In contrast, intramuscular EMG is selective and enables recording of deep muscle activity (McManus et al., 2020).

Although sEMG signals are often considered more complex to analyze than intramuscular EMG, they tend to be used in rehabilitation medicine applications due to their non-invasive nature. Additionally, their analysis provides a global measurement of the level of muscle activity, which may be more appropriate in movement analysis.

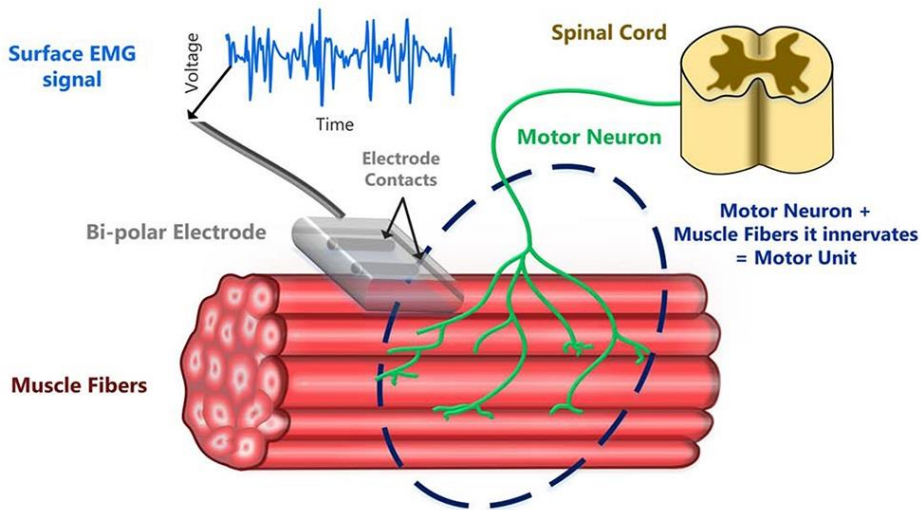


Figure 1.5. EMG signal recording using a surface electrode, including a motor unit and muscle fibers (McManus et al., 2020).

In fact, sEMG has been regarded as the most suitable physiological signal for implementing biocooperative controls due to their good accuracy and robustness in predicting the intention of human motion (Li et al., 2020). Analyzing sEMG signals from the target muscles is widely used as an alternative strategy for integrating force sensors into the rehabilitation robot for motion control. Force sensors have intrinsic problems such as their placement that can obstruct the sense of feeling, or it cannot be distinguished between user-applied and external forces. Robotic control systems based on EMG signals are the most popular approach in rehabilitation robotics (Meattini et al., 2018).

EMG-based motion intention recognition can be broadly categorized as classification and regression problems. While classification-based myoelectric control detects the type of movement, regression-based control can output continuous variables such as joint angle and joint torque. Therefore, the first strategy enables discrete motion control and is limited to a specific number of motions, whereas the latter allows for continuous motion control, resembling the continuous movement of the human body (Bi et al., 2019). Despite this fact, classification-based myoelectric controls are still the most widely implemented due to their reliable results. In both approaches, the kinematics

parameters estimated from the analysis of the EMG signals are fed into the robot control, causing it to behave according to the human intention (see Figure 1.6).

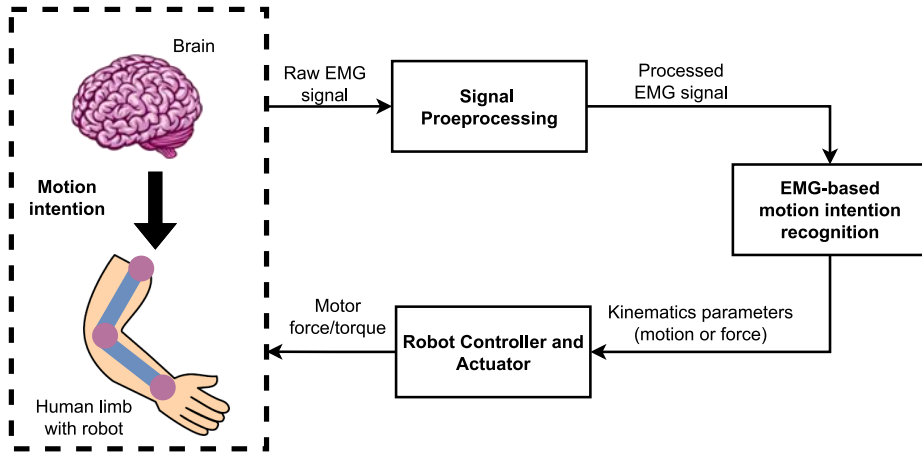


Figure 1.6. Conceptual block diagram for myoelectric control system.

Regarding to discrete motion control, it can be classified into non-pattern recognition and pattern recognition methods. Non-pattern recognition methods, also known as threshold methods, generates the input commands for the robot's assistance controller by comparing the amplitude or statistical features of EMG signals with some thresholds. Pattern recognition methods detect the type of movement using classification machine learning models, such as: support vector machines (SVM), artificial neural networks (ANN), linear discriminant analysis (LDA), among others. The classification results are used as an input of the robot controller. Non-pattern recognition based myoelectric control methods have the lowest computational cost (Fu et al., 2022).

In contrast, the continuous motion control outputs variables such as joint angle or joint torque from the analysis of EMG signals. The use of a biomechanical model and machine learning (ML) models are the main methods for mapping the EMG signals to the continuous control input. The most widely used biomechanical model is Hill's Muscle Model, which represents the human skeletal muscle with a 3-element system: a contractile element and two non-linear spring elements, one in series and another in parallel (Figure 1.7) (Battista et al., 2017). On the other hand, time-domain or statistical features extracted from the EMG signals are often used as an input of regression models, such as linear regression or ANN, to estimate joint angle or applied torque (Fu et al., 2022). However, ML-based systems have not been implemented in real applications mainly because of reliability issues (Meattini et al., 2018).

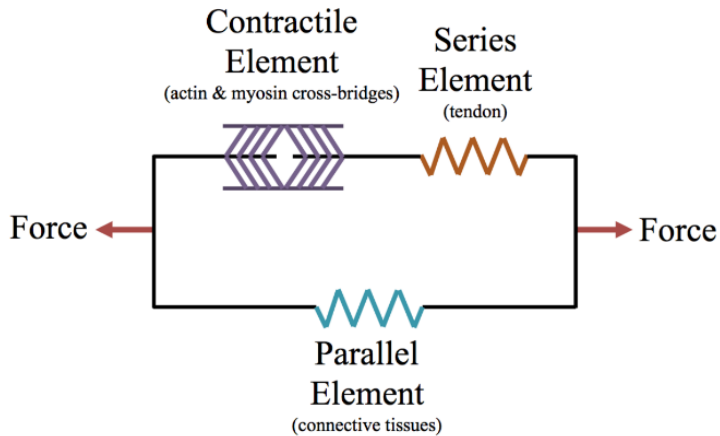


Figure 1.7. Schematic diagram of the 3-element Hill model of the human skeletal muscle: a contractile element, series element, and parallel element modelling acting and myosin cross-bridges, tendons, and connective tissues, respectively (Battista et al., 2017).

The potential applications of myoelectric control extend beyond motor recovery in rehabilitation; they also include assistance in ADL and human augmentation to enhance physical capacities of healthy population (Fu et al., 2022). In the case of rehabilitation robotics, the choice of the type of EMG control must not only consider the DoFs of the assistive device, but also user-acceptance in terms of number of electrodes and the system response. For instance, a high number of electrodes allows the implementation of an accurate continuous EMG control at the cost of poorer usability and a higher computational cost, which may be reflected in the system response. In their review (Fu et al., 2022), Fu et al. found out that 42% of the articles focused on controlling only one DoF, while 15%, 3%, 13 % and 15 % of the studied articles integrated two, three, four and more than four DoFs, respectively.

Clinical studies have been undertaken to evaluate the effectiveness of EMG-driven therapies in stroke patients. They found that while passive training mainly reduced spasticity, EMG-driven therapies also improved muscle coordination (Hu et al., 2009). However, some stroke patients exhibit sEMG signals that are excessively weak to effectively detect their motion intention. In such cases, a popular strategy is the implementation of bilateral myoelectric control, which consist of estimating the motion intention using EMG signals recorded from an unimpaired limb to rehabilitate the impaired limb with the assistance of a robotic device.

Moreover, sEMG can serve as an indirect measure to identify changes in muscle force during isometric muscle contractions, making it a potential tool for assessing muscle fatigue objectively. It can be also used as real-time

feedback to make patients more aware of their muscle activity and support re-learning of movement patterns. The amplitude of the sEMG signals can be fed back to the user to provide an objective measure of the level of muscle activation (McManus et al., 2020). Biofeedback has been generally delivered using visual displays or acoustic signals.

The biofeedback technique was introduced more than forty years ago in rehabilitation settings (Tate and Milner, 2010). sEMG biofeedback has been found to be beneficial in the treatment of many musculoskeletal conditions, including stroke rehabilitation, pelvic floor muscle dysfunction, and even in alleviating pain caused by muscular tension (Giggins et al., 2013). EMG biofeedback allows users to learn to self-regulate their muscle activity and facilitate the process of strengthening weak or paretic muscles and reducing tone in spastic muscles. However, clinical studies that had assessed the effectiveness of EMG biofeedback in musculoskeletal and neuromotor rehabilitation did not include the use of this technique in combination with RT.

1.2.4. Current limitations

The concept of utilizing robotic devices for neurorehabilitation was initially introduced by Hogan at MIT (Hogan et al., 1992). Despite the gradual introduction of traditional rehabilitation robots into clinical settings, the current level of development of biocooperative rehabilitation robots is insufficient to transition them from laboratory settings to practical real-world applications. While biocooperative controls promoting active participation that has been proven to enhance neural plasticity and motor (Blank et al., 2014), their high cost does not provide sufficient incentives for extensive investigation, hindering their current application and commercialization. Therefore, in order to advance the research and facilitate the utilization of biocooperative systems in clinical environments, it is necessary to address, at minimum, the following primary limitations:

I. Hardware

Recent research emphasizes the importance of compact, affordable sensing devices with advanced computational capabilities for detecting human physical activity and emotions through multimodal fusion strategies (Qiu et al., 2022). Despite the decreasing cost of computing and the emergence of real-time control support through embedded solutions (Harwin et al., 2006), biocooperative systems still rely on expensive, computationally limited, and occasionally bulky commercially available acquisition systems (Cisnal et al., 2023a), which impacts on accessibility and user acceptance.

II. Reliability

Biocooperative controls currently lack the required reliability and robustness to be effectively implemented in real-world scenarios. This includes the specific control method based on EMG signals, which, despite being widely utilized in the field of neuromotor rehabilitation robotics due to their accurate and robust prediction of motion intentions (Li et al., 2020), have not been successfully applied in clinical practice due to reliability concerns (Meattini et al., 2018).

1.3. Hypothesis and objectives

The pursuit of developing cost-effective and reliable biocooperative systems for neuromotor rehabilitation, with the aim of improving the quality of life for individuals with motor disabilities, has emerged as a significant concern in recent years. Consequently, the proposal developed in this Doctoral Thesis have been directed towards the creation of low-cost embedded systems for physiological data acquisition and the implementation reliable control paradigms. The primary objective of these systems is to enhance the accessibility and integration of biocooperative technologies into real clinical practices. To provide a comprehensive framework for this thesis, the hypotheses that have served as the basis for each study, as well as the overarching hypothesis that justifies the present Doctoral Thesis, are explicitly declared in section 1.3.1. Additionally, section 1.3.2. outlines the principal objective and the specific sub-objectives that must be fulfilled in order to accomplish this overarching goal.

1.3.1. Hypothesis

Despite the increasing interest in biocooperative systems for neuromotor rehabilitation in scientific literature, their current limitations have confined their application primarily to laboratory settings. As a result, studies often overlook their potential utilization in real-world scenarios and focus solely on academic purposes. Thus, a naïve hypothesis can be formulated: *limitations of current biocooperative control systems that restrict their application outside laboratory settings can be mitigate*. However, while this statement serves as a starting point, it is not comprehensive enough to address a specific research question. Therefore, further exploration and examination of lower-level hypotheses are necessary to advance toward this goal.

As stated in subsection 1.2.4, current biocooperative systems encounter two primary limitations: (I) hardware, and (2) reliability. Regarding to the hardware limitations (I) improving user acceptance requires a compact set of appropriately positioned sensors, thereby necessitating size reduction, even if it imposes limitations on battery capacity (Qiu et al., 2022). Additionally, the development of integrated multimodal approaches is crucial for user-centric systems in rehabilitation applications, fostering engagement within the user community (Rodgers et al., 2019). Real-time embedded systems play a vital role in reducing system response time, as lengthy delays can have detrimental effects, such as decreased task completion accuracy, reduced perceptual sensitivity, and increased task error rates, all of which can negatively impact user acceptance and satisfaction (Yang and Dorneich, 2015).

By developing small multimodal platforms with high computational capacities, user acceptance can be improved in terms of comfort and faster system response. Furthermore, the creation of affordable and versatile platforms that support real-time multimodal controls would encourage further research in the field of biocooperative controls. With improved accessibility to this technology and continued research, it would be possible for researchers to effectively translate biocooperative control strategies that rely on physiological signals into practical and affordable real-world solutions.

The limitation of reliability (II) largely arises as a result of hardware limitations. By enhancing accessibility, research can be increased, leading to the development of robust and effective controls that can be implemented in the clinical setting. Moreover, when considering the specific case of myoelectric EMG-driven controls, which are the most common in the field of robotic rehabilitation, their implemented in real-world applications is not viable due to reliability issues (Meattini et al., 2018). Although various sEMG-based pattern recognition methods have shown promising results, their practical application is limited due to the need for a large number of DoFs in the robot and the associated high computational costs, making them unsuitable for real-time embedded systems.

The development of EMG-driven control systems should focus on providing controls that can be integrated into existing robotic platforms with a limited number of DoFs. This approach reduces the number of electrodes, improving both user and clinician acceptance by reducing the time required for electrode attachment. Moreover, a lower number of DoFs and restricted movements contribute to increased system reliability, robustness, and decreased computational costs, resulting in appropriate response times. Collectively, these factors enhance user acceptance. These statements form the core of the present Doctoral Thesis, and they can be combined into the following:

Biocooperative system may be oriented toward a real use outside laboratory by developing cost-effective, real-time, embedded physiological data acquisition systems, which promote further research in developing reliable and robust controls.

1.3.2. Objectives

The overall goal of this Doctoral Thesis was to design, develop and evaluate biocooperative control strategies in the context of upper-limb neuromotor rehabilitation, and to provide affordable technology for their implementation in an attempt towards widespread use in clinical settings. This general objective involved the design and development of embedded systems for physiological signal acquisitions and its integration in neuromotor rehabilitation systems by implementing and evaluating assistive control strategies. In order to achieve this general objective, the following specific objectives arise:

- I. Conduct a comprehensive literature review and examine the current state-of-the-art in upper-limb neuromotor rehabilitation platforms, with particular emphasis on control strategies that integrate the human element into the control loop through the analysis of physiological signals.
- II. Design and development affordable embedded systems for physiological signal recording and data processing for real-time execution of the control paradigm of the rehabilitation systems.
- III. Design and development of biocooperative control strategies for the developed real-time embedded solutions and their integration into pre-existing rehabilitation platforms.
- IV. Perform a comprehensive evaluation of the performance of the proposed biocooperative rehabilitation systems, including the assessment of control accuracy, time response, and user performance.
- V. Evaluation of the performance of the wearable multimodal embedded acquisition system, focusing on its versatility, power consumption and reliability of the recorded signals for the implementation of biocooperative controls.
- VI. To disseminate the results of this study in JCR indexed journals, as well as, in national and international conferences.

Chapter 2

2. Materials and methods

This chapter describes the materials and methods that have been applied throughout the compendium of publications. Section 2.1 details the robotic platforms used within the scope of this study. Section 2.2 is dedicated to a comprehensive review of the relevant literature pertaining to biocooperative controls. Afterwards, section 2.3 focuses on the experimental designs and setups. Finally, section 2.4 offers a description of the applied metrics for performance assessment.

2.1. Robotic rehabilitation platforms

Two robotics platforms were used in this Doctoral Thesis: the RobHand and the M3Rob. The RobHand was used in the first (Cisnal et al., 2021) and second articles (Cisnal et al., 2023b), in combination with the designed EMG acquisition system. On the other hand, the M3Rob was employed in the last article (Cisnal et al., 2023a) to assess the performance of the wearable multimodal acquisition system. The electromechanical structures of these robotics platforms offer unique features and capabilities that enable the investigation of different biocooperative controls. In this section, an overview of each platform's specifications is provided to help readers understand the technology behind them.

2.1.1. RobHand, a Robot for Hand Rehabilitation

The RobHand (Robot for Hand Rehabilitation) project aimed to develop a robot for hand rehabilitation for patients with neuromotor disabilities resulting from a cerebrovascular accident. The project was developed in partnership between the TICCYL Digital S.L. enterprise and the ITAP Robotics Research Group at the School of Industrial Engineering of the University of Valladolid. The work was supported by CDTI (Center of Development of Industrial Technology), a Public Business Entity of the Spanish Ministry of Science and Innovation, under project IDI-20170263 with the European Regional Development Fund (ERDF).

RobHand is an exoskeleton-type robot for neuromotor rehabilitation, which assists flexion and extension of the hand fingers (Figure 2.1). It was specifically designed to be lightweight, easy-to-use, cost effective and versatile. Its mechanical design is based on a direct-driven under-actuated serial-bar linkage paradigm. In particular, the mechanical structure is based on a platform located on the back of the hand and five subassemblies, each one associated to one finger. All of them are mounted on the platform except the one for the thumb, which is connect with the platform using a linkage device. The subassemblies are composed of an underactuated linkage-rotate mechanic and a flexible double-ring to transmit the linear force from the actuator to the ring attached to the proximal and medial phalanges (Moreno-San Juan et al., 2021).

Thus, the device is characterized by independent finger motion and has two DoFs for each finger: one active DoF associated with the metacarpophalangeal (MCP) joint and passive DoF associate with the proximal interphalangeal (PIP) joint. The robot provides a ROM of 8° of extension and 62° of flexion in the MCP joint. The exoskeleton incorporates five L12-30-100-6-I linear actuators (Actuonix Motion Devices Inc., Saanichton, BC, Canada). The actuators have a 30 mm stroke, provided up to 23N force and are low-cost, reducing the overall cost of the system and making it more affordable.

Additionally, the flexible-double rings ensure an easy donning and doffing of the exoskeleton even in case of patients suffering from severe hand spasticity. First, the rings are placed on the fingers and then, they are joint to their corresponding the linkage-rotate mechanisms. The exoskeleton is adjusted to the hand by using two Velcro straps. Additionally, the thumb submodule is manually adjustable, providing an easy adaptation to different hand sizes. The system is built in aluminum except from the linkage-rotate mechanisms and the flexibles double-rings, which are 3D printed, resulting in a total weight of 610 g. The system also incorporates a forearm support to compensate the forces created by the exoskeleton weight.



Figure 2.1. The RobHand robotic platform and forearm support for hand rehabilitation (Cisnal et al., 2021).

2.1.2. M3Rob, a robot for wrist rehabilitation

The M3Rob (in Spanish, *Mente-Mano-Muñeca*, Mind-Hand-Wrist-Robot) project aimed to develop a platform for neuromotor and cognitive hand and wrist rehabilitation for people who have suffered a cerebrovascular accident. The project is developed by TICCYL Digital S.L. company, the ITAP Robotics Research Group and the Biomedical Engineering Group, both from the University of Valladolid, and the *Benito Menni* Hospital Center in Valladolid. The project is supported by the Ministry of Science and Innovation of Spain, under grant RTC2019-007350-1.

The rehabilitation robot assists the pronation/supination (PS), flexion/extension (FE), and radial/ulnar (RU) deviation motions of the wrist. It is based on a three serial revolute active joints (3-DoF RRR) mechanism (Figure 2.2). Each rotational joint is powered by one independent brushed DC motor (Maxon Motors, Switzerland) equipped with a 3-channel encoder. Cables are used to transmit the force generated by the motors to the mechanical structure, and thus, assist the wrist motion. The mechanism also incorporates a one passive DoF that allows manual adjustment of the forearm support. A 6-axis torque-force sensor K6D27 50N/1Nm (Me&Systeme, Germany) is embedded in a cylindrical handle. The range of motion of PS, FE and RU joints are 180°, 135° and 110°, respectively (Cisnal et al., 2022a).



Figure 2.2. The M3Rob robotic platform for wrist rehabilitation, which provides assistance of the pronation/supination, flexion/extension, and radial/ulnar deviation motions.

2.2. Biocooperative controls

The first section 2.2.1 describes some physiological signals, which are necessary for the development of biocooperative controls. Subsequently, in section 2.2.2, is focused on reviewing relevant literature on non-pattern recognition-based myoelectric controls. EMG-driven control can be classified into two main types: discrete and continuous control, with the former further categorized into non-pattern (or threshold) methods and pattern recognition methods. Considering our emphasis on developing an embedded control system with intrinsic limited computation capacity and intended for real applications, we have opted to concentrate only on non-pattern recognition controls. Finally, in section 2.2.3, a brief summary of the state of the art on multimodal controls will be presented.

2.2.1. Physiological signals

Based on wide range of physiological signals used in related studies (Table 1.2) and considering both usability and wearability, we decided to only focus on

four sensor technologies from which valuable physiological data can be extracted:

Electromyogram (EMG) provides important information on muscle activation patterns and muscle properties. EMG has the potential to offer an objective and quantitative approach to evaluate not just movement pattern, but also muscle function and local fatigue muscle (McManus et al., 2020). Hence, it can be used for progress assessment and evaluation of the rehabilitation outcomes.

Electrocardiogram (ECG) provides information about the activity of the rate. Several parameters can be extracted, such as HR or HRV. The HR can indicate the body's need for oxygen and provide insights into the physical effort. Additionally, HR and arousal are strongly correlated (Malmstrom et al., 1965). HRV as well as HR has been also used as an indicator of arousal, physical effort and mental workload (Meshkati, 1988).

Galvanic Skin Response (GSR) signal can be divided into tonic and phasic component. The tonic component, also known as SCL, exhibits slow changes over time and is related to skin hydration, dryness, and autonomic regulation, indicating general changes in arousal. On the other hand, the phasic component, referred to as SCR, represents the rapidly changing part of the signal that responds to emotionally stimulating events. SCL is a good indicator for physical workload, while the frequency of SCR increases with arousal and mental workload (Novak et al., 2010).

Peripheral Skin Temperature (SKT) is an effective way to estimate emotional state (Ekman et al., 1983). When the sympathetic nervous system is activated due to stress, it causes vasoconstriction, which reduces peripheral circulation and lowers skin temperature. SKT changes can also indicate significant physical activity as the shunting of blood in the body helps regulate temperature and meet the oxygen demands of organs.

2.2.2. Non-pattern EMG-based controls

Non-pattern EMG-based controls require the comparison of EMG activity between muscles. To achieve this, signal normalization is necessary to mitigate the effects of interferences on the signals, including power line noise, skin perspiration, sensor contact impedance, and crosstalk interference from active muscles (Halaki and Ginn, 2012). These factors contribute to high signal variability, and small differences in electrode placement between sessions can compromise the repeatability of EMG signals (Chowdhury et al., 2013). EMG

processing involves rectifying the raw EMG signal and mapping it into a normalized signal ranging from 0 to 1.

EMG rectification involves converting all negative signal values to positive amplitudes. The average rectified value (AVR), root mean squares (RMS) and signal envelope are commonly used methods for full-wave signal rectification, typically followed by a low-pass filtering (Conforto, 2009). However, while RMS measures the signal power, AVR and envelope do not possess a specific physical meaning (Luca, 2002).

Normalization typically involves using the maximal voluntary contraction (MVC) as a reference value. This approach allows for the comparison of muscle activation patterns within an individual over time. However, it is not suitable for comparing between different individuals, muscles, or tasks. In clinical applications, where patients may not be capable of exerting maximum efforts or repeating certain movements, EMG is often normalized to submaximal contractions or reference voluntary contractions (RVC) as they provide a more reliable indicator of changes in muscular activity (Lehman and McGill, 1999).

Various non-pattern recognition EMG-based controls for hand robot have been previously proposed in the literature. These controls share a similar nature but are referred to differently, such as binary control (Lucas et al., 2016), ON-OFF control (Serpelloni et al., 2016), time-over-threshold control (Polygerinos et al., 2015a), or triggered mode (Chen et al., 2009; Ho et al., 2011).

A binary control was developed to regulate the pressure level of a pneumatic hand exoskeleton (Lucas et al., 2016). The biceps EMG signal was recorded, rectified, smoothed using a Butterworth low-pass filter, and normalized using the MVC. The resulting EMG signal was then used to determine the controller binary output: if the EMG signal exceeded a specified threshold value, the output was set to "on", and if it was below the threshold, the output was set to "off". To avoid output oscillation, a hysteresis mechanism was implemented in the valve triggering system. Initially, the threshold values were set at 55% MVC to activate the "on" state and 45% MVC to initiate the "off" state. However, before each experiment, these threshold values were adjusted to ensure they corresponded to the subject's comfortable level.

A triggered ON-OFF EMG-driven control for the GLOREHA glove was designed to identify three different states, namely hand opening, hand rest and hand closing, with a predefined speed command (Serpelloni et al., 2016). Electrodes were placed on the extensor digitorum (ED) and the extensor carpi radialis to detect muscle activation during hand opening, while the palmaris longus and the flexor carpi ulnaris muscles were used to detect hand closing.

The EMG signals were sampled at a rate of 25 KHz, and a temporal segmentation of 1-second windows with a 99.5% overlap between adjacent windows was employed, resulting in a temporal resolution of 5 ms. Within each window, the signal was rectified using RMS method. The difference between the rectified signals of the extensor and flexor EMG signals was then calculated. This difference, along with two threshold values, was employed to determine the three states (Figure 2.3).

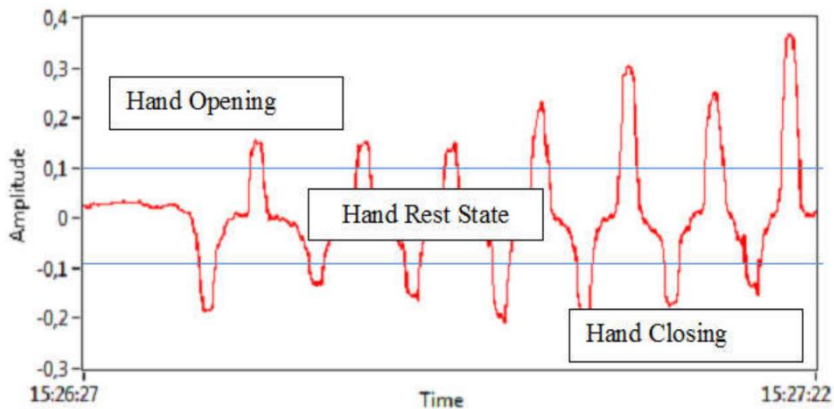


Figure 2.3. EMG differences and thresholds used in the triggered ON-OFF EMG-driven control (Serpelloni et al., 2016).

Another EMG-triggered control utilized two EMG signals obtained from the ED and the abductor pollicis brevis (APB) muscles to detect the intention of hand opening and closing (Chen et al., 2009). The EMG signals were subjected to full-wave rectification and then smoothed by applying a moving average filter with a window size of 100 ms, followed by normalization using the MVC. The hand rehabilitation robot was programmed to initiate movement when the EMG signal exceeded a threshold of 30% of the MVC.

An open-loop time-over-threshold EMG-driven control was designed for a hydraulically actuated soft rehabilitation glove (Polygerinos et al., 2015a). It detected user intention by measuring electromyographic signals from electrodes attached to the forearm, specifically the flexor digitorum superficialis (FDS) and the ED. The control system continuously monitors and compares the FDS and EDC muscle signals to detect predefined conditions: flex, extend, and hold. The flex condition pressurizes the soft actuators, causing the glove to flex along with the fingers, while the extend condition depressurizes the actuators, returning the fingers to the extended position. The hold condition maintains the present fluidic pressure within the actuators. To avoid misinterpretation of involuntary muscle contractions, the conditions require the processed signals to cross predefined thresholds for a specified duration (Figure 2.4). These conditions are manually adjusted.

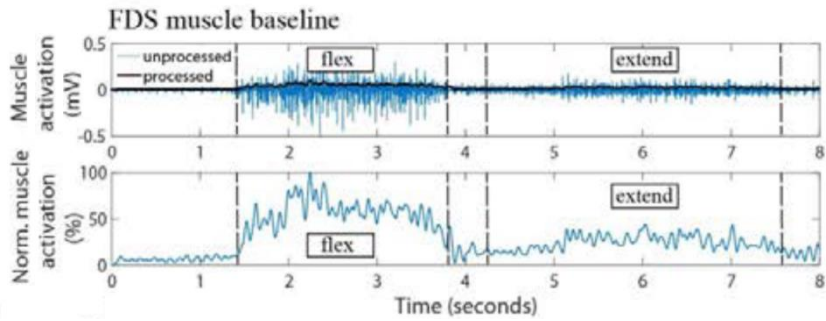


Figure 2.4. EMG signal processing for the FDS muscle in the time-over-threshold EMG-driven control (Polygerinos et al., 2015a).

An EMG-triggered mode strategy was developed to control the Hand of Hope exoskeleton by recording the EMG signals from the APB and ED muscles (Ho et al., 2011). The EMG signals were normalized with respect to the MVC, which was determined at the beginning of each training session. A threshold of 20% of the MVC was employed to initiate hand opening and closing motions. During hand closing triggering mode, the robotic system awaited EMG signals from the APB muscle surpassing 20% MVC before initiating hand closure. Similarly, during hand opening mode, the system awaited EMG signals from the ED muscle exceeding 20% MVC before starting the hand opening action (Figure 2.5).

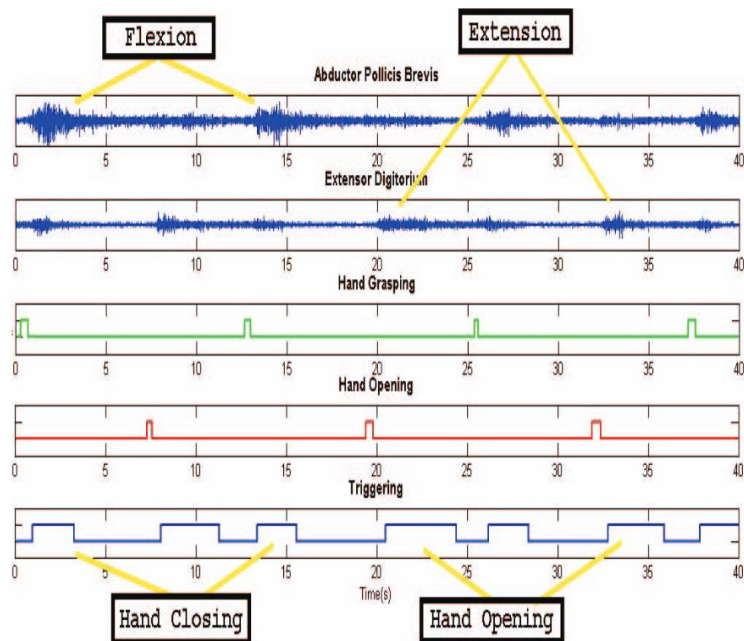


Figure 2.5. Raw EMG signals from the APB and ED muscles and the EMG-triggered status (Ho et al., 2011).

2.2.3. Multimodal controls

Multimodal controls and methods for recognizing emotions through physiological signals have been previously proposed in the literature. One study adapted the level of assistance provided by an upper-limb rehabilitation robot based on the patient's performance and fatigue. Patient performance was determined using biomechanical information from an IMU sensor, while muscular fatigue was estimated using EMG signals (Scotto Di Luzio et al., 2018). Another study adjusted the difficulty of an upper extremity rehabilitation task using biomechanics (force and movement), task performance, and physiological signals, such as ECG, GSR, RESP, and SKT (Novak et al., 2011).

A two-stage fuzzy logic model was used to generate the next action primitives of an upper extremity rehabilitation device (Figure 2.6). The first stage calculated motor performance, arousal, and valence based on position, force, RESP, GSR, and SKT. The second stage selected the action primitives based on physical effort associated with motor performance, arousal, and valence (Mihelj et al., 2009).

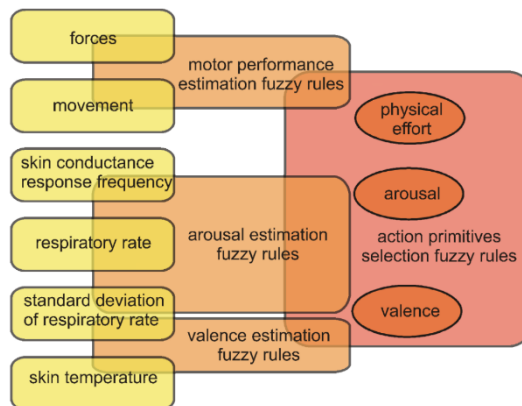


Figure 2.6. Simplified diagram of the two-stage fuzzy logic model for generating action primitives in an upper extremity rehabilitation robot (Mihelj et al., 2009).

Affective and emotional states have also been used to control devices, such as modulating the assistance provided by a haptically controlled robot based on user emotions. Emotions were estimated by a fuzzy logic model that considered the 3-dimensional emotion model (arousal, dominance, and valence) using HR mean, SCL mean, and SCR frequency as inputs (Guerrero et al., 2013). Similarly, arousal and valence have been determined using normalized GSR, HR, and EMG signals as inputs to a fuzzy logic control scheme characterized by 22 rules as shown in Figure 2.7 (Mandryk and Atkins, 2007).

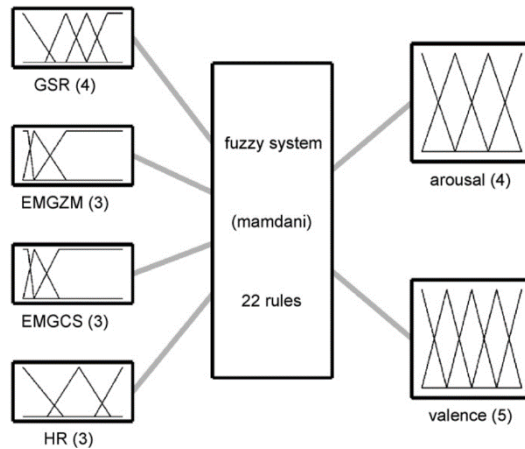


Figure 2.7. Determination of arousal and valence from GSR, EMG and HR information (Mandryk and Atkins, 2007).

Emotion recognition, considering either pleasant, neutral, or unpleasant states, has been addressed using EEG, BVP, SKT, and SCL recordings and developing gradient boosting machines (GBMs) and convolutional neural networks (CNNs) (Gümüslü et al., 2020). Models were developed to recognize six and even eight basic emotions employing various classification methods such as SVM and k-nearest neighbors (KNN) (Khezri et al., 2015; Picard et al., 2001). Detection of basic emotions considering two, three, or four states was also investigated using HR and SCL measurements and employing a Classification and Regression Trees (CART) algorithm (Hariharan and Adam, 2015). Several studies have used physiological signals to map emotions in a two-dimensional model of arousal and valence (Kim and André, 2008; Koelstra et al., 2012).

Affection recognition has been developed considering three target affective states, such as anxiety, engagement, and liking, using SVM-based recognition models with different features derived from physiological signals (Liu et al., 2008). Differentiating of stress and normal states has been carried out using SVM and features derived from BVP, GSR, and PD signals. Finally, a classification method was developed to detect three levels of stress using pulse rate, RESP rate, SKT, and GSR features (Badesa et al., 2014).

2.3. Experimental design

This section details the experimental design employed to investigate the accuracy and responsiveness of EMG-driven control (section 2.3.1) and the impact of the EMG-based visual feedback on user performance (section 2.3.2).

2.3.1. Accuracy and responsiveness of the EMG-driven control

The first study was conducted to evaluate the accuracy and responsiveness of the EMG-driven bilateral assistance with the RobHand exoskeleton (Cisnal et al., 2021). Ten healthy subjects (7 males, 3 females) over 18 years old with no neurological or motor impairment, volunteered for the study and provided written informed consent.

The subjects wore a 5DT Data Glove (5DT Technologies) to measure the actual position of the dominant hand (corresponding to the non-paretic hand of the patient), while the sEMG of the muscles responsible for that hand movement were recorded, and also the recognized hand gesture. The subjects wore the hand exoskeleton on the non-dominant hand (corresponding to the paretic hand of the patient), which replicated the gestures recognized from the sEMG signals analysis (Figure 2.8).

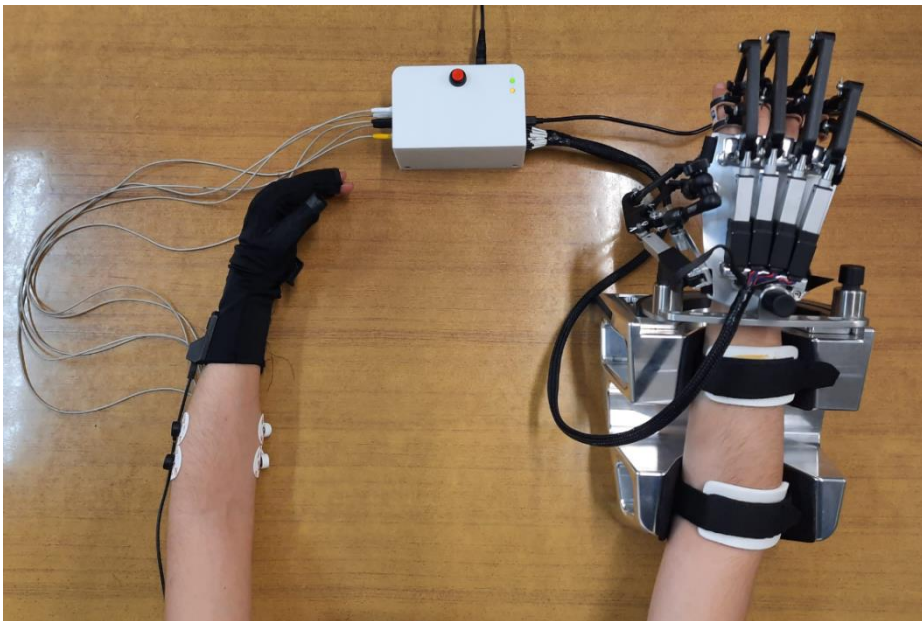


Figure 2.8. The left-handed subject wearing the 5DT Data Glove on the dominant hand and the exoskeleton on the non-dominant hand. The sEMG electrodes are attached to the target muscles of the forearm of the dominant hand (Cisnal et al., 2021).

The subjects were asked to perform an initial calibration followed by ten one-minute tests, with a 5-minute rest between tests to avoid the appearance of muscle fatigue. Each test consisted of performing and maintaining hand gestures (rest, open and close) with the dominant hand. The gesture to be performed was indicated on the computer screen and was randomly generated every 5s.

2.3.2. Influence of the feedback on the user's performance

The second study was conducted to evaluate the influence of the visual EMG-based visual feedback on the subject's performance when performing EMG-driven bilateral therapies with the RobHand exoskeleton (Cisnal et al., 2023). Eighteen subjects (23 ± 3.4 years old) with no neurological or motor impairment volunteered and provided written informed consent.

The subjects wore the hand exoskeleton on the non-dominant hand (in the case of a patient, it would correspond to the paretic hand), while the sEMG signals were recorded from the target muscles of the dominant hand (in the case of a patient, it would correspond to the healthy hand) (Figure 2.9).

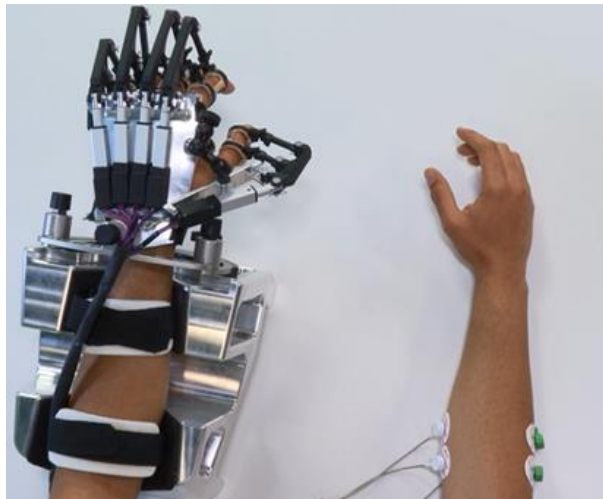


Figure 2.9. The right-handed subject wearing the hand exoskeleton on the non-dominant hand while the sEMG electrodes are attached to the target muscles of the forearm of the dominant hand (Cisnal et al., 2023).

Subjects performed an initial calibration and four one-minute experimental tests (named A, B, C and D) with a three-minute break between tests to avoid muscular fatigue. To avoid the appearance of learning order effect, the four tests were randomly performed. Each test consisted of performing and maintaining a hand gesture (rest, open or close) with the dominant hand. The target gestures were randomly generated every three seconds. Each test was characterized by a different combination of two feedback sources (Table 2.1): kinesthetic and EMG-based visual feedback. While the kinesthetic feedback was provided by the movement of the hand exoskeleton based on the EMG-driven bilateral control, the EMG-based visual feedback was provided by the computer screen.

Table 2.1: Test configuration for evaluating user performance based on the presence of feedback sources, including kinesthetic and EMG-based visual feedback.

	Kinesthetic Feedback	EMG-Based Visual Feedback
Test A	(✓)	(✓)
Test B	(✓)	(x)
Test C	(x)	(✓)
Test D	(x)	(x)

The overall system configuration employed in the experimental protocol is depicted in Figure 2.10. The participant is instructed to execute a specific hand gesture (i.e., open, close, or rest) using their dominant hand, guided by visual and auditory information provided by the computer. Concurrently, the recorded EMG signals are transmitted to the microcontroller for gesture recognition and generation of control signals to actuate the exoskeleton accordingly. The recognized gestures are then transmitted to the PC to update the EMG-based visual feedback. Additionally, both the recognized and target gestures are stored in a SQL database as temporal series for subsequent offline analysis. The provision of EMG-based visual feedback and kinesthetic feedback from the exoskeleton movement is dependent on the specific test being conducted (i.e., test A, B, C, or D).

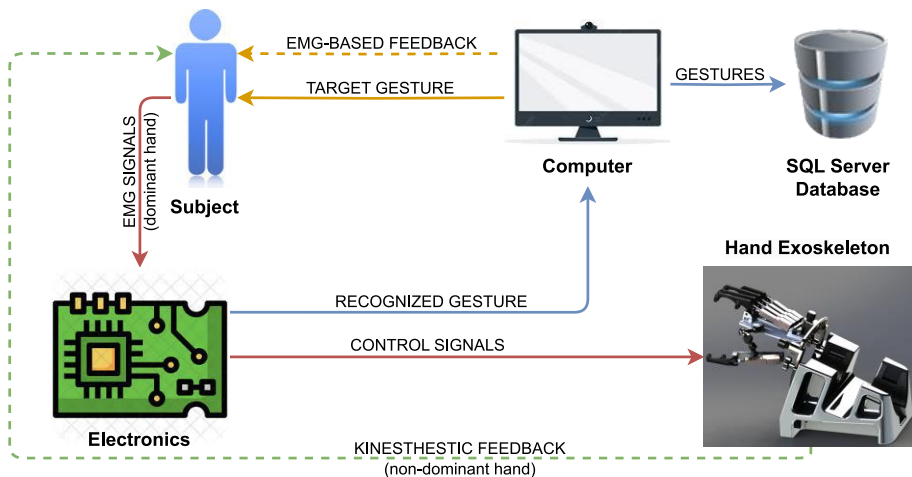


Figure 2.10. Experimental setup diagram, showing the data flow between subsystems: visual information from the computer (yellow lines), EMG and control signals (red lines), data transmission (blue lines), and exoskeleton movement (green lines). The presence of the source of feedback (dotted lines) varies depending on the specific test (Cisnal et al., 2023b).

2.4. Performance assessment

During the different studies that compose the present Doctoral Thesis, performance assessments were carried out to evaluate the real-time control performance of the rehabilitation system based on motion intention recognition. In the specific case of an assistive rehabilitation robot based on gesture recognition, a reliable and natural human-robot interaction requires a combination of a good responsiveness and accurate gesture detection. Large delay times can exert adverse consequences and can negatively influence the user satisfaction towards robot-assisted therapy (Yang and Dorneich, 2015). Likewise, wrongly movement assistance negatively affects satisfaction and can even lead to physical damage. Hence, determining the relevant time delays and gesture classification metrics of the robotic system for an efficient HRI is essential (Cisnal et al., 2021). Additionally, similarity measurements for time series and parametric statistical tests are used to evaluate user performance under different feedback setup conditions when using the EMG-driven hand exoskeleton (Cisnal et al., 2023b).

2.4.1. Classification accuracy

Evaluation metrics play a critical role in evaluating the effectiveness of classification problems. There are two types of classification problems according to the number of classes: binary classification and multi-class classification (Tharwat, 2018). The quality of the classifier can be expressed using a confusion matrix, which is a table that records the number of occurrences between two raters: the rows of the table represent the predicted classes, while the columns show the actual/true classes.

For binary classification, the confusion matrix is shown in Figure 2.11. True Positive (TP) and True Negative (TN) are the number of positive and negative classes that are correctly classified. Meanwhile, the numbers of misclassified negative and positive instances are denoted by False Positive (FP) and False Negative (FN), respectively (Hossin and Sulaiman, 2015).

From the confusion matrix, many metrics for evaluating the classification effectiveness can be calculated (Grandini et al., 2020). Accuracy (Acc) is the most popular classification, although some complement metrics such as precision or recall, are also used to express all the relevant information about the algorithm performance. Accuracy measures how much the algorithm is correctly predicting in the entire set of data by evaluating the percentage of correct predictions over the total number of samples. Accuracy is calculated

using equation (1), which considers the sum of TP and TN elements at the numerator and the sum of all entries at the denominator.

		True/Actual Class	
		Positive (P)	Negative (N)
Predicted Class	True (T)	True Positives (TP)	False Positive (FP)
	False (F)	False Negative (FN)	True Negative (TN)
		P=TP+FN	N=FP+TN

Figure 2.11. Confusion matrix for a binary classification problem. There are two true classes: positive (P) and negative (N). The output of the predicted class is either true (T) or false (F).

$$Accuracy = \frac{TP + TN}{TP + FP + FN + TN} \quad (1)$$

The precision, or positive predictive value (PPV), quantifies the correctly predicted positive classes among the total predicted positive classes. Precision is calculated using equation (2).

$$Precision = \frac{TP}{TP + FP} \quad (2)$$

Recall measures the fraction of positive classes that are correctly classified. It is also known as true positive rate (TPR), and it is calculated using equation (3).

$$Recall = \frac{TP}{TP + FN} \quad (3)$$

The EMG-based gesture recognition control is considered a classification problem since it requires determining one gesture out of three possible gestures (open, close and rest). Hence, the confusion matrix and abovementioned metrics are used to evaluate the performance of the gesture recognition algorithm (Cisnal et al., 2021).

2.4.2. Time delay analysis

The study of responsiveness of the EMG-based rehabilitation system is carried out using the following time-related metrics (Cisnal et al., 2021). Some of them were proposed by Li. et al. in the work in which they quantified the time delay of an EMG-based pattern recognition control of a virtual arm (Li et al., 2010), the rest are proposed in the context of this work.

Motion-selection time (MST) is the time needed by the controller to accurately determine a certain gesture. Hence, MST is calculated as the time interval from the onset of the motion to the instant the controller accurately predicts that motion.

Motion-onset time (MOT) is calculated as the time interval from the onset of the gesture change movement to the instant the assistive robot starts that movement.

Motion-completion time (MCT) is calculated as the time interval from the onset of the gesture change movement to the instant the assistive robot correctly reaches the next gesture.

Motion-completion rate is the percentage of successfully motions, considering that a motion is successful when it is performed within a time limit. The time limit is established based on clinical experience and is 5s to ensure that the movement is not too slow so as not to demotivate or annoy the user.

A time diagram representing the time parameters (MST, MOT and MCT) is shown in Figure 2.12 to enhance comprehension. These time-delay metrics are characterized by events that define their onset and end time: motion onset time of the subject (MO_{Human}), the motion onset time of the assistive robot (MO_{ROBOT}), the motion end time of the assistive robot (ME_{ROBOT}), and the time in which the controller accurately detects the gesture (AGD_{CTRL}).

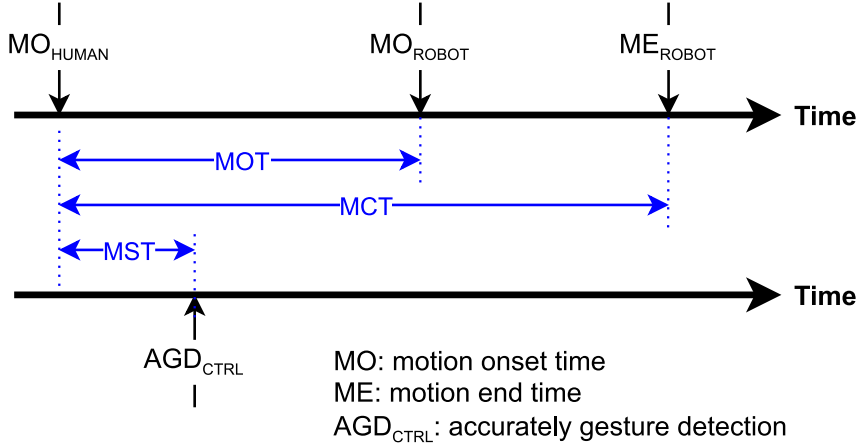


Figure 2.12. Timing diagram showing the time-related metrics: MST, MOT, MCT (Cisnal et al., 2021).

2.4.3. Time series similarity measurement

A similarity measure is mathematically defined as a real-valued function that quantified the similarity between two entities, in this context between two time series. Similarity measures can be divided into lock-step measures that calculate the one-to-one point Lp-norm or distance between two series or using elastic measurements that do not considered a fixed step, such as the Dynamic Time Warping (DTW) or the Longest Common Subsequence (LCSS) (Ding et al., 2008).

Lock-step measures are commonly used since they are relatively straightforward, intuitive and their low linear computational cost. However, since distance is computed from i -th point of one time series to the i -th point of another series, this method is highly sensitive to noise and time misalignments (Ding et al., 2008). Therefore, two time series must be time-synchronized before calculating the distance measurements, since local time shifting can't be handled.

Synchronization of two time series x and y can be performed by calculating the lag at which their cross-correlation (r_{xh}) is the highest. r_{xh} is computed based on equation (4), where h is the lag and $*$ denote the complex conjugate.

$$r_{xy}(h) = \begin{cases} \sum_{n=0}^{N-h-1} x(n+h) \cdot y^*(n), & 0 \leq h \leq N-1 \\ r_{yx}^*(h), & -(N-1) \leq h \leq 0 \end{cases} \quad (4)$$

The most typical examples of distance metrics are the Manhattan distance (L1 norm) and the Euclidean distance (L2 norm). L1 norm is calculated as the sum of the absolute difference of the values of the time series as shown in equation (5), while L2 norm is calculate as the square root of the sum of the square time series values as expressed in equation (6).

$$L_1(x, y) = \sum_{i=0}^{n_{samples}} |x_i - y_i| \quad (5)$$

$$L_2(x, y) = \sqrt{\sum_{i=0}^{n_{samples}} (x_i - y_i)^2} \quad (6)$$

were x_i and y_i are elements of x and y , respectively. The comparison of distance measurements between time series with different durations requires a previous normalization. These metrics can be normalized by multiplying by the sampling period (T_s).

2.4.4. Statistical analysis

Statistical analysis is a powerful tool in scientific research, allowing for fair comparisons of data across multiple groups and provides valuable insights into the relationship between variables. One commonly used method for this type of analysis is Multifactorial additive Analysis of Variance (ANOVA), which enables researchers to assess multiple dependent variables simultaneously. This approach is particularly useful when dealing with more than two independent groups, as it allows researchers to determine whether there is a statistically significant difference between the means of those groups.

The ANOVA is based on testing the null hypothesis that the mean values of all groups are equal. If the null hypothesis is rejected, it means that at least one pair of groups differs significantly on at least one variable, indicating that the independent variable explains a significant amount of variance in the dependent variable. However, ANOVA does not provide information about which group means are significantly different from each other. To uncover specific differences between three or more group means, post hoc tests are used. Post hoc tests, such as Duncan's Multiple Range test, measure specific differences between pairs of means.

Duncan's Multiple Range test is a post hoc test that compares all possible pairs of group means to identify which pairs differ significantly. This test is based on a ranking system that compares the distance between group means with the standard error of the mean. The test identifies significant differences

between groups by dividing the mean square error by the number of degrees of freedom to calculate the standard error of the mean. This standard error is then compared to the difference between the means of each pair of groups. If the difference between the means is greater than the standard error, the two means are significantly different.

The statistical analysis of ANOVA and Duncan's Multiple Range test relies on several important assumptions: normality, homogeneity of variances, and independence. Normality refers to the requirement that the data follows a normal distribution, ensuring that the sample means are normally distributed. Homogeneity of variances implies that the variability among the groups being compared is approximately equal. Independence requires that each observation is independent to the others, meaning that the values of one observation do not influence or depend on the values of other observations.

It is important to note that obtaining reliable and valid results depends on adhering to these assumptions. When the assumption of normality is violated, it can lead to Type I or Type II errors. Type I error occurs when a significant difference is detected between groups when no true difference exists. Type II error occurs when a true difference between groups exists, but it is not detected as statistically significant. Violations of homogeneity of variances assumption can lead to biased estimates of group differences and impact the validity of the statistical tests. Therefore, assessing the assumptions of normality and homogeneity is crucial to ensure the reliability and validity of the results and minimize the potential for Type I and Type II errors.

Overall, statistical analysis, including ANOVA and post hoc analysis, is a crucial tool for making fair comparisons between groups and determining specific differences between means. They allow to identify significant relationships between variables and gain a deeper understanding of the mechanisms underlying their research questions.

In the present Doctoral thesis, we evaluated the influence of EMG-based visual biofeedback on users' performance (Cisnal et al., 2023). Prior conducting the analysis, normality and homogeneity of variances were verified. ANOVA was used for evaluating the effects of independent variables such as the type of test, test order, and individual on user performance. Next, we performed a Duncan's Multiple Range test to evaluate the differences in user performance with the presence or absence of two different types of feedback (EMG-based visual feedback and kinesthetic feedback from the motion exoskeleton) by calculating the difference between pairs of means.

Chapter 3

3. Results

In this chapter, the most relevant results of the Doctoral Thesis are summarized. Section 3.1 introduces the designed embedded solutions for physiological signal acquisition, while section 3.2 elaborates on the development of biocooperative control strategies. The results of the performance assessment are provided in section 3.3.

3.1. Embedded systems for physiological signal acquisition

This section presents the two embedded system for physiological signal acquisition that have been developed. The first one was specially designed for the implementation of rehabilitation therapies based on sEMG signals (Cisnal et al., 2021). The second solution features a wearable design with enhanced versatility, enabling the acquisition of a broader range of physiological signals to facilitate the development of multimodal biocooperative controls (Cisnal et al., 2023a).

The primary objective behind the design and develop embedded electronic systems for physiological signal acquisition is to overcome certain limitations identified in prior studies. Specifically, these include the high cost of such systems, which is a major obstacle to universal access, as well as the use of computers as the data processing platforms, which presumably increases the latency time of the entire rehabilitation platform. As a solution of these challenges, custom-made systems have been developed with the goal of minimizing overall costs. Additionally, these systems incorporate a real-time microcontroller (MCU) for advanced on-board processing.

Both systems are based on the TMS320F28069M MCU (Texas Instruments, Texas, USA), whose Harvard architecture is optimized to perform real-time tasks. The MCU is characterized by a two-core architecture resulting in a large system bandwidth. C28x core and CLA (Control Law Accelerator) execute code independently and interface using a specialized data bus (CLA Bus). The high efficiency 32-bit C28x core runs up to 90 MHz and is also equipped with 256 Kb Flash embedded memory, 100KB of RAM and 2 KB of one-time programmable (OTP) ROM. Additionally, the MCU integrates multiple peripherals such as a 12-bit analog-to-digital converter (ADC) with a sampling rate up to 3.46 MSPS (mega samples per second), serial port communication peripherals (SPI, I2C, UART...), ePWM (enhanced Pulse Width Modulation) modules and timers. Normal current consumption is 245 mA, allowing low-power operating modes.

3.1.1. EMG acquisition system

EMG-driven control strategies are widely used in rehabilitation robotics. Muscular electrical activity resulting from MUAP superposition (raw sEMG signals) can be acquired by surface electrodes and proper conditioning circuits. Therefore, a custom-made application-specific integrated circuit (ASIC) was designed to capture and preprocess the sEMG signals, which are subsequently converted by an ADC for its transmission to the TMS320F28069M MCU, especially dedicated to real-time processing operations.

The 2-channel EMG data acquisition ASIC developed is characterized by a 24-bit resolution differential channels and 112 dB of dynamic range (DR). The channels consist of an instrumentation amplifier of gain 50 followed by an RC low-pass filter with a cutoff frequency of 150 Hz. The channels are designed to compensate differential input offset to prevent the instrumentation amplifier from saturation. Additionally, the ASIC has the MCP3912 (Microchip Technology Inc., AZ, USA) Analog Front End (AFE), which is characterized by synchronous Delta-Sigma ADCs, which interfaces with the TMS320F28069M MCU using SPI communication and other digital control signals.

The 4-layer Printed Circuit Board (PCB) has split ground planes to separate analog, digital, and power circuitries to ensure signal integrity (Figure 3.1, a). Discrete Surface Mounted Device (SMD) components are placed on the top and bottom layers, resulting in a board size of 50.8×33 mm, with an active area of 10 cm² (Figure 3.1, b). The PCB was purposely designed to enable direct fit of the LAUNCHXL-F28069M MCU, thereby eliminating the need for wiring (Figure 3.1, c). The chip consumes 3 mW from 3.3 V DC power supply.

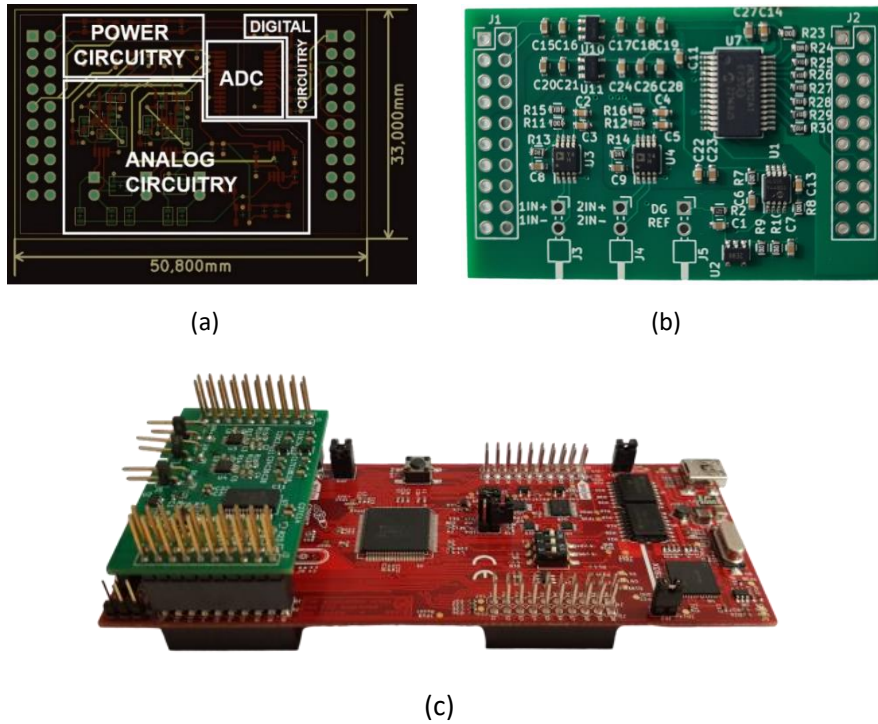


Figure 3.1. EMG acquisition system layout (a) PCB layout (b) final solution (c) board plugged-in the MCU.

The main characteristics of the proposed EMG signal acquisition system are outlined in Table 3.1. The system is powered by a 5 V supply derived from the MCU, despite the admissible power supply ranging from 3 to 12V. Additionally, the Delta-Sigma ADCs are fully configurable, and the configuration details specifically established in this thesis are presented in Table 3.1.

3.1.2. Multimodal acquisition system

The proposed embedded wearable system integrates multiple sensors modalities, high-efficiency real-time MCUs, and wireless communication, providing a highly flexible and capable platform for the development of biocooperative controllers. The system is battery-powered and integrates five sensors (IMU, ECG, EMG, GSR, and SKT), which directly interface with the TMS320F28069M MCU for real-time data processing and control (Figure 3.2). The recorded and processed data can be transmitted by a CC2650 (Texas Instruments, TX, USA) Bluetooth low energy (BLE) MCU. Additionally, a JTAG port allows temporary access to the MCUs.

Table 3.1: Technical specifications of the EMG acquisition system, encompassing general characteristics and configuration parameters of the Delta-Sigma ADCs.

General Characteristics	Values
Supply voltage	3.3-12 V / 5V ^(a)
Supply voltage	5V
Total Current Consumption	0.9 mA
Active area	10 cm ²
Board dimensions	50.8×33 mm
EDS input protection	17 KV
Acquisition channels	2 ch.
ΔΣ- ADC Performance	Values
Frequency sample	200 Hz ^(a)
Acquisition bandwidth	195 Hz ^(a)
Digital Signal Resolution	24 bits ^(a)
Operating frequency	3.3 MHz ^(a)
Differential input impedance	232 KΩ ^(a)
DD CMRR	100 dB
Signal-to-Noise Ratio (SNR)	94 dB

^(a) Established configuration.

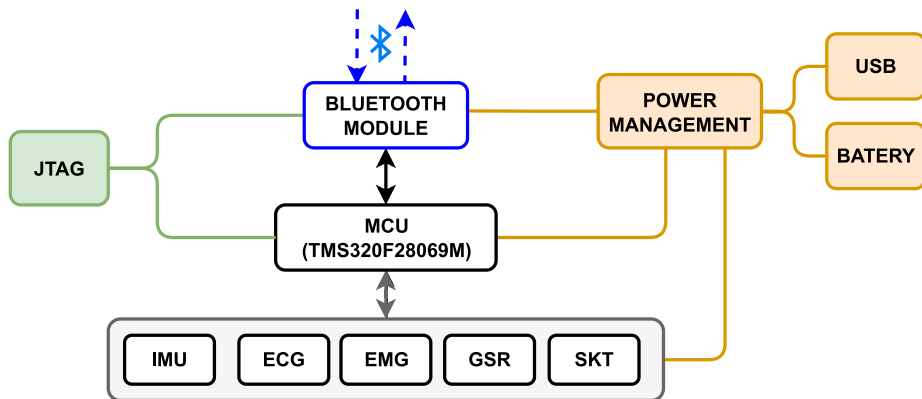


Figure 3.2. High level block diagram of the proposed multimodal embedded system (Cisnal et al., 2023a).

An ICM-20948 9-axis MEMS device (InvenSense, CA, USA) allows to track the motion of the user wearing the device. It consists of a gyroscope, an accelerometer and a compass with programmable sensitivities and filters. It also embeds a digital motion processor (DMP) aimed to reduce the computational load associated to the motion algorithm from the MCU, thus improving system performance. The ICM-20948, which is powered at 1.8 V, communicates with the TMS320F28069M using Fast Mode i2C.

The fully integrated single-lead ECG front-end AD8232 (Analog Devices Inc., MA, USA), powered at 3.3 V, amplifies, and filters the ECG signals. It also

incorporates an AC lead-off detection mode. The recorded ECG signals are analog-to-digital converted in the MCU with 12-bit resolution and two additional digital signals interface with the MCU to indicate whether the snap-lead pre-gelled electrodes are properly attached and connected using a jack connector.

A 2-channel electromyographic signal acquisition module is also integrated into the printed circuit board. The electronic circuit of the module is the same as described in section 3.1.1. The GSR measurements are based on a low constant voltage technique. A low electrical potential is applied between two electrodes attached to two hand fingers and the resulting current flow is amplified by the LM324 quadruple operational amplifier (Texas Instruments, TX, USA) and then, filtered. The analog output is transmitted to the MCU to be ADC.

The MLX90614 infrared (IR) thermometer (Melexis, Belgium) allows to measure the body temperature without physical contact and thus, facilitating its continuous monitoring. The MLX90614 is characterized by an IR-sensitive thermopile detector chip and conditioning circuit, which includes a low-noise amplifier, a 17-bit ADC and a digital signal processing unit. It transmits the temperature measurements with up to 0.02 °C resolution to the MCU via i2C and it is powered at 3.3 V.

The CC2650 MCU is a system-on-chip (SOC) that provides an ultralow power BLE using a 2.4 GHz RF transceiver. The MCU is built on an ARM® Cortex®-M3 processor for the application layer and BLE protocol stack management and on ARM Cortex®-M0 processor for the autonomous low-level radio control and processing related to the physical and link layers. The CC2650 MCU interfaces with the TMS320F28069M using one of the following serial communications: i2C, SPI or UART. No external antenna is required since the PCB integrates one on the top cooper layer, following TI's design specifications.

The device is powered by a battery or via a USB-C port if the battery is being recharged. The system integrates a MCP73831 dedicated integrated circuit (Microchip Technology Inc., AZ, USA), which is based on a constant voltage/constant current (CVVC) charging method. The charge management controller continuously monitors the battery voltage and starts its recharge if the voltage drops below a threshold. A 3.7V 3500 mAh rechargeable lithium-ion polymer battery (68x55x7 mm) provides an estimated life of 5 hours, considering that a maximum power consumption of 1250 mW.

The 2-layer PCB was designed to optimize signal integrity and its layout is based on the different submodules (Figure 3.3, a). The power planes are split, and 12 mil wide traces are used, except for 24 mil wide power signals. For reducing assembling costs, all components are placed on the top layer, except

for the thermometer. The resulting board size is 63x83 mm, including three holes for screw fixing to the box (Figure 3.3, b).

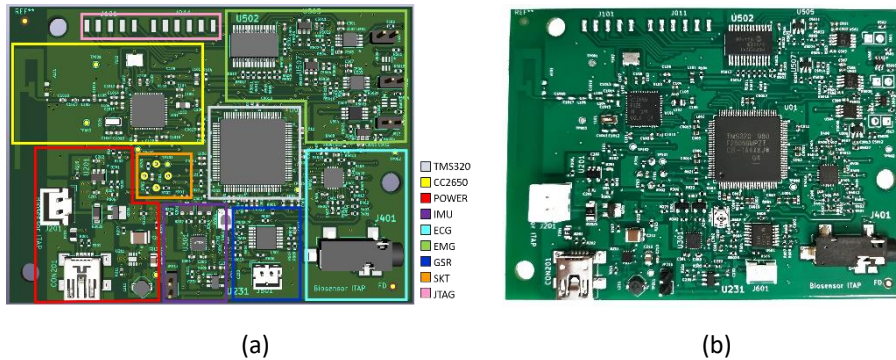


Figure 3.3. Multimodal acquisition system (a) PCB layout (b) Final solution (Cisnal et al., 2023a).

3.2. Biocooperative rehabilitation systems

This section aims to present three biocooperative control strategies for upper-limb rehabilitation using the acquisition systems described in the previous section 3.1. An EMG-driven bilateral control for hand robotic rehabilitation is detailed in section 3.2.1. In section 3.2.2, a VR-based exergame using hand gesture detection and arm tracking is presented. Lastly, an AAN control for robotic wrist rehabilitation therapy is described in section 3.2.3.

3.2.1. EMG-driven control for hand robotic rehabilitation

A threshold EMG-driven control has been proposed for conducting bilateral training with the RobHand rehabilitation robot (section 2.1.1). The exoskeleton is worn on the impaired hand to provide assistance in motion, while surface electrodes are attached to the forearm muscles and olecranon of the healthy limb for recording the EMG signals (Figure 3.4).

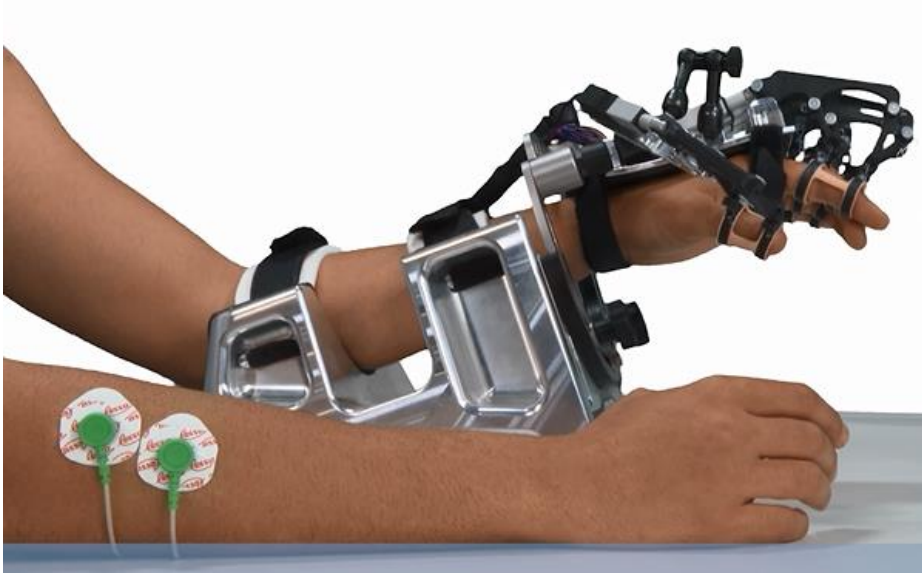


Figure 3.4. User performing EMG-driven bilateral therapy using the RobHand rehabilitation platform. The exoskeleton is worn on the impaired hand, while disposable electrodes are attached to the forearm muscles of the healthy hand to capture EMG signals (Cisnal et al., 2023b).

The embedded system described in section 3.1.1 was used to record the sEMG signals of the ED and the FDS muscles, responsible for the extension and flexion of the hand fingers. The acquired signals were processed by the MCU to recognize the gesture performed by the healthy hand (rest, open or close), generating the proper pulse width modulation (PWM) signals so the rehabilitation exoskeleton placed on the paretic hand moves to replicate the detected gesture (Figure 3.5).

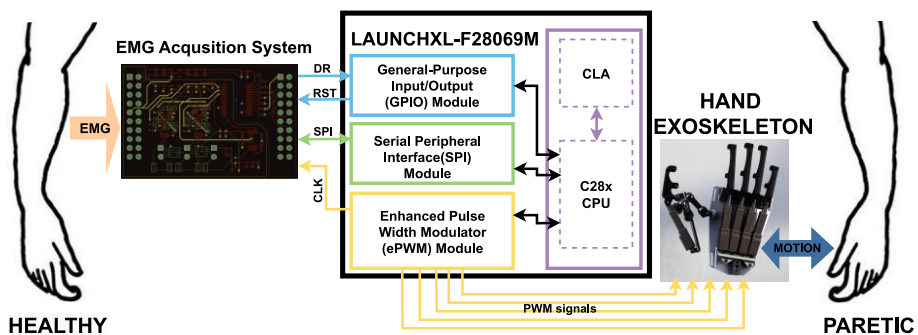


Figure 3.5. Simplified block diagram of the implementation of the EMG-driven control on the RobHand platform for assisted bilateral therapy (Cisnal et al., 2021).

The EMG signals, which are recorded at 200 Hz, are filtered for baseline noise and electromagnetic interferences removal and then, rectified and

normalized to compare the electrical activity between muscles (Figure 3.6). A notch center frequency (50 Hz cutoff frequency; 20 Q-factor) and a high-pass FIR filter (0.01 Hz stopband frequency; 10 Hz passband frequency; 80 dB minimum stopband attenuation; 0.1 dB maximum passband ripple) are applied to the raw EMG signals. The rectification is based on a 10-point RMS and a low-pass FIR filter (1 KHz passband edge frequency; 2 Hz stopband edge frequency; 4 dB maximum passband ripple; 10 dB minimum stopband attenuation), resulting in a down-sampling of 20 Hz. The normalization is performed with respect to the MVC.

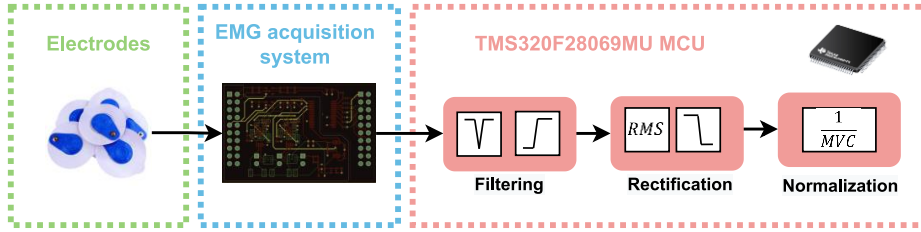


Figure 3.6. sEMG signal recording and processing, including filtering, rectification, and normalization (Cisnal et al., 2021).

The MVC values and EMG-based thresholds are computed in a calibration, which is user and rehabilitation session-specific. In the calibration procedure, subjects are asked to relax, open, and close their hand for 8 s each (Figure 3.7). The MVC values (MVC_{ED} and MVC_{FDS}) are calculated as the maximum value of their corresponding rectified EMG signal (rEMG), as indicated in equation (7).

$$MVC_{FDS/ED} = \max(rEMG_{FDS/ED}) \quad (7)$$

The extensor and flexor threshold, defined as ε and μ , correspond to the maximum limit values corresponding to muscular deactivation of the FDS and ED muscles, respectively. They are calculated following equations (8) and (9).

$$\varepsilon = \frac{\min(rEMG_{ED})}{MVC_{ED}} + 0.1 \quad (8)$$

$$\mu = \frac{\min(rEMG_{FDS})}{MVC_{FDS}} + 0.1 \quad (9)$$

The gesture recognition module (Figure 3.7) only depends on the instantaneous normalized EMG signals (nEMG) and the two EMG-based thresholds (μ and ε). Considering that A, B and C are defined according to equations (10)-(12).

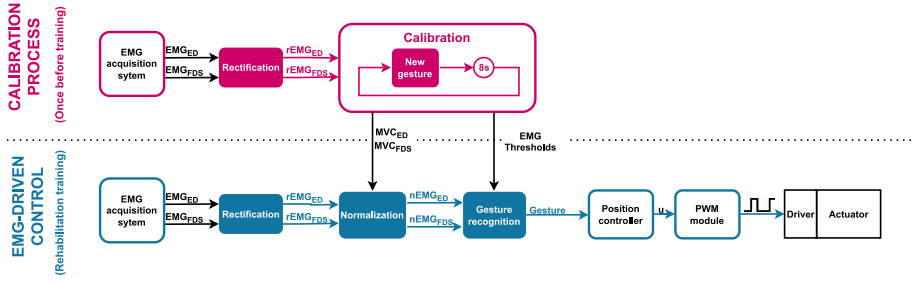


Figure 3.7. Control loop implemented for the calibration process and threshold-based EMG-driven control (Cisnal et al., 2021).

$$A \rightarrow nEMG_{ED} > \varepsilon \quad (10)$$

$$B \rightarrow nEMG_{FDS} > \mu \quad (11)$$

$$C \rightarrow nEMG_{ED} > nEMG_{FDS} \quad (12)$$

The gesture (rest, open or close) is updated every 50 ms based on equations (13)-(15) Note that for any combination of inputs, only one output (REST, OPEN or CLOSE) is true.

$$REST = \bar{A} \cdot \bar{B} \quad (13)$$

$$OPEN = A \cdot (\bar{B} + C) \quad (14)$$

$$CLOSE = B \cdot (\bar{A} + \bar{C}) \quad (15)$$

The rest gesture is recognized when the normalized signals are lower than their corresponding EMG-based threshold. The open gesture is detected when the normalized sEMG signal from the ED muscle is larger than both the extensor threshold (ε) and the normalized signal from the FDS muscle if it exceeds the flexor threshold (μ). Analogously, the closed gesture is detected when the normalized sEMG signal from the FDS muscle is larger than the flexor threshold (μ) and the normalized signal from ED muscle in case it exceeds the extensor threshold (ε). Figure 3.8 shows the signal processing of the presented EMG-driven control: raw and normalized signals based on user's residual muscle activity, thresholds, and recognized gestures.

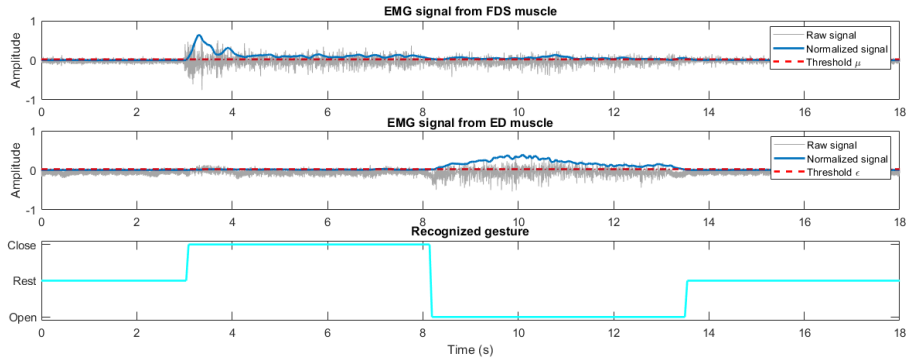


Figure 3.8. Threshold EMG-driven control: raw EMG signals of ED and FDS muscles, normalized signals, EMG-based threshold, and recognized gestures (Cisnal et al., 2023b).

Incorporation of EMG-based visual feedback to the presented EMG-driven bilateral therapy is feasible. The proposed biofeedback approach involves two variable-length bars, labelled as ‘Opening force’ and ‘Closing force’. These bars are named so as to correspond to the extensor and flexor muscle activity and have been designed to enhance the user-friendliness of the therapy (Figure 3.9).

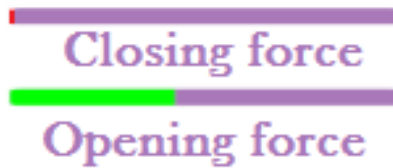


Figure 3.9. EMG-based visual feedback consisting of two variable length bars (Cisnal et al., 2023b).

The length of the bar indicates the instantaneous value of the normalized sEMG signals ($nEMG_{ED}$ and $nEMG_{FDS}$) and their color indicates the recognized gesture (Table 3.2) according to equations (13)-(15). The visual feedback is updated at 20 Hz, corresponding to the frequency of the normalized EMG signals and gesture recognition rate.

Table 3.2: Color of the bars of the EMG-based visual feedback depending on the recognized gesture.

Recognized gesture	Opening force bar	Closing force bar
Rest	Red	Red
Closed	Red	Green
Opened	Green	Red

3.2.2. EMG&IMU-based control for upper-limb rehabilitation

A VR-based exergame for upper-limb rehabilitation was developed using the multimodal embedded system (section 3.1.2). The system is worn on the user's arm to track the arm and hand movements, and thus enabling interaction with the virtual environment. Two pairs of surface electrodes are attached to the ED and FDS forearm muscles, along with one reference electrode to the olecranon, for recording EMG signals.

The objective of the exergame is to collect as many coins as possible within a fixed time by moving the arm towards the coins with a relaxed or open hand, and then closing the hand to take the coin (Figure 3.10). The difficulty of the game is adjusted online based of the elapsed time from each coin collection. Modifications are made to the degree of hand closure as well as size and relative position of the new coin respect to the last one to maintain patient motivation.



Figure 3.10. Upper-limb rehabilitation using a VR-based exergame. The embedded platform is place on the arm user and two pairs of surface electrodes are attached to the ED and FDS muscles and the reference electrode is attached to the olecranon (Cisnal et al., 2023a).

The sEMG signals captured from the ED and FDS muscles as well as the linear acceleration and angular velocity data from the ICM-20948 are transmitted to the TMS320F228069M MCU. Real-time algorithms for arm orientation estimation and hand gesture detection (open, rest and close) are executed on the MCU. The gesture and orientation are then transmitted via

BLE at a rate of 20 Hz to a PC, which updates the limb movements in the VR environment, allowing the hand to interact with the virtual coins (as shown in Figure 3.11). The VR scenario was developed using the Unity game engine.

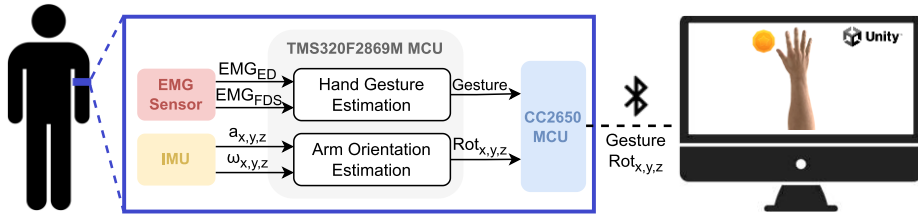


Figure 3.11. Schematic diagram of the VR-based exergame for upper-limb rehabilitation (Cisnal et al., 2023a).

The hand gesture recognition algorithm is the one presented in section 3.2.1. Regarding arm orientation estimation, the 16-bits 3 axis gyroscope and accelerometer of the ICM-20948 are set to full-scale range of ± 250 dps (degrees per second) and ± 2 g (19.6 m/s²), resulting in 131 LSB/dps and 16384 LSB/g ADC resolution, respectively. The sample rate is configured to 100 Hz and 400 KHz Fast Mode i2C is selected to transmit both linear acceleration and angular velocity to the MCU. On the MCU, the orientation estimation is carried out by implementing the model developed by M. Stanley (“Open Source Sensor Fusion,” 2015). The accelerometer and gyroscope readings are entered to this model, which is based on an indirect Kalmar filter. The linear acceleration, angular velocity and estimated arm orientation readings are shown in Figure 3.12.

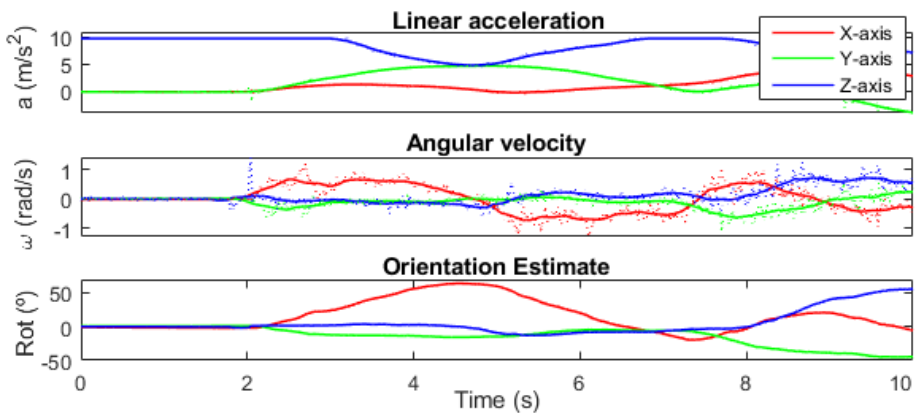


Figure 3.12. Recorded linear acceleration (top plot), recorded angular velocity (middle plot) and estimated orientation (bottom plot). Solid lines indicate raw data and dashed lines indicate filtered data (Cisnal et al., 2023a).

3.2.3. Assist-as-needed control for wrist robotic rehabilitation

An AAN control strategy that adapts the level of assistance of a wrist rehabilitation robot (section 2.1.2) based on the emotional state and the motor performance of the patient has been proposed. Biomechanical measurements from the encoder and force sensor embedded on the rehabilitation robot are used to determine the motor performance. ECG, GSR and SKT values recorded with the embedded system (section 3.1.2) are used to estimate the emotional state of the user considering the two-dimensional model (arousal and valence).

The user must wear the embedded system to register their SKT with the IR thermometer. Two disposable pre-gelled electrodes are attached to the torso, and one on the umbilical region of the user for ECG recording. GSR measurement is accomplished by placing two electrodes on the index and middle fingertips (Figure 3.13).



Figure 3.13. User undergoing rehabilitation using the wrist robotic platform based on an AAN control strategy, while wearing the embedded platform on the arm to register SKT. To record ECG signals, disposable electrodes are attached to the user's torso, and electrodes are placed on the fingertips of the hand to capture GSR (Cisnal et al., 2023a).

The AAN paradigm is applied to a closed-loop admittance control with a reference trajectory. The mechanical admittance (Y) of a system is defined as the ratio of its displacement (x) and its force (F), as expressed in equation (16). This definition is usually related to a mass-spring-damper system, characterized by a mass (m), a stiffness (k) and a viscous damping (b) (Mihelj and Podobnik, 2013).

$$Y(s) = \frac{X}{F} = \frac{1}{ms^2 + bs + k} \quad (16)$$

The objective of an admittance control is to shape the mechanical admittance of a device such that it possesses desired characteristics. Hence, M, B, and K parameters are updated (increase, decrease, or no change) every second according to assistance level of the robot. The level of assistance is determined by a two-stage fuzzy logic model (Figure 3.14), which is similar in nature to that presented by Mihelj et al. (Mihelj et al., 2009).

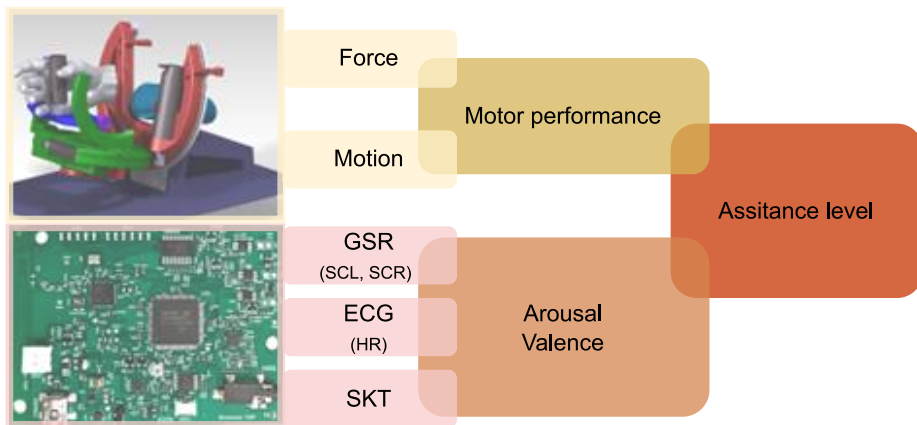


Figure 3.14. AAN control strategy based on a two-stage fuzzy logic model which consider the motor performance and emotional state of the user (Cisnal et al., 2023a).

Before the training session, the user must relax for 30 seconds to determine their physiological resting values. The first stage of the fuzzy logic evaluates the motor performance based on the biomechanical information (force and motion) provided by the force sensor and encoders of the rehabilitation robot. The first stage also determines whether to increase, decrease or maintain the arousal and valence in function of the variations in HR, SCL, SCR frequency and SKT, all of them normalized with respect to their resting values. The algorithm that determines the changes in valence and arousal is based on the ones presented by Mandryk et al. (Mandryk and Atkins, 2007) and Guerrero et al. (Guerrero et al., 2013).

The Pan–Tompkins’s algorithm (Pan and Tompkins, 1985) was used to detect the R events, and hence the heart rate from the ECG signals recorded at 500 Hz (Figure 3.15). The algorithm applies a series of filters to the ECG signal and squares the filtered signal to amplify the QRS contribution and then, uses adaptive thresholds to detect the peaks of the processed ECG signals.

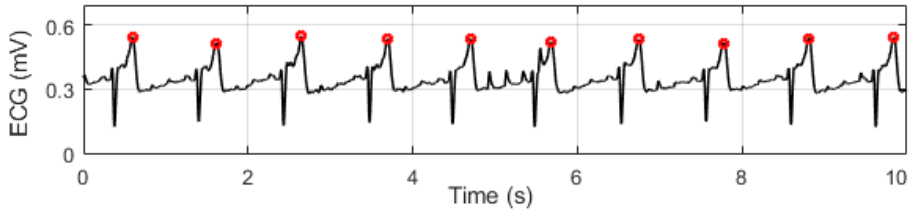


Figure 3.15. R events of an ECG signal from a person at rest (Cisnal et al., 2023a).

The skin conductance (SC), recorded by the GSR module at a 225 Hz, is low pass filtered (10 Hz cut-off frequency) to eliminate the high-frequency noise, which may cause false-positive detection of phasic events. The tonic component (SCL) and phasic component (SCR) are extracted from the filtered SC (Figure 3.16) using a deconvolution technique (Muñoz et al., 2018).

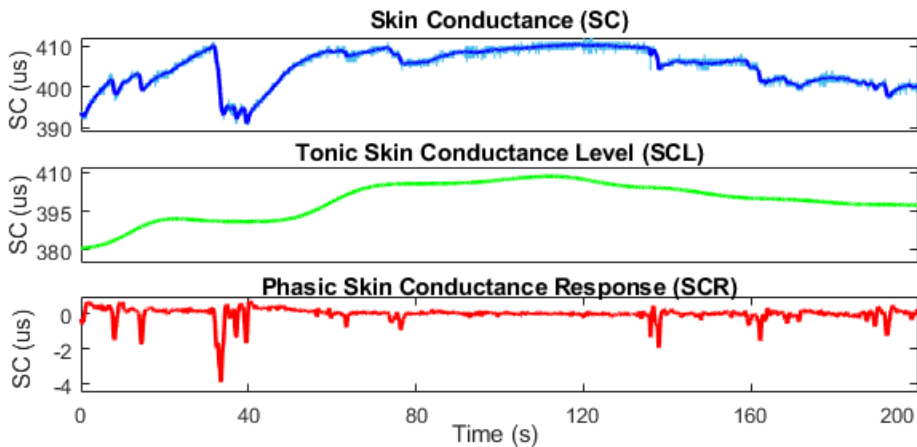


Figure 3.16. Raw and filtered skin conductance and its tonic (SCL) and phasic (SCR) components (Cisnal et al., 2023a).

In the second stage, the decision involves determining whether to increase, maintain or decrease the assistance level based on the variations in arousal, valence, and motor performance identified in the previous stage. The physiological signals (GSR, ECG and SKT) are processed in the MCU and the extracted features (HR, SCL, SCR, and SKT) are sent to the PC via BLE. These features are then combined with the biomechanical data (force, position, and velocity) are entered into the fuzzy model. This model estimates the assistance level and updates the mechanical admittance of the robot. The force, position and velocity data are sent from the robot to the PC, while the admittance parameters, namely K , B and M , are transmitted from the PC to the robot (Figure 3.17).

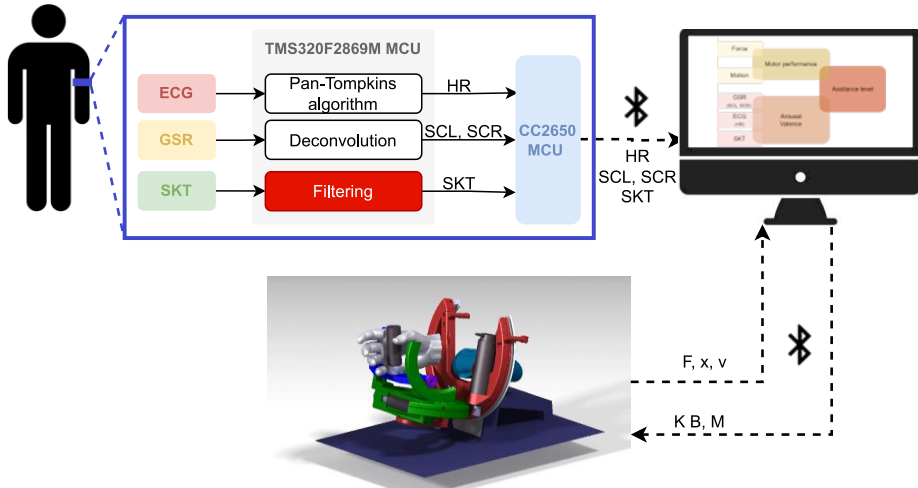


Figure 3.17. Schematic diagram of the AAN control strategy for wrist rehabilitation.

3.3. Performance assessment

The evaluation of the HRI of the EMG-driven hand exoskeleton was performed by assessing system responsiveness and gesture recognition accuracy (section 2.4.2). The experimental setup, as detailed in section 2.3.1, was used. The results of the time delay analysis are presented in Figure 3.18. The mean and standard deviation of the MST and the MOT were 0.48 ± 0.59 s and 0.55 ± 0.60 s, respectively. The MCT was 1.90 ± 1.65 s, varying from 0.98 s (from close to rest gesture) to 3.42 s (from open to close gesture). The MCT is dependent on the actuators speed and was deemed to be sufficiently long to ensure user safety during the rehabilitation. The motion-completion rate was 100 %, as MCT did not exceed the predefined time limit of 5 s in any case.

The confusion matrix that presents the performance of the EMG-based gesture recognition control is depicted in Figure 3.19. The confusion matrix was obtained by comparing the actual hand gestures recorded by the 5DT Data Glove and the corresponding gestures recognized by the EMG-based control. Before calculating the confusion matrix, data was cleaned to eliminate the gesture transition period (time needed to move the hand from one gesture to another) to avoid false negatives. The gesture transition period was considered 0.9s (maximum MST value) starting when a transient period is detected by the glove. The overall accuracy of the gesture recognition is 97% and misclassifications during the gestures are minimal (fewer than 0.06 s). This means that in 98.4% of cases, error is not noticeable in the exoskeleton, as the actuators do not start moving in the opposite direction to the intended movement.

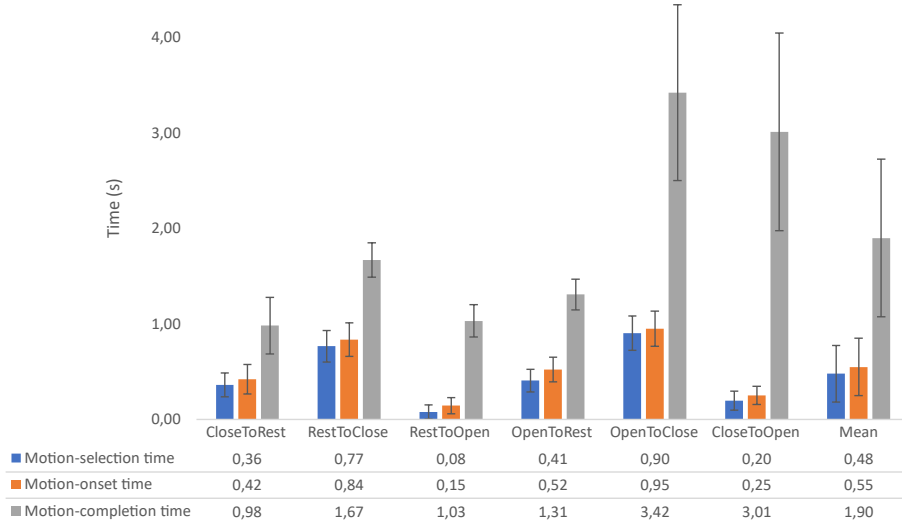


Figure 3.18. Time delay analysis of the EMG-driven bilateral control with the hand exoskeleton (Cisnal et al., 2021).

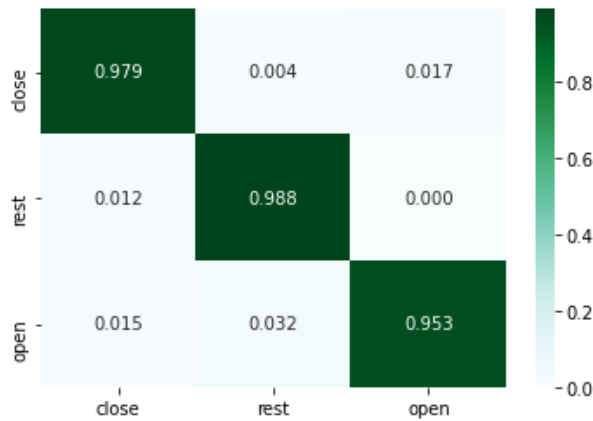


Figure 3.19. Confusion matrix of the EMG-based gesture recognition (Cisnal et al., 2021).

The influence of the EMG-based visual feedback on the user performance when performing EMG-driven bilateral assisted therapies was also evaluated. The experimental setup was detailed in section 2.3.2. The sequences of recognized gestures are delayed with respect to the sequence of target gestures (Figure 3.20, a). Both signals were time-synchronized (Figure 3.20, b) by calculating the delay based on the cross-correlation (section 2.4.2). The average time delay (T_d) used for the synchronization, which depends on the user response time (T_R) and the motion-selection time (MST), was 0.88 ± 0.14 s.

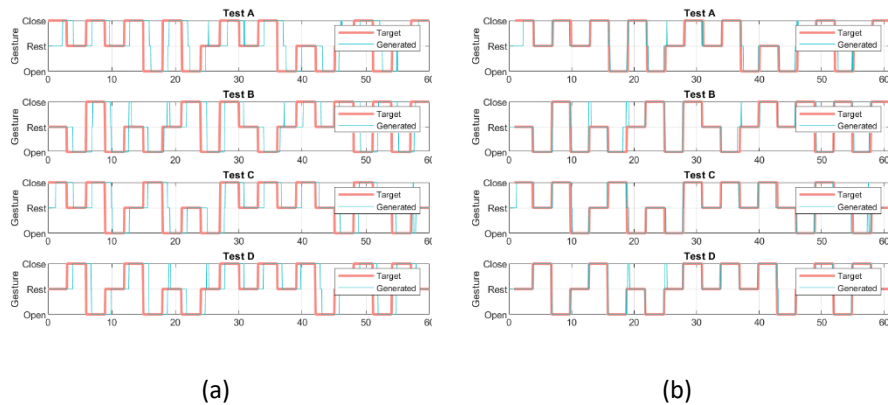


Figure 3.20. Target and recognized sequence of gestures of one subject (a) Raw data; (b) Time-synchronized data (Cisnal et al., 2023b).

The user performance was evaluated by using lock-step distance measure (section 2.4.2). The time series related to hand gestures are coded considering the following order: “Open < Rest < Closed” (“Open” = -1, “Rest” = 0 and “Close” = 1). As an error between open and closed gesture is more serious than an error between either of them or rest gesture, the L2 norm is used since the quadratic cost penalize this type of error more than the L1-norm. Hence, the L2 distance between the target gesture and the synchronized gesture time series are computed as a similarity measurement.

Table 3.3 shows the results of the multifactorial additive ANOVA, which was performed to evaluate the influence of three independent variables (type of test, test order and individual) on the L2 distances.

Table 3.3: Results of the Multifactorial additive ANOVA assessing the impact of the three independent variables (type of test, test order and individual) on the L2 distances.

		Df	Sum Sq.	Mean Sq.	F Value	Pr (>F)
Test	*	3	3.366	1.1221	4.028	0.0124
Order		3	1.037	0.3456	1.241	0.3054
Individual	***	17	20.933	1.2313	4.420	2.43 e-05
Residuals		48	13.373	0.2786		

*** Denotes significance at the (<0.001) level and * at the (<0.5) level.

No statistically significant differences were found in the order in which the tests were perform ($F(3) = 1.241$, $p = 0.3054$). Additionally, statistically significant differences were found in the average of L2 by type of test performed ($F(3) = 4.028$, $p=0.0124$). A Duncan post-hoc test (Table 3.4) revealed significant pairwise difference between performance in test A and C ($p = 0.0497$) and between performance in test B and C ($p = 0.0412$).

Table 3.4: Results of the Duncan's Multiple Range Test showing pairwise comparisons and significant differences among the variables.

	Test A	Test B	Test C
Test B	0.8775	-	-
Test C	0.0497 *	0.0412 *	-
Test D	0.3557	0.3121	0.2451

* Denotes significance at the (<0.5) level.

The distribution of the L2 distances according to the type of performed test is shown in Figure 3.21. L2 distances were 3.39 ± 0.70 , 3.43 ± 0.75 , 2.89 ± 0.71 , 3.17 ± 0.73 for test A, B, C and D, respectively. Finally, homoscedasticity was verified.

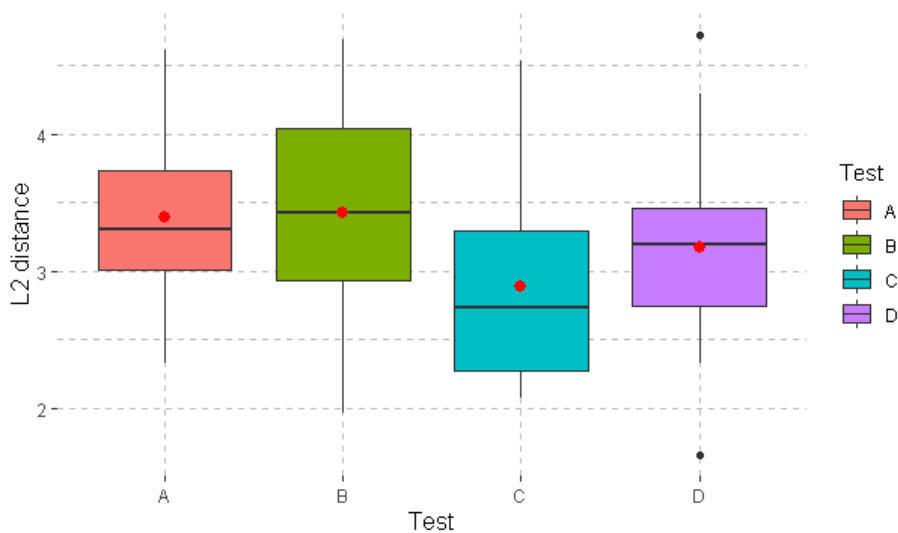


Figure 3.21. L2 distances for the four performed tests (Cisnal et al., 2023b).

An important feature of the wearable and multimodal embedded system presented in section 3.1.2, apart from its notable computational capabilities and high versatility, is its power consumption. It has a battery life of 5 hours and maximum power usage of around 1250 mW. To perform a power consumption analysis, the system is divided into three components: the sensor modules, TMS320F28069M MCU, and CC2650 MCU.

Regarding to the sensor modules, when active and set to the defined specifications, the EMG, IMU, ECG, GSR, and TEMP modules consume 40.6 mW, 5.6 mW, 0.6 mW, 3.3 mW, and 5.6 mW, respectively. In sleep mode, these modules consume 9.6 mW, 0.02 mW, 0.001 mW, 2.6 mW, and 0.01 mW, respectively.

Additionally, the power consumption of the TMS320F28069M MCU was analyzed for the two presented rehabilitation scenarios: EMG&IMU-based

control for upper-limb VR-based exergame (section 3.2.2) and the AAN control for a wrist rehabilitation robot (section 3.2.3). Figure 3.22 details the average power consumption of each peripheral for each application. During data acquisition from the sensors, the DMA is triggered to transfer the data to the internal memory, while the CLA module independently processes the signal. The DMA's energy consumption is proportional to the number of active channels and the amount of data and transfer rate, while the CLA energy consumption depends on the algorithm's complexity.

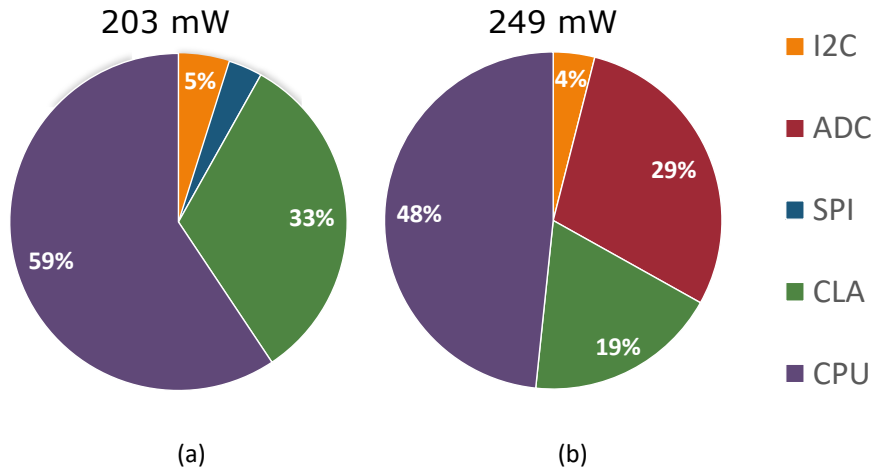


Figure 3.22. Breakdown of the power consumption for the two scenarios: (a) EMG&IMU-based control and (b) AAN control (Cisnal et al., 2023a).

The system's power consumption is heavily influenced by the application and MCU configuration, with the energy consumption of the MCU being highly variable based on the computational load. When the computation is over, the MCU can be programmed to enter an IDLE mode, which reduces power consumption from 272.3 mW to 82.5 mW. Motion recognition control has a power consumption of 203 mW, while adaptive control has a power consumption of 249 mW.

The CC2650 module's power consumption is primarily due to BLE communication, with the average power consumption being proportional to the amount of data transmitted. When streaming raw data from all five sensor modules at 1 kHz, the maximum power consumption for BLE communication can reach 32.7 mW. In the proposed scenarios, the CC2650 MCU only receives information through the i2C interface and sends it to a central node using BLE, with no additional modules or data processing being carried out, which would increase the module's power consumption.

Chapter 4

4. Discussion

In this Doctoral Thesis, the main aspects that limit the use of biocooperative systems have been addressed: hardware and reliability. First, a real-time embedded system is developed for acquisition of EMG signals. This system is integrated into a hand robotic exoskeleton, enabling EMG-driven bilateral assistive therapies. The evaluation focuses on assessing the impact of the real-time embedded system on the performance of the developed EMG-driven rehabilitation platform. The accuracy and responsiveness of the system were determined, which are essential parameters for assessing the quality of the human-robot interaction. The proposed EMG-driven rehabilitation system is further investigated by incorporating EMG-based visual feedback. The influence of this visual biofeedback on the user's performance during the execution of bilateral therapies is evaluated. The findings suggest that this type of feedback could benefit patients in increasing their control over the movement of the robotic platform. Lastly, a wearable real-time embedded system for multimodal signal acquisition was developed and tested by implementing two biocooperative control strategies. This versatile and low-cost system provides reliable signals for the implementation of real-time biocooperative controls for a wide range of neuromotor rehabilitation applications.

In this chapter, the aforementioned findings are discussed in accordance with the hypothesis and results presented in previous chapters. Each finding is given its own dedicated section, resulting in three distinct sections. Within these sections, a comprehensive analysis of the research findings and their implications in the field of rehabilitation robotics is provided.

4.1. EMG-driven hand rehabilitation robot

A systematic review according to PRISMA (Reporting Items for Systematic Reviews and Meta-Analyses) was conducted to compare the performance in terms of accuracy and latency of the proposed EMG-driven robotic rehabilitation platform with other similar works. Articles in various databases (IEEE Explorer, Web of Science and PubMed) using specific keywords and inclusion/exclusion criteria were searched to answer the question “What is the latency time of EMG-driven hand rehabilitation robots?”. Nine articles met the criteria, and only two of them reported latency times (Table 4.1).

Table 4.1: Published data regarding the accuracy and temporal information of EMG-driven robots for hand rehabilitation.

Ref	Control type	Accuracy	Delay ²
(Secciani et al., 2020)	Point-in-Polygon (PIP) (3 predefined gestures)	Accuracy: 0.944	-
(Leonardis et al., 2015)	EMG-driven (neural network to determine force)	Force error: 20.7 %	-
(Ben et al., 2017)	Threshold algorithm	-	-
(Lu et al., 2017)	Linear Bayes classifier (6 predefined gestures)	Accuracy ¹ : 98.1±4.9 %	Yes
(Zhang et al., 2019)	Classification algorithm (6 predefined gestures)	Accuracy: 86.38 %	Yes
(Park et al., 2020)	EMG-based intent inference method	-	-
(Burns et al., 2019)	Neural network	-	-
(Park et al., 2018)	Forest classifier (3 predefined gestures)	Accuracy: 77.9 - 85.2 %	-
(Chen et al., 2021)	Neural Network (4 predefined gestures)	Accuracy: 98.7±0.53 %	-

¹Accuracy for neurologically intact subjects. ²Whether delay analysis of the system is carried out.

The overall accuracy of the gesture recognition module was 0.97, and misclassifications during the gesture were small, which means that the error is not perceived in the exoskeleton in most cases. The accuracy results are comparable to other control systems proposed in the literature, varying from 77.9% to 98.7% (Table 4.1).

Regarding to the responsiveness analysis, (Lu et al., 2017) conducted a temporal analysis of a hand exoskeleton controlled by EMG signals. However, the five time parameters provided are not readily comparable with our

findings. Additionally, they were inconclusive regarding the delay experienced by the user, as they were primarily influenced by the mechanical structure of the exoskeleton and the waiting time for commands. In (Zhang et al., 2019), the "control speed" was measured as the number of actions correctly performed in one minute and provided an average "time per action" of 1.4s, which is comparable to the MCT (the MCT of the proposed control in the RobHand is 1.90 ± 1.65 s). However, the "time per action" value alone does not provide enough information about the lag, as the computational time could be very large while the actuators could be very fast, resulting in a low "time per action."

Due to the limited results, the systematic review was expanded to look for embedded systems for EMG gesture recognition integrated in hand rehabilitation robots. It yielded some studies that specify the computational time of the classification algorithm, ranging from 0.58-2.8 ms (Benatti et al., 2014, 2015; J. Liu et al., 2014), but comparisons are not possible due to the lack of information on EMG acquisition and data preprocessing. More information on control latency was available in studies on hand prostheses based on EMG, with reported times ranging from 100-600 ms (Chu et al., 2006; Ryser et al., 2017; Tam et al., 2020), but no reliable comparison can be made due to inaccurate definitions and uncertain time periods.

In summary, the presented system is characterized by its low-cost embedded EMG acquisition system, which has enabled the implementation of a real-time EMG-driven control for performing rehabilitation bilateral therapies with a hand robotic exoskeleton. The distinctive feature of the designed 2-channel EMG acquisition device is its cost, estimated at approximately 30€ for low-scale production. The key advantage of implementing EMG-based control within the real-time embedded system lies in the reduction of latency, while maintaining high accuracy in gesture recognition.

4.2. Influence of visual biofeedback on the users' performance

Significant statistical differences in subject performance were observed during execution of EMG-driven bilateral therapies based on the type of provided feedback. Specifically, users' performance significantly improved when only the EMG-based visual feedback (test C) was present compared to the presence of only kinesthetic feedback (test B) and both feedbacks (tests A). Therefore, it can be concluded that the visual biofeedback enhanced the user motor control. It provided users a simple way to monitor and regulate their EMG

activation levels with respect to the previously predefined activation thresholds, and thus enabling to have a better self-control the movement of the hand exoskeleton.

The biofeedback is provided earlier in time than the kinesthetic feedback and therefore, the user has a longer reaction time to self-regulate their EMG activation levels. In fact, the user can directly adjust the force being exerted at the moment by influencing the position controller input through real-time visual EMG feedback. On the other hand, kinesthetic feedback requires the user to first feel the movement performed by the exoskeleton's actuators before modulating the exerted force, resulting in a delayed force modulation (Figure 4.1). Consideration should be given to the electromechanical characteristics of the actuators, including their low dynamic response and limited speed due to the rehabilitation application. Note that relevant time delays for the human-robot interaction have been precisely determined, MST, MOT and MCT.

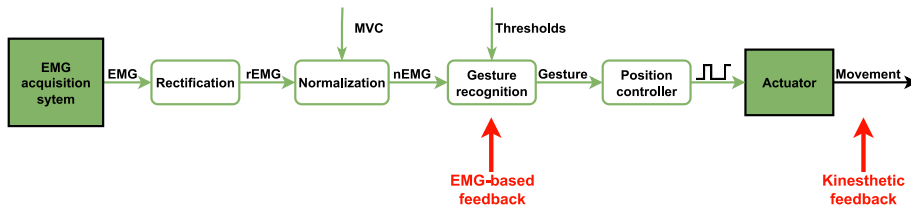


Figure 4.1. The control loop used for the threshold EMG-driven control of the RobHand specifying the origin of each feedback (Cisnal et al., 2023b).

On the other hand, the fact that EMG-biofeedback results in a significantly higher performance than in the presence of both feedbacks may be due to the fact that the kinesthetic feedback is more straightforward than the visual biofeedback and hence, users do not need to consciously pay attention to it.

In summary, in the presence of visual feedback, the user adjusts his/her force based on the data provided by the gesture recognition module (nEMG signals and detected gesture) and anticipates the response of the exoskeleton. On the other hand, with kinesthetic feedback, the user adjusts his/her force after the exoskeleton has performed the action. If the user notices that the movement performed by the exoskeleton does not align with their intention, the user can correct it by modulating their muscle activity, but this process takes longer than if they had corrected it based on real-time EMG visual feedback.

4.3. Wearable embedded multimodal acquisition system

The research introduced a cost-effective wearable embedded multimodal platform designed for the implementation of biocooperative control in the field of neuromotor rehabilitation. A significant observation from the examination of related studies in biocooperative control is that most of them incorporated only a restricted set of sensors and relied on expensive and often bulky commercial systems, lacking the necessary processing capabilities.

One approach to reduce the bulkiness of acquisition systems is the integration of sensors directly into the system. For instance, a previous study proposed integrating multiple sensors, including ECG, GSR, SKT, PPG, and force sensors, into the handle of an end-effector rehabilitation (Jakopin et al., 2017). Similarly, in other fields, researchers have embedded ECG, GSR, accelerometers, and force sensors onto wheelchairs (Postolache et al., 2014) or integrated direct contact sensors onto steering wheels to measure ECG, GSR, SpO2 levels, and SKT signals (Heuer et al., 2010). However, it should be noted that while this integration approach reduces bulkiness, it may also limit flexibility.

Recent research emphasizes the need for wearable sensing devices that are small, low-cost, and possess high computational power to detect human physical activity and emotions through multimodal fusion strategies. In order to promote portability and comfort, the number of sensors used must be chosen carefully, ensuring that the system is fast, energy-efficient, and convenient. Additionally, a smaller set of sensors placed in optimal locations can increase user acceptance (Qiu et al., 2022).

Several studies have attempted to create affordable wearable platforms. For instance, some works have focused on the development of integrated EMG sensors (Benatti et al., 2015; Brunelli et al., 2016; Örüçü and Selek, 2019), while others have specifically developed ECG sensors (Athavipach et al., 2019; Nguyen et al., 2017), or solely utilized IMU sensors (Marta et al., 2020). In contrast, other works have integrated more than one sensor into the platform, such as ECG and GSR (Villar et al., 2021), IMU and ECG (D’Mello et al., 2019) and GSR, SKT and IMU (Huan et al., 2022). However, these studies have not sufficiently addressed the need for versatility in terms of the number of sensors required to implement biocooperative control systems.

The presented wearable, multimodal and low-cost solution overcome these limitations. It integrates five sensors (IMU, EMG, SKT, GSR, and ECG) and its highly configurable, thus offering a more comprehensive approach for biocooperative control strategies in the context of neurorehabilitation. The

platform's high-efficiency real-time MCU provides ample processing capabilities and its high flexibility, concerning sensor diversity and wireless communication, allows the development of a numerous rehabilitation applications.

Two potential applications using different signals and rehabilitation approaches were proposed. Arm motion tracking using IMU data, hand gesture recognition through EMG signals, HR detection from ECG signals, SCL and SCR extraction from GSR data and SKT monitoring were carried out. It was verified that the system's low cost does not compromise the quality of the signals, that is reliable enough for the proposed scenarios and good performance is expected in other related applications. Additionally, the system power consumption for the two scenarios were analyzed and showed that they are within the energy constraints of the system. It can record and process real-time multimodal information for at least 5 hours.

The wearable system was design by balancing complexity, price, and performance, taking into account parameters such as volume, flexibility, energy consumption, onboard processing, and signal quality. Due to its low cost, compact size, and comfort, the platform shows great potential for rehabilitation applications. While it may not be appropriate for applications that demand high signal quality or a long-term battery life, such requirements are not typically expected in rehabilitation applications. Therefore, the presented platform is a promising advancement in the development of wearable technologies for neuromotor rehabilitation.

Chapter 5

5. Conclusions

In recent years, the developing of affordable biocooperative rehabilitation systems for improving the QOL of people suffering neuromotor disabilities has become a major challenge. Despite the growing interest of scientific literature in neuromotor rehabilitation robotics, limitations in current systems have made them accessible only to large academic medical centers and researcher laboratories. The excessive cost of physiological recording systems limits the accessibility of biocooperative controls for neuromotor rehabilitation even further.

Current research focuses on design innovative controls aiming to achieve a more natural HRI that enhances patient motivation towards rehabilitation. However, these studies overlook the potential utilization of biocooperative systems in clinic practice and focus on merely academic purposes. For instance, numerous EMG-based robotic control strategies have been suggested in literature, detecting numerous hand gestures with high accuracy. However, these approaches require robots with multiple degrees of freedom and entail substantial computational expenses, rendering them infeasible and unreliable for practical applications. Moreover, these techniques rely on numerous EMG signals, which call for several electrodes to be fixed onto the patient, thereby adding to the already time-intensive clinical regimen of physical therapy personnel. By reducing the number of electrodes, costs, power consumption, and user comfort can all be improved.

The present Doctoral Thesis is focused on providing affordable technology and developing control strategies, intended to provide a real use of biocooperative systems by motor-disabled people. In this chapter, the main

contributions and conclusions of the articles included in this compendium of publications are indicated in section 5.1 and section 5.2, respectively. In the last section 5.3., future endeavors related to this research are enumerated.

5.1. Contributions

In this section, the contributions of three articles that address the use of technology in neuromotor rehabilitation are highlighted. The first article presents a hand exoskeleton that supports EMG-driven assisted rehabilitation by using a custom-made low-cost EMG real-time embedded solution. The second article evaluates the influence of EMG-based visual biofeedback on the user performance when performing EMG-driven bilateral exercises with the robotic hand exoskeleton. Finally, the third article presents a low-cost and wearable embedded system that integrates the most used sensors in neuromotor rehabilitation and hence, enables the development of real-time biocooperative controls for a wide of range applications in this field. These articles showcase the potential of technology in promoting motor recovery and improving rehabilitation outcomes in patients with neuromotor impairments. The main contributions and potential impact in the field of neuromotor rehabilitation provided by the results of this compendium of publications are the following:

- I. Design and development of a low-cost EMG acquisition system for real-time EMG-driven therapies. Integration of the system in the Robhand rehabilitation platform, including additional electronic circuitry (Cisnal et al., 2021).
- II. Development of a non-pattern recognition-based EMG-driven control for bilateral robotic hand rehabilitation. Integration of the control in the real-time embedded platform (Cisnal et al., 2021).
- III. Performance evaluation of the EMG-driven exoskeleton in terms of accuracy and latency and comparison with previous works. It was detected that the HRI evaluation of EMG-based robotic rehabilitation systems in the current literature is inadequate. While studies have concentrated on providing accuracy metrics to evaluate the performance of gesture recognition, they have failed to provide latency metrics, which is essential for achieving optimal HRI (Cisnal et al., 2021).
- IV. Design and implementation of an EMG-based visual feedback. Despite the usefulness of EMG feedback in neuromotor rehabilitation applications has been demonstrated, to the best of our knowledge, this was the first time that EMG feedback in combination with rehabilitation robots have been investigated (Cisnal et al., 2023b).

- V. Evaluation of the performance of the users when providing EMG-based visual feedback during EMG-driven bilateral therapies. We found that EMG feedback led to significant improvements in performance (Cisnal et al., 2023b).
- VI. Design and development of a low-cost, wearable, embedded and multimodal acquisition system for the implementation of biocooperative systems in neuromotor rehabilitation. Feasibility of the system and power consumption was tested (Cisnal et al., 2023a).
- VII. Design and development of two biocooperative control strategies for neuromotor rehabilitation by means of the proposed embedded multimodal acquisition system. An EMG&IMU-based control using VR-based therapies and AAN control using a wrist rehabilitation robot (Cisnal et al., 2023a).

5.2. Main conclusions

The development and evaluation of the proposed low-cost biocooperative rehabilitation systems have shown promising results (Cisnal et al., 2021) (Cisnal et al., 2023a). These systems have proven the feasibility of implementing biocooperative controls without the need for expensive commercial systems that are typically bulky and lack processing capabilities. The advantages associated with these embedded solutions for physiological signal acquisition, in addition to their low cost and versatility, include enabling the development of real-time biocooperative controls with reduced latency while maintaining high accuracy. These characteristics make embedded acquisition solutions an attractive option for the development of biocooperative control systems that are accessible and affordable for rehabilitation in clinical settings. Furthermore, the use of these systems can also pave the way for the development of new applications in the fields of human-robot interaction and assistive robotics.

It has been shown that the incorporation of EMG-based visual feedback can significantly improve the performance of individuals undergoing EMG-driven assisted therapies. By providing real-time biofeedback, the subjects were able to monitor and modulate their EMG responses, resulting in better control of the exerted force. Thus, it can be inferred that EMG-based visual feedback has the potential to facilitate the rehabilitation learning process, as it helps users develop a better understanding of how to self-regulate their muscle activations. This could ultimately enhance patient motivation and contribute to better motor recovery outcomes (Cisnal et al., 2023b).

As a last point, there is a need for greater emphasis on responsiveness and latency times in EMG-driven rehabilitation systems (Cisnal et al., 2021). Previous studies have primarily focused on accuracy of gesture classification, neglecting important information regarding system latency. While some studies have addressed system latency, the measured values are often imprecisely defined. It is crucial to establish clear and standardized definitions of latency times for rehabilitation robotics to ensure homogeneity in this field of research. By doing so, we can ensure that the development of EMG-based rehabilitation systems is optimized for the benefit of patients.

5.3. Future research lines

Research on neurorehabilitation using biocooperative systems has shown promising results in recent years, highlighting the potential of these technologies to improve the quality of life of patients undergoing neurorehabilitation. Several future research questions can be derived from this investigation.

Firstly, it is important to focus on people with neurological disabilities. While this research has shown positive results in healthy individuals, it is important to explore the potential benefits for motor recovery in individuals with neurological impairments. By doing so, it may be possible to identify specific adaptations or modifications that can further enhance its effectiveness for this population. Additionally, it would be convenient to develop a unified protocol for the evaluation of the human-robot interface by measuring latency times, which would allow comparisons between different rehabilitation robots.

The use of EMG-based visual feedback is another area where future research can be directed. As the technology has been proven effective in healthy individuals through this study, it is crucial to investigate its potential advantages for those with neurological disorders. Additionally, the use of more complex visualizations of EMG-based feedback, such as in combination with other virtual reality objects, should be further explored to determine if it has a positive impact on user performance.

Finally, future research should focus on implementing more advanced biocooperative controls using the proposed multimodal embedded platform, which could provide further insights into the capabilities of the system. Additionally, the reduction of electronic size and energy consumption will improve its wearability, resulting in better user acceptance. Therefore, researchers should work towards developing energy-efficient and compact systems that could be easily integrated into wearable devices, making them

more comfortable for the user to wear. This would not only improve user acceptance but also enable remote monitoring of patients' progress, leading to more personalized treatment plans.

Overall, the potential benefits of biocoperative systems in neurorehabilitation are clear, and future research should focus on refining these systems to better serve the needs of individuals with neurological impairments. Continued research in this area has the potential to make a significant impact on the quality of life for those undergoing neurorehabilitation.

Appendix A

**Articles included in this
Doctoral Thesis**

A.1. (Cisnal et al., 2021)

A. Cisnal, J. Pérez-Turiel, J.C. Fraile, D. Sierra and E. de la Fuente, "*RobHand: A Hand Exoskeleton With Real-Time EMG-Driven Embedded Control. Quantifying Hand Gesture Recognition Delays for Bilateral Rehabilitation*," in IEEE Access, vol. 9, pp. 137809-137823, 2021, <https://doi.org/10.1109/ACCESS.2021.3118281>

A.2. (Cisnal et al., 2023b)

A. Cisnal, P. Gordaliza, J. Pérez-Turiel and J.C. Fraile, "*Interaction with a Hand Rehabilitation Exoskeleton in EMG-Driven Bilateral Therapy: Influence of Visual Biofeedback on the Users' Performance*," in Sensors, vol. 23, 2048, 2023, <https://doi.org/10.3390/s23042048>

A.3. (Cisnal et al., 2023a)

A. Cisnal, D. Antolínez, J. P. Turiel, J. C. Fraile and E. De La Fuente, "*A Versatile Embedded Platform for Implementation of Biocooperative Control in Upper-Limb Neuromotor Rehabilitation Scenarios*," in IEEE Access, vol. 11, pp. 35726-35736, 2023, <https://doi.org/10.1109/ACCESS.2023.3265898>

Appendix B

About the author

B.1. Biography



Ana Ciscal de la Rica received a B.S. degree in industrial electronics and automation engineering and an M.S. degree in industrial engineering from the University of Valladolid, Spain, in 2017 and 2019, respectively. S'18). She is currently pursuing a Ph.D. degree in industrial engineering at the University of Valladolid.

During her Bachelor's program, she participated in quality internships at Technology Center CARTIF (Valladolid, Spain) and Fraunhofer Institute for Biomedical Engineering (Sankt Ingbert, Germany). At the Health Division of Technology Center CARTIF, she contributed to the development of a control for the E2REBOT robotic platform for upper-limb rehabilitation in patients with neuromotor disabilities. During her internship in Fraunhofer IBMT, she designed and developed a measurement instrument for the characterization of electrodes in the context of functional electrostimulation.

From 2017 until now, she has been working at the Advanced Production Technologies Institute (ITAP) Medical Robotics Research Group of the University of Valladolid as a research advisor, research fellowship and contract researcher. Her work focuses on the development of neuromotor rehabilitation and surgical robotics applications. She became IEEE Student Member in 2018. In 2020, he worked at IDIMAS Gestion SLNE (Salamanca, Spain) developing a neck-mounted sensorized wearable device for individual cow control in extensive livestock. Since 2020, she is also an assistant professor at the Department of Systems Engineering and Automation of the University of Valladolid.

She joined the SCAI (Spinal Cord Artificial Intelligence) Lab as a visiting PhD student in September 2022, where she is working on the estimation of blood pressure based using photoplethysmography for personalized healthcare for spinal cord injury individuals.

B.2. Publications

B.2.1. Papers indexed in the JCR

1. **Cisnal, A.**, Fraile, J-C., Pérez-Turiel, J., Muñoz-Martinez, V., Müller, C, R., Ihmig, F. (2018) A Measurement Setup and Automated Calculation Method to Determine the Charge Injection Capacity of Implantable Microelectrodes. *Sensors*. 2018; 18(12):4152. <https://doi.org/10.3390/s18124152>
2. **Cisnal, A.**, R. Ihmig F, Fraile J-C, Pérez-Turiel J, Muñoz-Martinez V. (2019) Application of a Novel Measurement Setup for Characterization of Graphene Microelectrodes and a Comparative Study of Variables Influencing Charge Injection Limits of Implantable Microelectrodes. *Sensors*. 19(12):2725. <https://doi.org/10.3390/s19122725>
3. Moreno-San Juan, V., **Cisnal, A.**, Fraile, J., Pérez-turiel, J., & de la Fuente, E. (2021). Design and Characterization of a Lightweight Underactuated RACA Hand Exoskeleton for Neurorehabilitation. *Robotics and Autonomous Systems* 143, 143 (2021), 103828. <https://doi.org/https://doi.org/10.1016/j.robot.2021.103828>
4. **Cisnal, A.**, Perez-Turiel, J., Fraile, J. C., Sierra, D., & de La Fuente, E. (2021). RobHand: A Hand Exoskeleton with Real-Time EMG-Driven Embedded Control. Quantifying Hand Gesture Recognition Delays for

- Bilateral Rehabilitation. *IEEE Access*, 9, 137809–137823. <https://doi.org/10.1109/ACCESS.2021.3118281>
5. González-Sánchez C, Sánchez-Brizuela G, **Cisnal A**, Fraile J-C, Pérez-Turiel J, Fuente-López Edl. (2021) Prediction of Cow Calving in Extensive Livestock Using a New Neck-Mounted Sensorized Wearable Device: A Pilot Study. *Sensors*. 21(23):8060. <https://doi.org/10.3390/s21238060>
 6. **Cisnal, A.**, Moreno-SanJuan, V., Fraile, J. C., Turiel, J. P., de-la-Fuente, E., & Sánchez-Brizuela, G. (2022). Assessment of the Patient’s Emotional Response with the RobHand Rehabilitation Platform: A Case Series Study. *Journal of Clinical Medicine*, 11(15). <https://doi.org/10.3390/jcm11154442>
 7. Sánchez-Brizuela G, Santos-Criado F-J, Sanz-Gobernado D, de la Fuente-López E, Fraile J-C, Pérez-Turiel J, **Cisnal A.** (2022) Gauze Detection and Segmentation in Minimally Invasive Surgery Video Using Convolutional Neural Networks. *Sensors*. 22(14):5180. <https://doi.org/10.3390/s22145180>
 8. **Cisnal, A.**, Gordaliza, P., Pérez Turiel, J., & Fraile, J. C. (2023). Interaction with a Hand Rehabilitation Exoskeleton in EMG-Driven Bilateral Therapy: Influence of Visual Biofeedback on the Users’ Performance. *Sensors*, 23(4), 2048. <https://doi.org/10.3390/s23042048>
 9. Barria, P., Riquelme, M., Reppich, H., **Cisnal, A.**, Fraile, J.C., Pérez-Turiel, J., Sierra, D., Aguilar, R., Andrade, A., Núñez-Espinosa, C. (2023). Hand Rehabilitation Based on the RobHand Exoskeleton in Stroke Patients: a Case Series Study. *Front. Robot. Al.*, 10 (42). <https://doi.org/10.3389/frobt.2023.1146018>
 10. Fontúrbel, C., **Cisnal, A.**, Fraile-Marinero, J.C., Pérez-Turiel, J. (2023) Force-based Control Strategy for a Collaborative Robotic Camera Holder in Laparoscopic Surgery Using Pivoting Motion. *Front. Robot. Al.*, 10:1145265. <https://doi.org/10.3389/frobt.2023.1145265>
 11. **Cisnal, A.**, Antolínez, D., Turiel, J.P., Fraile, J.C., de la Fuente, E. (2023) A versatile Embedded Platform for Implementation of Biocooperative Control in Upper-Limb Neuromotor Rehabilitation Scenarios. *IEEE Access*, 11, 35726–35736. <https://doi.org/doi:10.1109/ACCESS.2023.3265898>
 12. Sánchez-Brizuela, G., **Cisnal, A.**, de la Fuente-López, E., Fraile, J.C., Pérez-Turiel, J. (2023) Lightweight Real Time Hand Segmentation Leveraging MediaPipe Landmark Detection. *Virtual Reality*. (Under Review)

B.2.2. International conferences

1. **Cisnal, A.**, Alonso, R., Turiel, J. P., Fraile, J. C., Lobo, V., & Moreno, V. (2019). EMG Based Bio-Cooperative Direct Force Control of an Exoskeleton for Hand Rehabilitation: A Preliminary Study. ICNR BIOSYSROB, 21, 390–394. https://doi.org/10.1007/978-3-030-01845-0_78
2. Villar, B. F., **Cisnal, A.**, Vargas, M.M, Turiel, J.P., Fraile, J.C. (2021). A Low Cost IoT Enabled Device for the Monitoring, Recording and Communication of Physiological Signals.. BIODEVICES, 135-143.
3. **Cisnal, A.**, Moreno-SanJuan, V., Sierra, D., Turiel, J.P., Fraile, J.C. (2022). An Embedded Implementation of EMG-Driven Control for Assisted Bilateral Therapy. In: Torricelli, D., Akay, M., Pons, J.L. (eds) Converging Clinical and Engineering Research on Neurorehabilitation IV. ICNR 2020. Biosystems & Biorobotics, vol 28. Springer, Cham. https://doi.org/10.1007/978-3-030-70316-5_130

B.2.2. National conferences

1. **Cisnal, A.**, Lobo, V, Moreno, V. Fraile, J.C., Alonso, R., Turiel, J.P (2018). Robhand, un exoesqueleto de mano para la rehabilitación neuromotora aplicando terapias activas y pasivas. XXXIX Jornadas de Automática, 34-41.
2. **Cisnal, A.**, Moreno, V., Turiel, J.P., Alonso, R., Fraile, J.C., Lobo, V. (2019). Estrategia para el control háptico, basado en electromiografía, de un exoesqueleto de mano para neurorehabilitación. 11º Simposio CEA de Bioingeniería, 164-178.
3. **Cisnal, A.**, Sierra, D., Turiel, J. P., Fraile, J. C. (2021). Solución integrada de control basado en EMG para la rehabilitación de terapias bilateral en exoesqueleto de rehabilitación de mano RobHand. XLII Jornadas de Automática, 152-159.
4. **Cisnal, A.**, Sierra, D., Turiel, J. P., Fraile, J. C., de la Fuente, E. (2021). Integración de Bio-realimentación visual de EMG en un exoesqueleto de rehabilitación de mano (RobHand) utilizando entornos de realidad virtual. XII Simposio CEA de Bioingeniería, 89–94.
5. **Cisnal, A.**, Martínez-Cagigal, V., Alonso-Linaje, G., Moreno-Calderón, S., Turiel, J. P., Hornero, R., Carlos, J., & Marinero, F. (2022). An Overview of M3Rob, a Robotic Platform for Neuromotor and Cognitive

Rehabilitation Using Augmented Reality. XL Congreso Anual de La Sociedad Española de Ingeniería Biomédica., 180–183.

6. **Cisnal, A.**, Alonso-Linaje, G., Granja, J., Veganzones, M., Pérez-Turiel, J., Fraile, J.C. (2023). M3Rob: Plataforma robotizada para la rehabilitación de muñeca. Aspectos de diseño y arquitectura de control. XLIV Jornadas de Automática 2023 (Under Review).

B.3. International internship

Four-month research internship at the Spinal Cord Injury & Artificial Intelligence (SCAI) Lab of the Swiss Federal Institute of Technology in Zurich (Eidgenössische Technische Hochschule Zürich, ETHZ), located at the Swiss Paraplegic Center (SPZ) in Nottwil (Switzerland).

The long-term goal of SCAI Lab is to develop personalized and cost-effective health care solution for Spinal Cord Injury (SCI) population to improve their functioning in daily life. The location of the laboratory offers optimal opportunities for interaction between patients, scientists, and clinicians. The laboratory is run by Dr. Diego Páez-Granados and is supervised by Professor Robert Riener.



September 2022 SMS group picture.

The SCAI Lab is part of the Sensory-Motor Systems (SMS) Lab, run by Professor Robert Riener. The SMS-Lab focuses on the study of human-sensory motor control, the design of robots and optimization of human-machine interaction, mainly applied to rehabilitation and sports fields.

The main purpose of the research stay was to develop machine learning models for ambulatory blood pressure (BP) estimation using photoplethysmography (PPG). PPG is a non-invasive optical method for the detection of volumetric changes in blood in peripheral circulation. This work was part of the project "Remote Continuous Cardiovascular Function Monitoring for Ambulatory SCI". The development of the study included: (1) a state-of-the-art revision of blood pressure techniques, (2) signal preprocessing, (3) feature extraction and selection, (4) development of BP estimation models, (5) validation and analysis of the results, and (6) presentation.

B.4. Participation in Research Projects

Contract researcher:

Robot para rehabilitación de las funciones de la mano mediante terapias activas, en personas con discapacidad neuromotora (RobHand)

Main researcher: Juan Carlos Fraile Marinero

Funding: CDTI, Proyecto de investigación y desarrollo (IDI-20170263)

Duration: January 2017 – December 2019

Sistema robótico para neurocirugía endoscópica endonasal

Main researcher: Juan Carlos Fraile Marinero

Funding: Ministerio de Economía y competitividad (DPI2016-80391-C3-3-R)

Duration: January 2017 - December 2019

Desarrollo de un nuevo modelo de gestión eficiente del rebaño de vacuno de carne en extensivo, basado en el control individual de cada animal (CIVEX).

Main researcher: Juan Carlos Fraile Marinero

Funding: CDTI (IDI-20180355)

Duration: January 2018 – December 2020

Research team member:

Robot háptico tipo exoesqueleto, para rehabilitación de las funciones de la mano mediante terapias activas, en personas con discapacidad neuromotora.

Main researcher: Eduardo Zalama Casanova

Funding: Consejería de Educación de la Junta de Castilla y León (VA007G19)
Duration: January 2019 – December 2021

Coordinación quirúrgica multi-robot - evaluación de competencias en cirugía robotizada de anastomosis

Main researcher: Juan Carlos Fraile Marinero and Javier Pérez Turiel
Funding: Ministerio de Ciencia e Innovación (PID2019-111023RB-C33)
Duration: June 2020 – December 2022

Plataforma para rehabilitación neuromotora y cognitiva mediante terapias activas, en personas que han sufrido un accidente cerebro-vascular - M3Rob.

Main researcher: Juan Carlos Fraile Marinero
Funding: Ministerio de Ciencia e Innovación. Retos colaboración (RTC2019-007350-1)
Duration: January 2020 – December 2023

Desarrollo y ensayos clínicos de una plataforma de rehabilitación para acelerar la recuperación de pacientes con secuelas neuromotoras producidas por el COVID.

Main researcher: Juan Carlos Fraile Marinero
Funding: ADE (Agencia de Desarrollo Económico) de la Junta de Castilla y León (Referencia: 14/21/SA/0005)
Duration: September 2021 – December 2022

Research advisor:

Desarrollo y realización de un prototipo de laboratorio de un dispositivo instrumental de análisis de suelos y fluidos en tiempo real (SINUMLAB)

Main researcher: Juan Carlos Fraile Marinero
Funding: ADE (Agencia de Desarrollo Económico) de la Junta de Castilla y León (04/18/SA/0016)
Duration: January 2020 – September 2022

Electrificación de la movilidad en minas chilenas: desarrollo de estrategias y servicios de gestión para movilidad sostenible

Main researcher: Juan Carlos Fraile Marinero and Javier Pérez Turiel
Funding: CDTI (IDI-20200746)
Duration: January 2022 – December 2022

Desarrollo de nueva tecnología de electroencefalografía para sistemas Brain Computer Interface asistenciales.

Main researcher: Juan Carlos Fraile Marinero

Funding: CDTI (IDI-20220556)
Duration: June 2022 – June 2024

B.5. Other activities

- 2019/2020: **Speaker** in the course *Wall-e-dolit: to BOT or not to BOT*, organized by the Local BEST Group Valladolid.
- 2019/2020: **Award** *Premio Prometeo* for the project *Exoesqueleto de mano para la recuperación de movimientos funcionales primarios*, at Departamento de Innovación de la Fundación General de la Universidad de Valladolid (FUNGE)
- 2019/2020: **Course** *CS50's Introduction to Game Development*, at HarvardX (EDX)
- 2019/2020: **Course** *Cómo comunicar la ciencia*, at Departamento de Innovación de la Fundación General de la Universidad de Valladolid (FUNGE)
- 2019/2020: **Course** *Propiedad industrial e Intelectual*, at Departamento de Innovación de la Fundación General de la Universidad de Valladolid (FUNGE)
- 2019/2020: **Course** *Inteligencia Computacional aplicada al Monitoreo de Condición*, at Departamento de Ingeniería de Sistemas y Automática, Universidad de Valladolid
- 2020/2021: **Virtual assistance** and **speaker** at *5th International Conference on NeuroRehabilitation (ICNR2020)*
- 2020/2021: **Assistant professor** at Departamento de Ingeniería de Sistemas y Automática, Universidad de Valladolid (26 hours)
- 2020/2021: **Course** *Machine Learning*, at Stanford Online (Coursera)
- 2020/2021: **Grant** from the *Regional Ministry of Education* for the predoctoral hiring of research personnel co-financed by the European Social Fund (ESF) (2020-2024)
- 2020/2021: **Course** *Estadística en R*, at Escuela de Doctorado Universidad de Valladolid (ESDUVA)
- 2021/2022: **Assistance** and **speaker** at *Jornadas de Automática 2021*
- 2021/2022: **Assistant professor** at *Departamento de Ingeniería de Sistemas y Automática*, Universidad de Valladolid (60 hours)

- 2021/2022: **Certificate** *in Advance English*, Cambridge
- 2021/2022: **Course** *Scopus: Presentación de Scopus LibGuide - Preguntas y Respuestas*, by FECYT/Elsevier
- 2021/2022: **Course** *Scopus: Perspectiva institucional/Más allá de Scopus*, by FECYT/Elsevier
- 2021/2022: **Course** *Scopus: Perfiles de autor*, by FECYT/Elsevier
- 2021/2022: **Course** *Scopus: Métricas*, by FECYT/Elsevier
- 2021/2022: **Course** *Deep Learning Specialization*, at Coursera. Completion of all 5 courses of Deep Learning Specialization: Neural Networks and Deep Learning, Improving Deep Neural networks: Hyperparameters Tuning, Regularization and Optimization, Structuring Machine Learning Projects, Convolutional Neural Networks and Sequence Models.
- 2021/2022: **Assistance** at the *2022 Summer School on Neurorehabilitation*
- 2021/2022: **Virtual assistance** and **speaker** at *Undécima Jornada de Ciencia y Tecnología*
- 2022/2023: **Assistant professor** at *Departamento de Ingeniería de Sistemas y Automática*, Universidad de Valladolid (60 hours)
- 2022/2023: **Grant** *Eramus+ Internship Programme* at the ETHZ, Swizertland (2022)
- 2022/2023: **Workshop** Enseñando Ingeniería Robótica con Matlab&Simulink, by MathWorks
- 2022/2023: **Webinar** El profesorado en la LOSU: Claves de la nueva ley universitaria, by Centro de Enseñanza Online, Formación e Innovación Docente de la Universidad de Valladolid (VirtUVA)
- 2022/2023: **Course** OnCampus CyL 2023, by Instituto para la Competitividad Empresarial (ICE) de Castilla y León
- 2022/2023: **Assistance** at Jornadas Nacionales de Robótica y Bioingeniería 2023

Appendix C

Resumen en castellano

C.1. Introducción

El empleo de robots en el ámbito de la neurorrehabilitación surgió como una herramienta innovadora para facilitar el entrenamiento intensivo y repetitivo y promover la recuperación motora y la independencia funcional en pacientes con trastornos neurológicos. A diferencia de la robótica de rehabilitación tradicional, que se basa principalmente en información biomecánica, los controles biocooperativos en la robótica de rehabilitación van más allá al incorporar información psicológica y/o fisiológica, integrando al paciente en el control de manera más eficiente (Riener and Muni, 2010). Estos dispositivos robóticos proporcionan diferentes tipos de asistencia y pueden ser controlados por diferentes modalidades de entrada, como la electromiografía (EMG), la electroencefalografía (EEG) y la información cinemática. Entre estas modalidades de entrada, la EMG es la más utilizada debido a su capacidad para proporcionar información en tiempo real sobre los patrones de activación muscular, lo que posibilita un control biocooperativo entre el usuario y el robot (Li et al., 2020).

Este enfoque biocooperativo proporciona una interacción bilateral entre el humano y el robot, promoviendo la participación activa del usuario (Koenig et al., 2011). Esto es de gran importancia en el contexto de la neurorrehabilitación, ya que se ha comprobado que la participación activa del paciente mejora la plasticidad neuronal y facilita el aprendizaje motor (Blank et al., 2014).

Sin embargo, el estado actual de los sistemas biocooperativos dificulta su introducción en entornos clínicos, principalmente debido a su falta de robustez y su limitada accesibilidad (Meattini et al., 2018). Los problemas de confiabilidad se deben fundamentalmente al alto coste asociado con los sistemas de adquisición de señales fisiológica necesarios, lo que representa una restricción significativa para la llevar a cabo la investigación necesaria en este campo. Además, la falta de capacidades de procesamiento de estos sistemas dificulta el desarrollo de estrategias de control biocooperativo en tiempo real y, en consecuencia, una interacción eficiente entre humanos y robots. Por último, el tamaño voluminoso de los sistemas de adquisición fisiológica afecta negativamente a la aceptación por parte de los usuarios (Rodgers et al., 2019).

En este contexto, esta Tesis Doctoral se enfoca en el diseño de sistemas embebidos de tiempo real y bajo coste para la adquisición de señales fisiológicas y el desarrollo de estrategias de control biocooperativo que contribuyan a brindar aplicaciones prácticas en el campo de la neurorrehabilitación motora del miembro superior. Esta es un área de gran importancia, considerando que la paresia del miembro superior es uno de los resultados más frecuentemente observados después de un accidente cerebrovascular, y tiene un profundo impacto en la calidad de vida y la independencia de los sobrevivientes de accidentes cerebrovasculares (Fischer et al., 2007).

En esta Tesis Doctoral se presenta un compendio de tres publicaciones indexadas en el *Journal Citations Reports* (JCR) entre los años 2021 y 2023. El primer artículo (Cisnal et al., 2021) se centra en el diseño de un sistema de tiempo real, embebido, y de bajo coste para la adquisición de señales de EMG. Se desarrolla un paradigma de entrenamiento bilateral basado en un control de EMG sin reconocimiento de patrones. El control reconoce los gestos realizados por la mano sana (apertura, cierre y reposo) mediante el análisis de las señales de EMG, y los replica en un exoesqueleto robótico colocado en la mano parética. En el segundo artículo (Cisnal et al., 2023b) se procede a la incorporación de un mecanismo de retroalimentación visual basado en EMG al sistema de rehabilitación propuesto anteriormente, con el fin de evaluar y analizar la influencia de dicha retroalimentación visual en el rendimiento de los usuarios.

Tras la evaluación del desempeño del sistema de control embebido basado en EMG integrado en el robot de rehabilitación de mano, se lleva a cabo un avance adicional y se desarrolla una solución asequible que permita no solo el registro de señales de EMG, sino también la captación de otras señales fisiológicas relevantes contexto del control biocooperativo aplicado a la neurorrehabilitación robótica de las extremidades superiores. En el tercer

artículo, se presenta un sistema embebido multimodal, de bajo costo y portátil (Cisnal et al., 2023a). El rendimiento del sistema se valida mediante la implementación de dos escenarios biocooperativo de neurorrehabilitación.

C.2. Objetivos

El objetivo general de esta Tesis Doctoral es diseñar, desarrollar y evaluar estrategias de control biocooperativo en el contexto de la rehabilitación neuromotora del miembro superior, y proporcionar tecnología asequible para su implementación con el objetivo de lograr un uso generalizado en entornos clínicos. Este objetivo general implicó el diseño y desarrollo de sistemas embebidos para la adquisición de señales fisiológicas y su integración en sistemas de rehabilitación neuromotora mediante la implementación y evaluación de estrategias de control asistido. Con el fin de lograr este objetivo general, surgen los siguientes objetivos específicos:

- I. Realizar una revisión exhaustiva de la literatura y examinar el estado actual de las plataformas de rehabilitación neuromotora del miembro superior, con énfasis particular en las estrategias de control que integran el elemento humano en el bucle de control a través del análisis de señales fisiológicas.
- II. Diseñar y desarrollar sistemas embebidos asequibles para el registro y procesamiento de señales fisiológicas y la ejecución en tiempo real del paradigma de control de los sistemas de rehabilitación.
- III. Diseñar y desarrollar estrategias de control biocooperativo para las soluciones embebidas en tiempo real desarrolladas y su integración en plataformas de rehabilitación preexistentes.
- IV. Realizar una evaluación exhaustiva del rendimiento de los sistemas de rehabilitación biocooperativos propuestos, incluyendo el análisis de la precisión, el tiempo de respuesta y el rendimiento del usuario.
- V. Evaluar el rendimiento del sistema embebido y portátil de adquisición multimodal, centrándose en su versatilidad, consumo de energía y confiabilidad de las señales registradas para la implementación de controles biocooperativos.
- VI. Diseminar los resultados principales y las conclusiones de este estudio en revistas indexadas en JCR, así como en conferencias nacionales e internacionales.

C.3. Materiales y métodos

La metodología de los distintos estudios comparte la misma estructura general, compuesta por las siguientes etapas: revisión del estado del arte y justificación del trabajo, descripción de la plataforma robótica de rehabilitación utilizada, definición del procedimiento experimental para la evaluación del sistema propuesto, y presentación de métricas y análisis estadísticos empleados.

Dos plataformas robóticas de rehabilitación son utilizadas en esta tesis doctoral con el fin de validar los sistemas embebidos de control biocooperativo desarrollados: RobHand y M3Rob. RobHand (*Robot for Hand Rehabilitation*) es un robot de rehabilitación de mano de tipo exoesqueleto que asiste a la flexión y extensión de los dedos de la mano (Moreno-San Juan et al., 2021). M3Rob (Mente-Mano-Mueca Robot) es un robot de rehabilitación de muñeca de tipo exoesqueleto que asiste a los movimientos de pronación/supinación, flexión/extensión y desviación radial/ulnar (Cisnal et al., 2022a).

Para la evaluación de los sistemas desarrollados se realizan dos estudios experimentales. Los estudios contaron con diez y dieciocho sujetos sanos mayores de 18 años, sin discapacidad neurológica o motora, que se ofrecieron voluntariamente para el estudio y proporcionaron su consentimiento informado por escrito. En ambos estudios los sujetos realizaban terapias bilaterales basadas en EMG con el exoesqueleto de mano RobHand. Los sujetos llevaban el exoesqueleto en su mano no dominante (correspondiendo a la mano parética del paciente) y se registraban las señales de EMG del brazo dominante (correspondiendo al miembro no afectado del paciente). En ambos estudios los sujetos realizaban una calibración previa y se les pedía que hicieran una serie de gestos con la mano (apertura, reposo y cierre) mientras se registraban las señales EMG. Un ordenador proporcionaba información visual y auditiva sobre la secuencia de gestos a realizar (gestos objetivos). Los datos relacionados con las señales EMG registradas y la secuencia de gestos objetivo fueron guardados en una base de datos para su posterior análisis. Además, en un estudio los sujetos llevaban el guante 5DT Data Glove (5DT Technologies) para registrar la posición de la mano sana. En el otro estudio, los sujetos realizaron las secuencias de gestos en cuatro condiciones diferentes, resultaron de la combinación de utilizar o no una retroalimentación visual de EMG y una retroalimentación visual cinestésica generada por el movimiento del exoesqueleto.

La evaluación del desempeño de un sistema de rehabilitación basado en el reconocimiento de gestos requiere una atención particular en la interacción humano-robot. Para lograr una interacción confiable y natural, se necesita una

combinación de capacidad de respuesta adecuada y una detección precisa de los gestos. Largos tiempos de retardo pueden tener consecuencias adversas e influir negativamente en la satisfacción del usuario hacia la terapia asistida por robot (Yang y Dorneich, 2015). Del mismo modo, la asistencia incorrecta en el movimiento afecta negativamente la satisfacción e incluso puede provocar daños físicos. Por lo tanto, es esencial determinar los retrasos temporales relevantes y la eficacia de la clasificación de gestos del sistema desarrollado.

Un control de reconocimiento de gestos basado en EMG puede ser abordado como un problema de clasificación. En este sentido, la matriz de confusión y las métricas derivadas de la misma son ampliamente utilizadas para evaluar la calidad de un clasificador (Grandini et al., 2020). Por otro lado, el análisis del tiempo de respuesta se realizará utilizando las siguientes métricas temporales: tiempo de selección de movimiento (*motion-selection time*, MST), tiempo de comienzo del movimiento (*motion-onset time*, MOT), tiempo de finalización de movimiento (*motion-completion time*, MCT) y tasa de movimientos completados (*motion-completion rate*). Algunas de estas métricas fueron utilizadas por (Li et al., 2010) y otras han sido propuestas en el contexto de este trabajo.

La evaluación del rendimiento del usuario bajo diferentes condiciones de configuración de retroalimentación de la plataforma es evaluada mediante medidas de similitud para series temporales y pruebas estadísticas paramétricas. Una medida de similitud se define matemáticamente como una función de valor real que cuantifica la similitud entre dos entidades, en este contexto entre dos series temporales. Una de las medidas de similitud más utilizadas son las de paso fijo ya que son relativamente sencillas, intuitivas y tienen un bajo coste computacional. Las métricas de paso fijo más típicas son la distancia Manhattan (norma L1) y la distancia Euclidiana (norma L2). Sin embargo, las métricas de paso fijo son altamente sensibles al ruido y a los desalineamientos temporales ya que la distancia se calcula desde el punto i de una serie temporal hasta el punto i de otra serie (Ding et al., 2008). Por lo tanto, antes de calcular las medidas de distancia, es necesario sincronizar de las dos series temporales. Una forma de sincronización de dos series temporales es calculando el desfase en el cual su correlación cruzada es la más alto. Por último, para el cálculo de las distancias entre series temporales es necesario codificar los gestos de la mano. Estos son codificados en el siguiente orden: "abierto" < "reposo" < "cerrado", de tal manera que un error entre "abierto" y "cerrado" se considera más grave que un error entre "abierto" y "reposo".

Los análisis estadísticos permiten realizar comparaciones de datos entre múltiples grupos proporcionan información valiosa sobre la relación entre variables. El test de análisis de la varianza (ANOVA) multifactorial permite

evaluar múltiples variables dependientes simultáneamente. El test de Rango Múltiple de Duncan es una prueba post hoc que compara todas las posibles combinaciones de medias de grupos para identificar cuáles pares difieren significativamente.

C.4. Resultados y discusión

Los resultados principales de esta tesis son: (1) el diseño de los sistemas embebidos para el registro de señales fisiológicas, (2) el desarrollo de estrategias de control biocooperativo desarrolladas y su implementación en estos sistemas, y (3) la evaluación del rendimiento. A continuación, se presenta los resultados principales de cada investigación y su correspondiente implicación en el campo de la robótica de neurorrehabilitación.

- Control embebido basado en EMG en tiempo real (Cisnal et al., 2021)

El sistema embebido para la adquisición de señales EMG se caracteriza por tener dos canales diferenciales de 24 bits de resolución y un rango dinámico de 112 dB. Los canales consisten en un amplificador de instrumentación con una ganancia de 50, seguido de un filtro paso bajo RC con una frecuencia de corte de 150 Hz. Los canales están diseñados para compensar el desplazamiento diferencia de entrada y evitar la saturación del amplificador de instrumentación. Además, el sistema cuenta con la interfaz analógica MCP3912 (Microchip Technology Inc., AZ, USA), que se caracteriza por tener convertidores Delta-Sigma ADC síncronos, los cuales se comunican con el microcontrolador TMS320F28069M (Texas Instruments, TX, USA) utilizando comunicación SPI y otras señales de control digital.

La placa de circuito impreso (PCB) de 4 capas tiene planos de tierra divididos para separar los circuitos analógicos, digitales y de alimentación y asegurar la integridad de la señal. Los componentes discretos de montaje en superficie se colocan en las capas superior e inferior, resultando en un tamaño de placa de 50.8 x 33 mm y un área activa de 10 cm² y un consumo de 3 mW de una alimentación de 3.3 V DC.

Se diseña un control embebido por umbrales basado en señales EMG para la realización de terapias bilaterales asistidas con el exoesqueleto de mano RobHand. La estrategia de control desarrollada detecta los gestos de la mano sana (apertura, cierre o reposo) mediante el análisis de las señales EMG y los replica en el exoesqueleto colocado en la mano paretica.

Las señales de EMG de los músculos *extensor digitorum* (ED) y *flexor digitorum superficiales* (FDS), responsables de la apertura y cierre de la mano, se registran a una frecuencia de 200 Hz y, son filtradas para eliminar el ruido

de base y las interferencias electromagnéticas. Posteriormente, son rectificadas mediante el cálculo RMS de 10 puntos y un filtro de pasa bajas, resultando en una señal con una frecuencia de 20 Hz. La normalización se realiza con respecto al MVC (contracción voluntaria máxima).

Los valores de MVC y los umbrales de EMG se calculan en una calibración previa, específica para cada usuario y sesión. En esta calibración se les pide a los usuarios que relajen, abran y cierran la mano durante 8 s. Los valores de MVC se calculan como el valor máximo de la señal rectificada de EMG correspondiente. Los umbrales de EMG corresponden a los valores límite máximos de desactivación muscular (es decir, al inicio de la activación muscular) más una constante de 0.1.

El algoritmo de reconocimiento de gestos se basa en una serie de expresiones algebraicas y solo depende de los valores normalizados de las señales EMG y de los umbrales determinados en la calibración. El módulo de reconocimiento de gestos actualiza los gestos cada 50 ms, que corresponde con el periodo de las señales de EMG normalizadas.

La precisión general del algoritmo de reconocimiento de gestos basado en EMG es del 97% y el tiempo de las clasificaciones erróneas durante los gestos es mínimo. Esto significa que en el 98,4% de los casos, el error no es perceptible en el exoesqueleto, ya que los actuadores no comienzan a moverse en dirección opuesta al movimiento previsto. Respecto al tiempo de respuesta del sistema, la media y la desviación estándar del MST y el MOT fueron de 0.48 ± 0.59 s y 0.55 ± 0.60 s, respectivamente. El MCT fue de 1.90 ± 1.65 s, variando desde 0.98 s (de gesto de reposo) hasta 3.42 s (de gesto de abrir a cerrar). El MCT depende de la velocidad de los actuadores y se consideró suficientemente largo para garantizar la seguridad del usuario durante la rehabilitación. La tasa de finalización del movimiento fue del 100%, ya que el MCT no superó el límite de tiempo predefinido de 5 s en ningún caso.

El control basado por EMG propuesto fue implementado en el sistema embebido desarrollado con el objetivo de permitir la rehabilitación mediante terapias bilaterales con un exoesqueleto de mano. La precisión del algoritmo de reconocimiento de gestos es adecuada y está en el rango de otros sistemas de control propuestos en la literatura, que varían del 77.9 al 98.7 %. En cuanto a la respuesta del sistema, los resultados no son comparables con los ofrecidos por la literatura ya que este aspecto no es estudiado en profundidad. Se puede concluir que el sistema embebido de tiempo real desarrollado, a pesar de su bajo coste (menos de 30€ para producción a baja escala), permite la implementación del control basado en EMG en tiempo real. Esto se traduce en una reducción del tiempo de latencia del sistema, mientras se mantiene una precisión elevada en el reconocimiento de gestos.

- Influencia de la retroalimentación visual basada en EMG en el rendimiento del usuario (Cisnal et al., 2023b)

La técnica de la retroalimentación basada en señales fisiológicas se introdujo hace más de cuarenta años en entornos de rehabilitación (Tate y Milner, 2010). Se ha demostrado que la retroalimentación basada en señales de EMG es beneficiosa en el tratamiento de diversas afecciones musculoesqueléticas, incluyendo la neurorrehabilitación (Giggins et al., 2013). Sin embargo, no hay estudios clínicos que hayan evaluado la efectividad de esta técnica en combinación con la rehabilitación física asistida por robots.

Por esta razón, se lleva a cabo un estudio sobre la influencia de la retroalimentación visual basada en EMG en el rendimiento del usuario durante la realización de terapias bilaterales con el sistema de rehabilitación propuesto. La retroalimentación visual involucra dos barras de longitud variable, etiquetadas como "*Fuerza de apertura*" y "*Fuerza de cierre*". Estas barras se nombran de esta manera para corresponder a la actividad de los músculos extensores y flexores, y mejorar la facilidad de uso. La longitud de la barra indica el valor instantáneo de las señales de EMG normalizadas, y su color indica el gesto reconocido. La retroalimentación visual se actualiza a 20 Hz, lo que corresponde a la frecuencia de las señales de sEMG normalizadas y la tasa de reconocimiento de gestos.

La influencia de la integración de la retroalimentación visual se evaluó mediante la distancia Euclidiana o norma L2. Antes del cálculo de la norma L2, las secuencias temporales de los gestos objetivos y reconocidos son codificadas y sincronizadas calculando el retraso mediante la correlación cruzada. El tiempo medio de retrasado calculado fue de 0.88 ± 0.14 s

Se observaron diferencias estadísticamente significativas en el rendimiento de los sujetos según el tipo de retroalimentación proporcionada (valor de p-valor = 0.0124). Específicamente, el rendimiento fue significativamente mejor cuando solo se presentaba la retroalimentación visual basada en EMG en comparación con la retroalimentación cinestésica por sí sola (p-valor = 0.0412) o la combinación de ambas (p-valor = 0.0497). Estos resultados sugieren que la retroalimentación visual de EMG permite aumentar el control de los sujetos sobre el movimiento de la plataforma robótica mediante la evaluación de su activación muscular en tiempo real.

La retroalimentación basada en EMG se proporciona antes en el tiempo que la retroalimentación cinestésica, por lo que el usuario tiene un mayor tiempo de reacción para autorregular sus niveles de activación muscular. De hecho, la retroalimentación basada en EMG es una representación visual de la señal de entrada del controlador de posición del robot, por lo que el usuario anticipa la respuesta del exoesqueleto y regula su fuerza si fuera necesario. En cambio,

la retroalimentación cinestésica requiere que el usuario sienta el movimiento realizado por el robot antes de poder regular su fuerza. Por otro lado, el hecho de que la retroalimentación basada en EMG resulte en un rendimiento significativamente mayor que en presencia de ambos tipos de retroalimentaciones puede deberse a que la cinestésica es más directa que la visual y, por lo tanto, los usuarios no muestran atención a la retroalimentación visual cuando la otra está presente.

En resumen, la retroalimentación visual basada en EMG permite a los usuarios monitorizar su activación muscular en tiempo real, y, por tanto, modular la fuerza ejercida. Este tipo de retroalimentación puede ser muy útil en la etapa de aprendizaje, permitiendo al usuario aprender más rápidamente cómo modular la activación de sus músculos para que el robot de rehabilitación se mueva según su intención. Esto puede resultar en una mejora de la motivación del paciente durante el proceso de rehabilitación al utilizar plataformas robóticas asistidas.

- Sistema embebido multimodal (Cisnal et al., 2023a)

Se diseña un sistema embebido y portátil integrado por múltiples sensores, microcontroladores en tiempo real de alta eficiencia y comunicación inalámbrica, proporciona una solución altamente flexible y configurable lo que ofrece amplias posibilidades para el desarrollo de controles biooperativos en el contexto de la neurorrehabilitación. El sistema funciona con batería e integra cinco sensores: unidad de medición inercial (*inertial measurement unit*, IMU), electrocardiograma (ECG), electromiografía (EMG), sensor galvánico de respuesta de la piel (*galvanic skin response*, GSR) y termómetro cutáneo (*skin thermometer*, SKT). Estos sensores se comunican con el microcontrolador TMS320F28069M (Texas Instrumentes, TX, USA) para el procesamiento y el control de datos en tiempo real. Los datos registrados y procesados pueden ser transmitidos por el microcontrolador CC2650 (Texas Instruments, TX, USA), con tecnología Bluetooth de baja energía (BLE). Además, el sistema dispone de un puerto JTAG para el acceso temporal de los microcontroladores.

La placa de circuito impreso fue diseñada para optimizar la integridad de la señal y su diseño se basa en nueve submódulos. Los planos de alimentación están separados y se utilizan pistas de 12 mil de ancho, excepto para las señales de alimentación de 24 mil. Para reducir los costos de ensamblaje, todos los componentes se colocan en la capa superior, excepto el termómetro. El tamaño resultante de la placa es de 63x83 mm, incluyendo tres agujeros para fijación con tornillos en la caja. La caja está diseñada para la colocación en el brazo.

Se proponen dos posibles aplicaciones de rehabilitación para la validación del sistema: control de reconocimiento de movimiento y control adaptativo. Las aplicaciones utilizan señales diferentes y los enfoques de rehabilitación son distintos. Mientras que la primera no requiere un dispositivo de robótico de asistencia y utiliza información del IMU y EMG, la segunda utiliza el robot de rehabilitación de mano M3Rob y utiliza información relativa al ECG, GSR y SKT. Se ha verificado que, aunque el sistema es de bajo costo, la calidad de las señales adquiridas es confiable para implementar los dos algoritmos de control biocooperativo propuestas. Además, se han probado las capacidades de procesamiento de alta eficiencia de la plataforma. Esta plataforma admite la ejecución en tiempo real de algoritmos más complejos que los presentados para los dos escenarios de rehabilitación.

Una característica importante del sistema embebido portátil y multimodal, aparte de sus destacadas capacidades computacionales y alta versatilidad, es su consumo de energía. Tiene una vida útil de la batería de 5 horas para un consumo máximo de energía de alrededor de 1250 mW. Se ha analizado detenidamente el consumo de energía del sistema para los dos escenarios de rehabilitación propuestos, resultando en un consumo de 203 mW para el control de reconocimiento de movimiento y de 249 mW para el control adaptativo. El consumo de las dos aplicaciones de rehabilitación cumple plenamente con las restricciones de energía del sistema portátil.

El sistema portátil fue diseñado buscando el equilibrio entre complejidad, el precio y el rendimiento, teniendo en cuenta parámetros como el volumen, la flexibilidad, el consumo de energía, el procesamiento a bordo y la calidad de la señal. Debido a su bajo costo, tamaño compacto y versatilidad, la plataforma muestra un gran potencial para aplicaciones de rehabilitación. Si bien puede no ser adecuada para aplicaciones que requieren una alta calidad de señal o una vida útil de la batería a largo plazo, dichos requisitos no son típicamente esperados en aplicaciones de rehabilitación. Por lo tanto, la plataforma presentada es un avance prometedor en el desarrollo de tecnologías portátiles y bajo coste para la rehabilitación neuromotora.

C.5. Conclusiones

La evaluación de los sistemas de rehabilitación biocooperativos de bajo coste propuestos han mostrado resultados prometedores (Cisnal et al., 2021) (Cisnal et al., 2023a). Estos sistemas han demostrado la viabilidad de implementar controles biocooperativos sin necesidad de sistemas comerciales costosos que suelen ser voluminosos y carecen de capacidades de procesamiento. Las ventajas asociadas con estas soluciones embebidas para la adquisición de señales fisiológicas, además de su bajo costo y versatilidad, incluyen la

posibilidad de desarrollar controles biocooperativos en tiempo real con una latencia reducida y un alto grado de precisión. Estas características hacen que las soluciones de adquisición integradas sean una opción atractiva para el desarrollo de sistemas de control biocooperativo accesibles y asequibles en entornos clínicos de rehabilitación. Además, el uso de estos sistemas también puede abrir el camino para el desarrollo de nuevas aplicaciones en los campos de la interacción humano-robot y la robótica asistencial.

Se ha demostrado que la incorporación de la retroalimentación visual basada en EMG puede mejorar significativamente el rendimiento de las personas que se someten a terapias asistidas impulsadas por EMG. Al proporcionar retroalimentación visual en tiempo real, los sujetos pudieron monitorear y modular sus respuestas EMG, lo que resultó en un mejor control de la fuerza ejercida. Por lo tanto, se puede inferir que la retroalimentación visual basada en EMG tiene el potencial de facilitar el proceso de aprendizaje de la rehabilitación, ya que ayuda a los usuarios a desarrollar una mejor comprensión de cómo autorregular sus activaciones musculares. Esto podría mejorar la motivación de los pacientes y contribuir a mejores resultados de recuperación motora (Cisnal et al., 2023b).

Como último punto, es necesario hacer mayor énfasis en la capacidad de respuesta y los tiempos de latencia en los sistemas de rehabilitación impulsados por EMG (Cisnal et al., 2021). Estudios anteriores se han centrado principalmente en la precisión de la clasificación de los gestos, descuidando información importante sobre el tiempo de latencia del sistema. Si bien algunos estudios han abordado la latencia del sistema, los valores medidos a menudo están imprecisamente definidos. Es crucial establecer definiciones claras y estandarizadas de los tiempos de latencia en la robótica de rehabilitación para garantizar la homogeneidad en este campo de investigación. Al hacerlo, podemos asegurarnos de que el desarrollo de los sistemas de rehabilitación basados en EMG esté optimizado en beneficio de los pacientes.

Bibliography

- Ada, L., Canning, CG., Low, SL., 2003. Stroke patients have selective muscle weakness in shortened range. *Brain* 126, 724–731. <https://doi.org/10.1093/brain/awg066>
- Almekkawy, M., Zderic, V., Chen, J., Ellis, M.D., Haemmerich, D., Holmes, D.R., Linte, C.A., Panescu, D., Pearce, J., Prakash, P., 2020. Therapeutic Systems and Technologies: State-of-the-Art Applications, Opportunities, and Challenges. *IEEE Rev Biomed Eng* 13, 325–339. <https://doi.org/10.1109/RBME.2019.2908940>
- Badesa, F.J., Morales, R., Garcia-Aracil, N., Sabater, J.M., Casals, A., Zollo, L., 2014. Auto-adaptive robot-aided therapy using machine learning techniques. *Comput Methods Programs Biomed* 116, 123–130. <https://doi.org/10.1016/j.cmpb.2013.09.011>
- Battista, N.A., Strickland, W.C., Miller, L.A., 2017. IB2d: A Python and MATLAB implementation of the immersed boundary method. *Bioinspir Biomim* 12. <https://doi.org/10.1088/1748-3190/aa5e08>
- Ben, I.A., Bouteraa, Y., Rekik, C., 2017. Design and development of 3d printed myoelectric robotic exoskeleton for hand rehabilitation. *International Journal on Smart Sensing and Intelligent Systems* 10, 341–366. <https://doi.org/10.21307/ijssis-2017-215>
- Benatti, S., Casamassima, F., Milosevic, B., Farella, E., Schönle, P., Fateh, S., Burger, T., Huang, Q., Benini, L., 2015. A Versatile Embedded Platform for EMG Acquisition and Gesture Recognition. *IEEE Trans Biomed Circuits Syst* 9, 620–630. <https://doi.org/10.1109/TBCAS.2015.2476555>
- Benatti, S., Milosevic, B., Casamassima, F., Schonle, P., Bunjaku, P., Fateh, S., Huang, Q., Benini, L., 2014. EMG-based hand gesture recognition with flexible analog front end, in: 2014 IEEE Biomedical Circuits and Systems Conference

- (BioCAS) Proceedings. IEEE, Lausanne, Switzerland, pp. 57–60. <https://doi.org/10.1109/BioCAS.2014.6981644>
- Bi, L., Feleke, A., Guan, C., 2019. A review on EMG-based motor intention prediction of continuous human upper limb motion for human-robot collaboration. *Biomed Signal Process Control* 51, 113–127. <https://doi.org/10.1016/j.bspc.2019.02.011>
- Blank, A.A., French, J.A., Pehlivan, A.U., O'Malley, M.K., 2014. Current Trends in Robot-Assisted Upper-Limb Stroke Rehabilitation: Promoting Patient Engagement in Therapy. *Curr Phys Med Rehabil Rep* 2, 184–195. <https://doi.org/10.1007/s40141-014-0056-z>
- Bo Nielsen, J., Willerslev-Olsen, M., Christiansen, L., Lundbye-Jensen, J., Lorentzen, J., 2015. Science-based neurorehabilitation: Recommendations for neurorehabilitation from basic science. *J Mot Behav* 47, 7–17. <https://doi.org/10.1080/00222895.2014.931273>
- Bosecker, C., Dipietro, L., Volpe, B., Igo Krebs, H., 2010. Kinematic Robot-Based Evaluation Scales and Clinical Counterparts to Measure Upper Limb Motor Performance in Patients With Chronic Stroke. *Neurorehabil Neural Repair* 24, 62–69. <https://doi.org/10.1177/1545968309343214>
- Burns, M.K., Pei, D., Vinjamuri, R., 2019. Myoelectric control of a soft hand exoskeleton using kinematic synergies. *IEEE Trans Biomed Circuits Syst* 13, 1351–1361. <https://doi.org/10.1109/TBCAS.2019.2950145>
- Carmeli, E., Peleg, S., Bartur, G., Elbo, E., Vatine, J.-J., 2011. HandTutor™ enhanced hand rehabilitation after stroke - a pilot study. *Physiotherapy Research International* 16, 191–200. <https://doi.org/10.1002/pri.485>
- Chen, M., Ho, S.K., Zhou, H.F., Pang, P.M.K., Hu, X.L., Ng, D.T.W., Tong, K.Y., 2009. Interactive rehabilitation robot for hand function training, in: 2009 IEEE International Conference on Rehabilitation Robotics (ICORR). Kyoto, Japan, pp. 777–780. <https://doi.org/10.1109/ICORR.2009.5209564>
- Chen, Y., Yang, Z., Wen, Y., 2021. A soft exoskeleton glove for hand bilateral training via surface EMG. *Sensors* 21, 1–18. <https://doi.org/10.3390/s21020578>
- Chien, W. tong, Chong, Y. yu, Tse, M. kei, Chien, C. woon, Cheng, H. yu, 2020. Robot-assisted therapy for upper-limb rehabilitation in subacute stroke patients: A systematic review and meta-analysis. *Brain Behav* 10, 1–16. <https://doi.org/10.1002/brb3.1742>
- Chowdhury, R.H., Reaz, M.B.I., Bin Mohd Ali, M.A., Bakar, A.A.A., Chellappan, K., Chang, T.G., 2013. Surface electromyography signal processing and classification techniques. *Sensors* 13, 12431–12466. <https://doi.org/10.3390/s130912431>

- Chu, J.U., Moon, I., Mun, M.S., 2006. A real-time EMG pattern recognition system based on linear-nonlinear feature projection for a multifunction myoelectric hand. *IEEE Trans Biomed Eng* 53, 2232–2239. <https://doi.org/10.1109/TBME.2006.883695>
- Cisnal, A., Alonso, R., Turiel, J.P., Fraile, J.C., Lobo, V., Moreno, V., 2019. EMG Based Bio-Cooperative Direct Force Control of an Exoskeleton for Hand Rehabilitation: A Preliminary Study, in: Masia, L., Micera, S., Akay, M., Pons, J. (Eds.), *Converging Clinical and Engineering Research on Neurorehabilitation III*. ICNR 2018. Biosystems & Biorobotics. Springer, Cham, pp. 390–394. https://doi.org/10.1007/978-3-030-01845-0_78
- Cisnal, A., Antolínez, D., Turiel, J.P., Carlos Fraile, J., De La Fuente, E., 2023a. A Versatile Embedded Platform for Implementation of Biocooperative Control in Upper-Limb Neuromotor Rehabilitation Scenarios. *IEEE Access* 11, 35726–35736. <https://doi.org/doi: 10.1109/ACCESS.2023.3265898>
- Cisnal, A., Gordaliza, P., Pérez Turiel, J., Fraile, J.C., 2023b. Interaction with a Hand Rehabilitation Exoskeleton in EMG-Driven Bilateral Therapy: Influence of Visual Biofeedback on the Users' Performance. *Sensors* 23, 2048. <https://doi.org/10.3390/s23042048>
- Cisnal, A., Martínez-Cagigal, V., Alonso-Linaje, G., Moreno-Calderón, S., Turiel, J.P., Hornero, R., Carlos, J., Marinero, F., 2022a. An Overview of M3Rob, a Robotic Platform for Neuromotor and Cognitive Rehabilitation Using Augmented Reality, in: *XL Congreso Anual de La Sociedad Española de Ingeniería Biomédica*. Valladolid, pp. 180–183.
- Cisnal, A., Moreno-SanJuan, V., Fraile, J.C., Turiel, J.P., de-la-Fuente, E., Sánchez-Brizuela, G., 2022b. Assessment of the Patient's Emotional Response with the RobHand Rehabilitation Platform: A Case Series Study. *J Clin Med* 11, 4442. <https://doi.org/10.3390/jcm11154442>
- Cisnal, A., Perez-Turiel, J., Fraile, J.C., Sierra, D., De La Fuente, E., 2021. RobHand: A Hand Exoskeleton with Real-Time EMG-Driven Embedded Control. Quantifying Hand Gesture Recognition Delays for Bilateral Rehabilitation. *IEEE Access* 9, 137809–137823. <https://doi.org/10.1109/ACCESS.2021.3118281>
- CNS Traumatic Brain Injury Rehab, 2023. What is Stroke | CNS Traumatic Brain Injury Rehab [WWW Document]. URL <https://www.neuroskills.com/brain-injury/stroke/what-is-stroke/> (accessed 3.8.23).
- Colebatch, J.G., Gandevia, S.C., 1989. The distribution of muscular weakness in upper motor neuron lesions affecting the arm. *Brain* 112, 749–763. <https://doi.org/10.1093/brain/112.3.749>
- Conforto, S., 2009. The role of the sEMG signal processing in the field of the Human Movement Analysis, in: Dösel, O., Schlegel, W.C. (Eds.), *World Congress on*

- Medical Physics and Biomedical Engineering, September 7 - 12, 2009, Munich, Germany. IFMBE Proceedings, Vol 25/9. Springer, Berlin, Heidelberg, pp. 523–526. https://doi.org/https://doi.org/10.1007/978-3-642-03889-1_140
- Corbetta, D., Imeri, F., Gatti, R., 2015. Rehabilitation that incorporates virtual reality is more effective than standard rehabilitation for improving walking speed, balance and mobility after stroke: a systematic review. *J Physiother* 61, 117–124. <https://doi.org/10.1016/J.JPHYS.2015.05.017>
- Ding, H., Trajcevski, G., Scheuermann, P., Wang, X., Keogh, E., 2008. Querying and Mining of Time Series Data: Experimental Comparison of Representations and Distance Measures. *Proceedings of the VLDB Endowment* 1, 1542–1552. <https://doi.org/10.14778/1454159.1454226>
- Ekman, P., Levenson, R.W., Friesen, W. V., 1983. Autonomic Nervous System Activity Distinguishes Among Emotions. *Science* (1979) 221, 1208–1210. <https://doi.org/10.1126/SCIENCE.6612338>
- Fasoli, S.E., Krebs, H.I., Stein, J., Frontera, W.R., Hogan, N., 2003. Effects of robotic therapy on motor impairment and recovery in chronic stroke. *Arch Phys Med Rehabil* 84, 477–482. <https://doi.org/10.1053/apmr.2003.50110>
- Fischer, H.C., Stubblefield, K., Kline, T., Luo, X., Kenyon, R. v., Kamper, D.G., 2007. Hand Rehabilitation Following Stroke: A Pilot Study of Assisted Finger Extension Training in a Virtual Environment. *Top Stroke Rehabil* 14, 1–12. <https://doi.org/10.1310/tsr1401-1>
- Fougner, A., Scheme, E., Chan, A.D.C., Englehart, K., Stavadahl, Ø., 2011. Resolving the limb position effect in myoelectric pattern recognition. *IEEE Transactions on Neural Systems and Rehabilitation Engineering* 19, 644–651. <https://doi.org/10.1109/TNSRE.2011.2163529>
- Frick, E.M., Alberts, J.L., 2007. Combined Use of Repetitive Task Practice and an Assistive Robotic Device in a Patient With Subacute Stroke. *Phys Ther* 86, 1378–1386. <https://doi.org/10.2522/ptj.20050149>
- Fu, J., Choudhury, R., Hosseini, S.M., Simpson, R., Park, J.H., 2022. Myoelectric Control Systems for Upper Limb Wearable Robotic Exoskeletons and Exosuits—A Systematic Review. *Sensors* 22, 8134. <https://doi.org/10.3390/s22218134>
- GBD 2016 Stroke Collaborators, 2019. Global, regional, and national burden of stroke, 1990–2016: a systematic analysis for the Global Burden of Disease Study 2016. *Lancet Neurol* 18, 439–458. [https://doi.org/https://doi.org/10.1016/S1474-4422\(19\)30034-1](https://doi.org/https://doi.org/10.1016/S1474-4422(19)30034-1)
- Giggins, O.M., Persson, U.M., Caulfield, B., 2013. Biofeedback in rehabilitation. *J NeuroEngineering Rehabil* 10, 1–11. <https://doi.org/https://doi.org/10.1186/1743-0003-10-60>

- Grandini, M., Bagli, E., Visani, G., 2020. Metrics for Multi-Class Classification: an Overview. *ArXiv* 1–17. <https://doi.org/10.48550/arXiv.2008.05756>
- Guerrero, C.R., Fraile Marinero, J.C., Turiel, J.P., Muñoz, V., 2013. Using “human state aware” robots to enhance physical human-robot interaction in a cooperative scenario. *Comput Methods Programs Biomed* 112, 250–259. <https://doi.org/10.1016/j.cmpb.2013.02.003>
- Gui, K., Tan, U.-X., Liu, H., Zhang, D., 2020. Electromyography-Driven Progressive Assist-as-Needed Control for Lower Limb Exoskeleton. *IEEE Trans Med Robot Bionics* 2, 50–58. <https://doi.org/10.1109/tmrb.2020.2970222>
- Gümüslü, E., Erol Barkana, D., Köse, H., 2020. Emotion recognition using EEG and physiological data for robot-assisted rehabilitation systems, in: Gümüslü, E., Barkana, D.E., Köse, H. (Eds.), *Companion Publication of the 2020 International Conference on Multimodal Interaction*. Association for Computing Machinery, New York, pp. 379–387. <https://doi.org/10.1145/3395035.3425199>
- Halaki, M., Ginn, K., 2012. Normalization of EMG Signals: To Normalize or Not to Normalize and What to Normalize?, in: Naik, G.R. (Ed.), *Computational Intelligence in Electromyography Analysis - A Perspective on Current Applications and Future Challenges*. InTech, Rijeka, Croatia, pp. 175–194. <https://doi.org/10.5772/3315>
- Hariharan, A., Adam, M.T.P., 2015. Blended Emotion Detection for Decision Support. *IEEE Trans Hum Mach Syst* 45, 510–517. <https://doi.org/10.1109/THMS.2015.2418231>
- Harwin, W.S., Patton, J.L., Edgerton, V.R., 2006. Challenges and opportunities for robot-mediated neurorehabilitation. *Proceedings of the IEEE* 94, 1717–1726. <https://doi.org/10.1109/JPROC.2006.880671>
- Herpich, F., Rincon, F., 2020. Management of Acute Ischemic Stroke. *Crit Care Med* 48, 1654–1663. <https://doi.org/10.1097/CCM.0000000000004597>
- Heuer, S., Chamadiya, B., Gharbi, A., Kunze, C., Wagner, M., 2010. Unobtrusive in-vehicle biosignal instrumentation for advanced driver assistance and active safety, in: *Proceedings of 2010 IEEE EMBS Conference on Biomedical Engineering and Sciences (IECBES)*. IEEE, Kuala Lumpur, Malaysia, pp. 252–256. <https://doi.org/10.1109/IECBES.2010.5742238>
- Ho, N.S.K., Tong, K.Y., Hu, X.L., Fung, K.L., Wei, X.J., Rong, W., Susanto, E., 2011. An EMG-driven Exoskeleton Hand Robotic Training Device on Chronic Stroke Subjects. *2011 IEEE International Conference on Rehabilitation Robotics* 149–153. <https://doi.org/10.1109/ICORR.2011.5975340>
- Hogan, N., Krebs, H.I., Charnnarong, J., Srikrishna, P., Sharon, A., 1992. MIT - MANUS: A workstation for manual therapy and training I. *1992 Proceedings IEEE*

- International Workshop on Robot and Human Communication (ROMAN) 161–165. <https://doi.org/10.1109/ROMAN.1992.253895>
- Holden, M.K., 2005. Virtual Environments for Motor Rehabilitation: Review. *CyberPsychology & Behavior* 8, 187–211. <https://doi.org/10.1089/cpb.2005.8.187>
- Hossin, M., Sulaiman, M.N., 2015. A Review on Evaluation Metrics for Data Classification Evaluations. *International Journal of Data Mining & Knowledge Management Process* 5, 1–11. <https://doi.org/10.5121/ijdkp.2015.5201>
- Hu, X.L., Tong, K.Y., Song, R., Zheng, X.J., Leung, W.W.F., 2009. A comparison between electromyography-driven robot and passive motion device on wrist rehabilitation for chronic stroke. *Neurorehabil Neural Repair* 23, 837–846. <https://doi.org/10.1177/1545968309338191>
- Jakopin, B., Mihelj, M., Munih, M., 2017. An Unobtrusive Measurement Method for Assessing Physiological Response in Physical Human-Robot Interaction. *IEEE Trans Hum Mach Syst* 47, 474–485. <https://doi.org/10.1109/THMS.2017.2681434>
- Jerath, R., Beveridge, C., 2020. Respiratory Rhythm, Autonomic Modulation, and the Spectrum of Emotions: The Future of Emotion Recognition and Modulation. *Front. Psychol.* 11, 1–7. <https://doi.org/10.3389/fpsyg.2020.01980>
- Kahn, L.E., Lum, P.S., Rymer, W.Z., Reinkensmeyer, D.J., 2006. Robot-assisted movement training for the stroke-impaired arm: Does it matter what the robot does? *J Rehabil Res Dev* 43, 619–30.
- Kamper, D.G., Harvey, R.L., Suresh, S., Rymer, W.Z., 2003. Relative contributions of neural mechanisms versus muscle mechanics in promoting finger extension deficits following stroke. *Muscle Nerve* 28, 309–318. <https://doi.org/10.1002/mus.10443>
- Katsigiannis, S., Ramzan, N., 2018. DREAMER: A Database for Emotion Recognition Through EEG and ECG Signals from Wireless Low-cost Off-the-Shelf Devices. *IEEE J Biomed Health Inform* 22, 98–107. <https://doi.org/10.1109/JBHI.2017.2688239>
- Khezri, M., Firoozabadi, M., Sharafat, A.R., 2015. Reliable emotion recognition system based on dynamic adaptive fusion of forehead biopotentials and physiological signals. *Comput Methods Programs Biomed* 122, 149–164. <https://doi.org/10.1016/j.cmpb.2015.07.006>
- Kim, J., André, E., 2008. Emotion recognition based on physiological changes in music listening. *IEEE Trans Pattern Anal Mach Intell* 30, 2067–2083. <https://doi.org/10.1109/TPAMI.2008.26>

- Koelstra, S., Mühl, C., Soleymani, M., Lee, J.S., Yazdani, A., Ebrahimi, T., Pun, T., Nijholt, A., Patras, I., 2012. DEAP: A database for emotion analysis; Using physiological signals. *IEEE Trans Affect Comput* 3, 18–31. <https://doi.org/10.1109/T-AFFC.2011.15>
- Koenig, A., Omlin, X., Novak, D., Riener, R., 2011. A review on bio-cooperative control in gait rehabilitation, in: *IEEE International Conference on Rehabilitation Robotics*. IEEE, Zurich, pp. 1–6. <https://doi.org/10.1109/ICORR.2011.5975454>
- Konrad, P., 2005. *The ABC of EMG: A Practical Introduction to Kinesiological Electromyography*, 1st ed, Noraxon INC. USA. Noraxon Inc. USA. <https://doi.org/10.1016/j.jacc.2008.05.066>
- Krasoulis, A., Vijayakumar, S., Nazarpour, K., 2019. Multi-grip classification-based prosthesis control with two EMG-IMU sensors. *IEEE Trans. Neural Syst. Rehabil. Eng.* 28, 508–518. <https://doi.org/10.1101/579367>
- Kutner, N.G., Zhang, R., Butler, A.J., Wolf, S.L., Alberts, J.L., 2010. Quality-of-life change associated with robotic-assisted therapy to improve hand motor function in patients with subacute stroke: a randomized clinical trial. *Phys Ther* 90, 493–504. <https://doi.org/10.2522/ptj.20090160>
- Kwakkel, G., Kollen, B.J., Krebs, H.I., 2008. Effects of Robot-Assisted Therapy on Upper Limb Recovery After Stroke: A Systematic Review. *Neurorehabil Neural Repair* 22, 111–121. <https://doi.org/10.1177/1545968307305457>
- Landgraf, M., Yoo, I.S., Sessner, J., Mooser, M., Kaufmann, D., Mattejat, D., Reitelsh, S., 2018. Gesture Recognition with Sensor Data Fusion of Two Complementary Sensing Methods, in: *2018 7th IEEE International Conference on Biomedical Robotics and Biomechatronics (Biorob)*. IEEE, Enschede, Netherlands, pp. 795–800. <https://doi.org/doi:10.1109/BIOROB.2018.8487949>.
- Lehman, G.J., McGill, S.M., 1999. The importance of normalization in the interpretation of surface electromyography: A proof of principle. *J Manipulative Physiol Ther* 22, 444–446. [https://doi.org/10.1016/S0161-4754\(99\)70032-1](https://doi.org/10.1016/S0161-4754(99)70032-1)
- Leonardis, D., Barsotti, M., Loconsole, C., Solazzi, M., Troncosi, M., Mazzotti, C., Castelli, V.P., Procopio, C., Lamola, G., Chisari, C., Bergamasco, M., Frisoli, A., 2015. An EMG-controlled robotic hand exoskeleton for bilateral rehabilitation. *IEEE Trans Haptics* 8, 140–151. <https://doi.org/10.1109/TOH.2015.2417570>
- Li, G., Member, S., Schultz, A.E., Kuiken, T.A., Member, S., 2010. Quantifying Pattern Recognition — Based Myoelectric Control of Multifunctional Transradial Prostheses. *IEEE Transactions on Neural Systems and Rehabilitation Engineering* 18, 185–192. <https://doi.org/10.1109/TNSRE.2009.2039619>.

- Li, K., Zhang, J., Wang, L., Zhang, M., Li, J., Bao, S., 2020. A review of the key technologies for sEMG-based human-robot interaction systems. *Biomed Signal Process Control* 62, 102074. <https://doi.org/10.1016/j.bspc.2020.102074>
- Liu, C., Conn, K., Sarkar, N., Stone, W., 2008. Physiology-based affect recognition for computer-assisted intervention of children with Autism Spectrum Disorder. *International Journal of Human Computer Studies* 66, 662–677. <https://doi.org/10.1016/j.ijhsc.2008.04.003>
- Liu, J., Zhang, F., Huang, H.H., 2014. An open and configurable embedded system for EMG pattern recognition implementation for artificial arms, in: 2014 36th Annual International Conference of the IEEE Engineering in Medicine and Biology Society (EMBC). IEEE, Chicago, IL, USA, pp. 4095–4098. <https://doi.org/10.1109/EMBC.2014.6944524>
- Lu, Z., Chen, X., Zhang, X., Tong, K.Y., Zhou, P., 2017. Real-Time Control of an Exoskeleton Hand Robot with Myoelectric Pattern Recognition. *Int J Neural Syst* 27, 1–11. <https://doi.org/10.1142/S0129065717500095>
- Luca, C.J. De, 2002. *Surface Electromyography: Detection and Recording*, Delsys Incorporated.
- Lucas, L., DiCicco, M., Matsuoka, Y., 2016. An EMG-Controlled Hand Exoskeleton for Natural Pinching. *Journal of Robotics and Mechatronics* 16, 482–488. <https://doi.org/10.20965/jrm.2004.p0482>
- Lum, P.S., Godfrey, S.B., Brokaw, E.B., Holley, R.J., Nichols, D., 2012. Robotic approaches for rehabilitation of hand function after stroke. *Am J Phys Med Rehabil* 91, 242–251. <https://doi.org/10.1097/PHM.0b013e31826bcedb>
- Lv, Y., Sun, Q., Li, J., Zhang, W., He, Y., Zhou, Y., 2021. Disability Status and Its Influencing Factors Among Stroke Patients in Northeast China: A 3-Year Follow-Up Study. *Neuropsychiatr Dis Treat* 17, 2567. <https://doi.org/10.2147/NDT.S320785>
- Maier, M., Ballester, B.R., Verschure, P.F.M.J., 2019. Principles of Neurorehabilitation After Stroke Based on Motor Learning and Brain Plasticity Mechanisms. *Front Syst Neurosci* 13, 1–18. <https://doi.org/10.3389/fnsys.2019.00074>
- Malmstrom, E., Opton, E., Lazarus, R., 1965. Heart Rate Measurement and the Correlation of Indices of Arousal. *Psychosom Med* 27, 546–556. <https://doi.org/10.1097/00006842-196511000-00005>
- Mandryk, R.L., Atkins, M.S., 2007. A fuzzy physiological approach for continuously modeling emotion during interaction with play technologies. *International Journal of Human Computer Studies* 65, 329–347. <https://doi.org/10.1016/j.ijhcs.2006.11.011>

- McManus, L., de Vito, G., Lowery, M.M., 2020. Analysis and Biophysics of Surface EMG for Physiotherapists and Kinesiologists: Toward a Common Language With Rehabilitation Engineers. *Front Neurol* 11. <https://doi.org/10.3389/fneur.2020.576729>
- Meattini, R., Benatti, S., Scarcia, U., De Gregorio, D., Benini, L., Melchiorri, C., 2018. An sEMG-Based Human-Robot Interface for Robotic Hands Using Machine Learning and Synergies. *IEEE Trans Compon Packaging Manuf Technol* 8, 1149–1158. <https://doi.org/10.1109/TCPMT.2018.2799987>
- Meshkati, N., 1988. Heart Rate Variability and Mental Workload Assessment. *Advances in Psychology* 52, 101–115. [https://doi.org/10.1016/S0166-4115\(08\)62384-5](https://doi.org/10.1016/S0166-4115(08)62384-5)
- Mihelj, M., Novak, D., Munih, M., 2009. Emotion-aware system for upper extremity rehabilitation. 2009 Virtual Rehabilitation International Conference, VR 2009 160–165. <https://doi.org/10.1109/ICVR.2009.5174225>
- Mihelj, M., Podobnik, J., 2013. Haptics for Virtual Reality and Teleoperation, *Journal of Chemical Information and Modeling*. Springer. <https://doi.org/10.1017/CBO9781107415324.004>
- Moggio, L., de Sire, A., Marotta, N., Demeco, A., Ammendolia, A., 2022. Exoskeleton versus end-effector robot-assisted therapy for finger-hand motor recovery in stroke survivors: systematic review and meta-analysis. *Topics in Stroke Rehabilitation* 29, 539–550. <https://doi.org/10.1080/10749357.2021.1967657>
- Moreno-San Juan, V., Cignal, A., Fraile, J., Pérez-turiel, J., de la Fuente, E., 2021. Design and Characterization of a Lightweight Underactuated RACA Hand Exoskeleton for Neurorehabilitation. *Robotics and Autonomous Systems* 143 143 (2021), 103828. <https://doi.org/https://doi.org/10.1016/j.robot.2021.103828>
- Muñoz, J.E., Gouveia, E.R., Cameirão, M.S., Badia, S.B.I., 2018. Physiolab - A multivariate physiological computing toolbox for ECG, EMG and EDA signals: A case of study of cardiorespiratory fitness assessment in the elderly population. *Multimed Tools Appl* 77, 11511–11546. <https://doi.org/10.1007/s11042-017-5069-z>
- Novak, D., Mihelj, M., Zihlerl, J., Olenšek, A., Munih, M., 2011. Psychophysiological measurements in a biocooperative feedback loop for upper extremity rehabilitation. *IEEE Transactions on Neural Systems and Rehabilitation Engineering* 19, 400–410. <https://doi.org/10.1109/TNSRE.2011.2160357>
- Novak, D., Zihlerl, J., Olenšek, A., Milavec, M., Podobnik, J., Mihelj, M., Munih, M., 2010. Psychophysiological responses to robotic rehabilitation tasks in stroke.

- IEEE Transactions on Neural Systems and Rehabilitation Engineering 18, 351–361. <https://doi.org/10.1109/TNSRE.2010.2047656>
- Open Source Sensor Fusion [WWW Document], 2015. URL <https://github.com/memsindustrygroup/Open-Source-Sensor-Fusion>
- Pan, J., Tompkins, W.J., 1985. A Real-Time QRS Detection Algorithm. IEEE Trans Biomed Eng BME-32, 230–236. <https://doi.org/10.1109/TBME.1985.325532>
- Park, S., Fraser, M., Weber, L.M., Meeker, C., Bishop, L., Geller, D., Stein, J., Ciocarlie, M., 2020. User-Driven Functional Movement Training with a Wearable Hand Robot after Stroke. IEEE Transactions on Neural Systems and Rehabilitation Engineering 28, 2265–2275. <https://doi.org/10.1109/TNSRE.2020.3021691>
- Park, S., Meeker, C., Weber, L.M., Bishop, L., Stein, J., Ciocarlie, M., 2018. Multimodal sensing and interaction for a robotic hand orthosis. IEEE Robot Autom Lett 4, 315–322. <https://doi.org/10.1109/LRA.2018.2890199>.
- Parker, M.E., Snyder-Shall, M., 2013. Recovery of Upper Extremity Function in Stroke Patients. Neurology Report 19, 46–47. <https://doi.org/10.1097/01253086-199519010-00028>
- Picard, R.W., Vyzas, E., Healey, J., 2001. Toward machine emotional intelligence: Analysis of affective physiological state. IEEE Trans Pattern Anal Mach Intell 23, 1175–1191. <https://doi.org/10.1109/34.954607>
- Polygerinos, P., Galloway, K.C., Sanan, S., Herman, M., Walsh, C.J., 2015a. EMG controlled soft robotic glove for assistance during activities of daily living, in: 2015 IEEE International Conference on Rehabilitation Robotics (ICORR). IEEE, Singapore, pp. 55–60. <https://doi.org/10.1109/ICORR.2015.7281175>
- Polygerinos, P., Wang, Z., Galloway, K.C., Wood, R.J., Walsh, C.J., 2015b. Soft robotic glove for combined assistance and at-home rehabilitation. Rob Auton Syst 73, 135–143. <https://doi.org/10.1016/j.robot.2014.08.014>
- Postolache, O., Viegas, V., Dias Pereira, J.M., Vinhas, D., Girão, P.S., Postolache, G., 2014. Toward developing a smart wheelchair for user physiological stress and physical activity monitoring, in: 2014 IEEE International Symposium on Medical Measurements and Applications (MeMeA). IEEE, Lisboa, Portugal, pp. 1–6. <https://doi.org/10.1109/MeMeA.2014.6860097>
- Qiu, S., Zhao, Hongkai, Jiang, N., Wang, Z., Liu, L., An, Y., Zhao, Hongyu, Miao, X., Liu, R., Fortino, G., 2022. Multi-sensor information fusion based on machine learning for real applications in human activity recognition: State-of-the-art and research challenges. Information Fusion 80, 241–265. <https://doi.org/10.1016/j.inffus.2021.11.006>

- Reinkensmeyer, D.J., Housman, S.J., 2007. "If I can't do it once, why do it a hundred times?": Connecting volition to movement success in a virtual environment motivates people to exercise the arm after stroke, in: 2007 Virtual Rehabilitation. IEEE, Venice, Italy, pp. 44–48. <https://doi.org/10.1109/ICVR.2007.4362128>.
- Riener, R., Munih, M., 2010. Guest editorial special section on rehabilitation via bio-cooperative control. *IEEE Transactions on Neural Systems and Rehabilitation Engineering* 18, 337–338. <https://doi.org/10.1109/TNSRE.2010.2060390>
- Rietman, J.S., Prange, G., Kottink, A., Ribbers, G., Buurke, J., 2014. The Effect of an Arm Supporting Training Device in Sub-Acute Stroke Patients: Randomized Clinical Trial. *Arch Phys Med Rehabil* 95, e8. <https://doi.org/10.1016/j.apmr.2014.07.382>
- Rodgers, M.M., Alon, G., Pai, V.M., Conroy, R.S., 2019. Wearable technologies for active living and rehabilitation: Current research challenges and future opportunities. *J. Rehabil. Assist. Technol. Eng.* 6, 1–9. <https://doi.org/10.1177/2055668319839607>
- Ryser, F., Bützer, T., Held, J.P., Lamercy, O., Gassert, R., 2017. Fully embedded myoelectric control for a wearable robotic hand orthosis, in: 2017 International Conference on Rehabilitation Robotics (ICORR). IEEE, London, UK, pp. 615–621. <https://doi.org/10.1109/ICORR.2017.8009316>
- Schmit, B.D., Dewald, J.P.A., Rymer, W.Z., 2000. Stretch reflex adaptation in elbow flexors during repeated passive movements in unilateral brain-injured patients. *Arch Phys Med Rehabil* 81, 269–278. [https://doi.org/10.1016/S0003-9993\(00\)90070-4](https://doi.org/10.1016/S0003-9993(00)90070-4)
- Scotto Di Luzio, F., Simonetti, D., Cordella, F., Miccinilli, S., Sterzi, S., Draicchio, F., Zollo, L., 2018. Bio-cooperative approach for the human-in-the-loop control of an end-effector rehabilitation robot. *Front Neurobot* 12, 1–12. <https://doi.org/10.3389/fnbot.2018.00067>
- Secciani, N., Topini, A., Ridolfi, A., Meli, E., Allotta, B., 2020. A novel Point-in-Polygon-based sEMG classifier for Hand Exoskeleton Systems. *IEEE Transactions on Neural Systems and Rehabilitation Engineering* 28, 3158–3166. <https://doi.org/10.1109/TNSRE.2020.3044113>
- Serpelloni, M., Tiboni, M., Lancini, M., Pasinetti, S., Vertuan, A., Gobbo, M., 2016. Preliminary study of a robotic rehabilitation system driven by EMG for hand mirroring, in: 2016 IEEE International Symposium on Medical Measurements and Applications (MeMeA). IEEE, Benevento, Italy, pp. 1–6. <https://doi.org/10.1109/MeMeA.2016.7533730>
- Simonetti, D., Zollo, L., Papaleo, E., Carpino, G., Guglielmelli, E., 2016. Multimodal adaptive interfaces for 3D robot-mediated upper limb neuro-rehabilitation: An

- overview of bio-cooperative systems. *Rob Auton Syst* 85, 62–72. <https://doi.org/10.1016/j.robot.2016.08.012>
- Sterr, A., Freivogel, S., 2003. Motor-improvement following intensive training in low-functioning chronic hemiparesis. *Neurology* 61, 842–4. <https://doi.org/10.1212/wnl.61.6.842>
- Subramanian, S.K., Lourenço, C.B., Chilingaryan, G., Sveistrup, H., Levin, M.F., 2013. Arm motor recovery using a virtual reality intervention in chronic stroke: Randomized control trial. *Neurorehabil Neural Repair* 27, 13–23. <https://doi.org/10.1177/1545968312449695>
- Sveistrup, H., 2004. Motor rehabilitation using virtual reality. *J Neuroeng Rehabil* 1, 1–8. <https://doi.org/10.1186/1743-0003-1-10>
- Tam, S., Boukadoum, M., Campeau-Lecours, A., Gosselin, B., 2020. A Fully Embedded Adaptive Real-Time Hand Gesture Classifier Leveraging HD-sEMG and Deep Learning. *IEEE Trans Biomed Circuits Syst* 14, 232–243. <https://doi.org/10.1109/TBCAS.2019.2955641>
- Tate, J.J., Milner, C.E., 2010. Real-time kinematic, temporospatial, and kinetic biofeedback during gait retraining in patients: A systematic review. *Physical Therapy and Rehabilitation Journal* 90, 1123–1134. <https://doi.org/10.2522/ptj.20080281>
- Teramae, T., Noda, T., Morimoto, J., 2018. EMG-Based Model Predictive Control for Physical Human-Robot Interaction: Application for Assist-As-Needed Control. *IEEE Robot Autom Lett* 3, 210–217. <https://doi.org/10.1109/LRA.2017.2737478>
- Tharwat, A., 2018. Classification assessment methods. *Applied Computing and Informatics* 17, 168–192. <https://doi.org/10.1016/j.aci.2018.08.003>
- Tran, P., Jeong, S., Herrin, K.R., Desai, J.P., 2021. Review: Hand Exoskeleton Systems, Clinical Rehabilitation Practices, and Future Prospects. *IEEE Trans Med Robot Bionics* 3, 606–622. <https://doi.org/10.1109/tmrb.2021.3100625>
- Ueki, S., Nishimoto, Y., Abe, M., Kawasaki, H., Ito, S., Ishigure, Y., Mizumoto, J., Ojika, T., 2008. Development of virtual reality exercise of hand motion assist robot for rehabilitation therapy by patient self-motion control, in: 2008 30th Annual International Conference of the IEEE Engineering in Medicine and Biology Society. IEEE, Vancouver, British Columbia, Canada, pp. 4282–4285. <https://doi.org/10.1109/IEMBS.2008.4650156>
- Volpe, B.T., Krebs, H.I., Hogan, N., Edelstein, L., Diels, C., Aisen, M., 2000. A novel approach to stroke rehabilitation: Robot-aided sensorimotor stimulation. *Neurology* 54, 1938–1944. <https://doi.org/10.1212/WNL.54.10.1938>

- Winstein, C.J., Stein, J., Arena, R., Bates, B., Cherney, L.R., Cramer, S.C., Deruyter, F., Eng, J.J., Fisher, B., Harvey, R.L., Lang, C.E., MacKay-Lyons, M., Ottenbacher, K.J., Pugh, S., Reeves, M.J., Richards, L.G., Stiers, W., Zorowitz, R.D., 2016. Guidelines for Adult Stroke Rehabilitation and Recovery: A Guideline for Healthcare Professionals from the American Heart Association/American Stroke Association, Stroke. Lippincott Williams and Wilkins. <https://doi.org/10.1161/STR.0000000000000098>
- Wolf, S.L., Winstein, C.J., Miller, J.P., Taub, E., Uswatte, G., Morris, D., Giuliani, C., Light, K.E., Nichols-Larsen, D., EXCITE Investigators, for the, 2006. Effect of Constraint-Induced Movement Therapy on Upper Extremity Function 3 to 9 Months After Stroke: The EXCITE Randomized Clinical Trial. *JAMA* 296, 2095–2104. <https://doi.org/10.1001/jama.296.17.2095>
- World Health Organization, 2020. The top 10 causes of death [WWW Document]. WHO. URL <https://www.who.int/news-room/fact-sheets/detail/the-top-10-causes-of-death> (accessed 2.8.23).
- World Health Organization, 1978. Cerebrovascular disorders: a clinical and research classification. World Health Organization, Geneva.
- Wu, J., Cheng, H., Zhang, J., Yang, S., Cai, S., 2021. Robot-Assisted Therapy for Upper Extremity Motor Impairment after Stroke: A Systematic Review and Meta-Analysis. *Phys Ther* 101, 1–13. <https://doi.org/10.1093/ptj/pzab010>
- Yang, E., Dorneich, M.C., 2015. The effect of time delay on emotion, arousal, and satisfaction in human-robot interaction, in: Proceedings of the Human Factors and Ergonomics Society 59th Annual Meeting 2015. pp. 443–447. <https://doi.org/10.1177/1541931215591094>
- Yue, Z., Zhang, X., Wang, J., 2017. Hand Rehabilitation Robotics on Poststroke Motor Recovery. *Behavioural Neurology* 2017, 1–20. <https://doi.org/http://dx.doi.org/10.1155/2017/3908135>
- Zhai, J., Barreto, A.B., Chin, C., Li, C., 2005. Realization of stress detection using psychophysiological signals for improvement of human-computer interactions, in: Proceedings. IEEE SoutheastCon, 2005. IEEE, Ft. Lauderdale, FL, USA, pp. 415–420. <https://doi.org/10.1109/secon.2005.1423280>
- Zhang, J., Wang, B., Zhang, C., Xiao, Y., Wang, M.Y., 2019. An EEG/EMG/EOG-based multimodal human-machine interface to real-time control of a soft robot hand. *Front Neurobot* 13, 1–13. <https://doi.org/10.3389/fnbot.2019.00007>

The research developed in this PhD thesis was in part supported by a Regional Ministry of Education grant for the pre-doctoral recruitment of research staff, co-financed by the European Social Fund (ESF).



**AYUDAS DESTINADAS A FINANCIAR LA
CONTRATACIÓN PREDOCTORAL DE PERSONAL
INVESTIGADOR COFINANCIADAS POR EL FONDO
SOCIAL EUROPEO**

*ORDEN de 12 de Diciembre de 2019, de la
Consejería de Educación*

PROGRAMA OPERATIVO FSE CASTILLA Y LEÓN 2014-2020.
ACTUACIÓN COFINANCIADA POR EL FONDO SOCIAL EUROPEO.



UNIÓN EUROPEA
FONDO SOCIAL EUROPEO